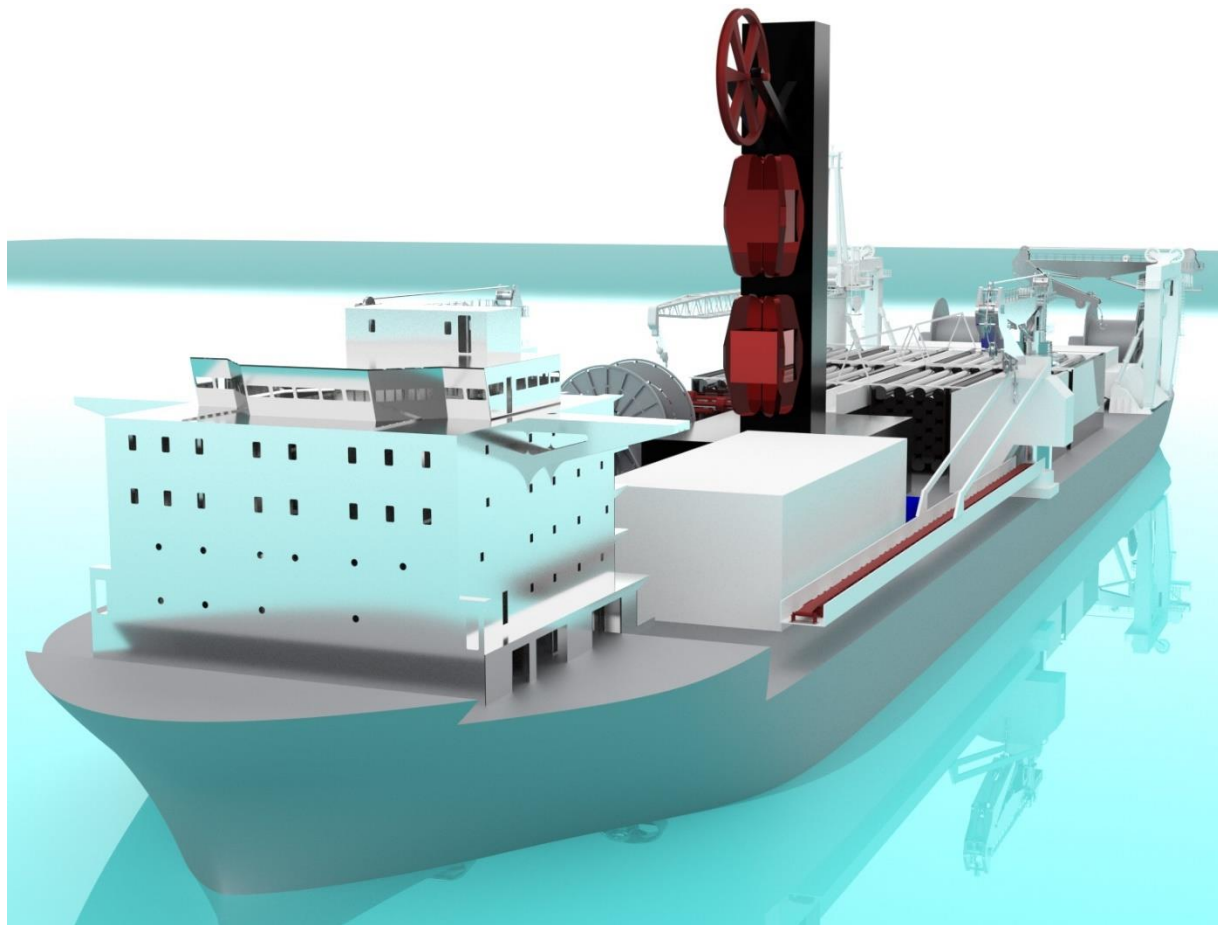


Preliminary Powerplant Concepts of a DSM production support vessel



Thesis for the degree of MSc in Marine Technology in the specialization of *Marine Engineering*

Preliminary Powerplant Concepts of a DSM production support vessel

By

Floris Roelofsen

Performed at

Norwegian University of Science and Technology

This thesis (MT.21/22.040.M) is classified as confidential in accordance with the general conditions for projects performed by the TUDelft.

15/08/2022

Company supervisors

Responsible supervisor: Prof. Bjørn Egil Asbjørnslett

Daily Supervisor(s):

Prof. Steinar Løve Ellefmo, Asst. Prof. Svein Aanond Aanondson,
PhD(c) Astrid Vamråk Solheim

Thesis exam committee

Chair/Responsible Professor: Dr. Ir. Klaas Visser

Staff Member: Dr. Ir. Rudy Helmons

Staff Member: Dr. Ir. Steinar Løve Ellefmo

Company Member: PhDc Astrid Vamråk Solheim

Author Details

Studynumber: 4468570

Summary

Mining for polymetallic nodules in the Clarion-Clipperton Zone in the Pacific Ocean is a new form of mining for minerals like copper, nickel, manganese, and cobalt. A collector vehicle moves across the seabed to suck up these nodules from the sand bed. To bring these nodules with their minerals from the seabed to the shore, a production support vessel is put into action. This vessel is the focus point of this thesis with an emphasis on matching a powerplant to its energy needs.

The production support vessel houses all the equipment to mine the nodules, transport them to the sea surface and process them for storage until they are offloaded to a transport vessel to shore. The mining operation is arranged to mine 400 tons of nodules per hour and offload these once every week to the transport vessel.

The main design consideration lies in transporting the nodules from the seabed to the surface. A hydraulic solution consists of a set of centrifugal slurry pumps, which pump a slurry of water and nodules to the surface in stages.

An alternative is the airlift system, which uses compressed air injected into the pipe to create the necessary upwards pressure. The expanding air forces the nodule-water slurry to move upwards. It also creates a suction effect under the air injection point to suck up the nodule-water slurry. This system is powered by a large compressor on the vessel to create the necessary air pressure to be able to inject air at significant water depth.

The hydraulic method is a derivation from the dredging industry and requires 7,2 MW of pump power. The airlift method in principle has a higher operability due to the systems being on board but requires 22,5 MW.

A 118 000 tons displacement production support vessel is designed. Its holds can hold 67 000 tons of nodules, equivalent to 7 days of mining. With the collectors, vertical transport system and processing plant being part of the deck layout.

The choice of hydraulic or airlift transport has a big effect on the power and as such requires different powerplants. The emissions of the powerplant are aimed to be in line with the most stringent IMO regulations to make the vessel futureproof.

So, 50 % less emission than the emission levels of 2008.



Hydraulic Powerplant – 29 MW

The vessel concept with a hydraulic system requires up to 29 MW of power. Two different powerplant concept are worked out:

- 4x 8 MW DF Engines to generate 32 MW of power. The engines are fueled by LNG to reduce emissions and the remaining CO₂ is captured and stored on board. An absorber in the exhaust separates the CO₂ and the cold from the LNG is used to liquify the CO₂ to store it at a density of around 1 t/m³. A fuel tank for 30 days of operation is installed together with a similar sized CO₂ tank.
- An alternative powerplant consist of a small modular reactor. Releasing 90 MW of thermal energy to generate 30 MW of electrical energy with a steam turbine. Nuclear energy does not emit the emissions of an internal combustion engine but faces technological – and social challenges. The reactor power output is constant but can be reduced by inserting control rods and reduce the heat generated. This process is slow and inconsistent, so a 10 MWh battery is added to the powerplant to increase its dynamic performance for dealing with power variations.

Airlift powerplant – 42 MW

With the added power of the compressor for the airlift system, a total of 42 MW of power is required. For this vessel, two powerplant are also worked out:

- A combine cycle gas turbine which consists of a 32 MW gas turbine with a 10 MW steam turbine which gets it steam from the exhaust heat of the gas turbine. The plant is chosen due to its high efficiency at 52 %. This powerplant also uses LNG as fuel like the hydraulic concept but doesn't capture the CO₂. This is due to the increase in power, requiring a bigger CO₂ tank which can't be fitted inside the chosen hull.
- A small nuclear reactor is also an option for the airlift system, two reactors can be used to achieve the 42 MW of power. Having two reactors would increase the dynamic behavior of the powerplant and adds a level of redundancy. Similar to the hydraulic nuclear option, a 10 MWh battery is installed to assist with power variations which the reactor can't react to.

Preface

To finish my studies as a Master of Marine Technology with a fitting end in the specialization of marine engineering, the subject of Deep Sea Mining was chosen. As it's a new and upcoming industry where only the resources are set in stone and the room is there to think a bit outside the box as to how to undertake an offshore mining operation.

This thesis was the result of a great collaboration between the Norwegian University of Science and Technology and TU Delft. At TU Delft, Rudy Helmons has the expertise on deep sea mining and was key in forming the collaboration with NTNU to set up a combined effort to research the vessel design and powerplant matching of a DSM production support vessel.

I'd like to personally thank Peter de Vos and Bjørn Egil Asbjørnslett for facilitating the groundwork for this inter-university collaboration.

Rudy Helmons has proven vital in being an endless supply of DSM knowledge, and always updating me on the latest developments. His support and passion for this subject has made this thesis and the overall DSM industry that much more interesting and exciting to me.

Klaas Visser's marine engineering expertise and interest in deepsea mining has formed the perfect bridge between this industry and my specialization as a Marine Engineer.

At NTNU, Astrid Solheim has been an irreplaceable help in guiding me through my thesis and always being open and supportive for new ideas. Steinar Ellefmo proved to be an extremely knowledgeable DSM expert, with a knack for asking the right questions to reevaluate the results from the research. And as such lift the work performed in this thesis to a higher level.

With the ship design part of this thesis, Svein Aanonsen was a great input to have an open and functional approach for such a unique ship.

I'm curious how this industry will develop in the coming years. How engineering can facilitate this type of mining, while also taking the environmental aspects of this industry into account. I hope this thesis can play a small part in this and open some new ways of how to mine for minerals offshore.

Contents

Summary	4
Preface	6
List of Figures	10
List of Tables	12
Abbreviations	13
1 Introduction	15
1.1 Polymetallic nodules	16
1.2 Production support vessel	16
2 DSM in the CCZ.....	18
2.1 Location & Environment	18
2.2 Nodule collector.....	20
2.3 Vertical Transport System.....	21
2.4 Dewatering Process	23
2.4.1 Blue nodules proposal.....	23
2.4.2 Boskalis Chatham Rise proposal	24
2.5 Offloading Process	25
2.5.1 Dry Offloading.....	25
2.5.2 Wet Offloading.....	26
2.6 Powerplant.....	28
2.6.1 Combined Cycle Gas Plant	28
2.6.2 Small Nuclear Reactors	28
2.7 Energy Storage	29
2.8 Regulation	30
2.8.1 Exhaust emissions	30
2.8.2 Mining License	32
3 Design Requirements.....	33
3.1 VTS Differences	34
3.2 Vessel Size	35
3.3 Emission	35
3.4 Dynamic Position System.....	35
3.5 Sea-states.....	36
4 Vessel blocks	37

4.1	Accommodation.....	37
4.2	Collector.....	38
4.3	Vertical Transport.....	39
4.3.1	Riser storage (Shaffer / Schlumberger).....	40
4.3.2	Hydraulic Transport.....	43
4.3.3	Airlift Transport.....	43
4.3.4	Return pipe.....	44
4.3.5	Assembly Tower.....	46
4.3.6	Energy Dynamics.....	49
4.3.7	Jumper Hose & ROV.....	50
4.4	Dewatering.....	51
4.5	Nodule Storage.....	53
4.6	Internal transport.....	54
4.7	Offloading.....	55
4.7.1	Dry Offloading.....	55
4.7.2	Wet Offloading.....	57
4.7.3	Offloading selection.....	61
4.8	Onboard cranes.....	62
5	Vessel Design.....	63
5.1	Hull Design.....	63
5.2	Stability.....	64
5.2.1	Transit scenario.....	64
5.2.2	Mining scenario.....	65
5.3	Deck layout.....	66
5.4	Propulsion.....	68
5.4.1	DP Vessel Force estimation.....	68
5.4.2	Thruster layout.....	69
5.4.3	Cruise speed.....	71
6	Hydraulic VTS – Powerplants.....	73
6.1	Operational profile.....	73
6.2	Powerplant concept – Diesel Generators.....	76
6.2.1	Energy Storage.....	78
6.2.2	CO ₂ – Reduction.....	79

6.3	Powerplant Concept – SMR	81
6.3.1	Dynamic Performance.....	82
7	Airlift VTS – Powerplants	83
7.1	Powerplant Concept – COGES.....	85
7.1.1	Energy Storage	88
7.1.2	CO ₂ – Reduction	88
7.2	Powerplant Concept – SMR	89
8	Discussion.....	91
8.1	Vessel systems	91
8.2	Vessel design.....	92
8.3	Powerplant.....	93
8.4	Energy storage – LAES.....	94
9	Recommendations	97
10	Conclusion.....	99
10.1	Modular design – subsystems.....	99
10.2	Ship design	100
10.3	Powerplant concepts	101
	Appendix A – Riser Assembly Power Breakdown	103
	Appendix B – Operational Profile Hydraulic Transport.....	104
	Appendix C – Operational Profile Airlift Transport	105
	Appendix D – COGES Plant Schematic	106
	Appendix E – Energy Flow Diagram	107
	Collector – EFD.....	107
	Hydraulic VTS – EFD	108
	Riser Assembly – EFD	109
	Dewatering – EFD.....	110
	Dry – Offloading – EFD	111
	Appendix F – Deck Layout.....	112
	Appendix H – Sleipnir LNG-fueled Ship Based Carbon Capture.....	114
	Appendix J – DP Vessel force Calculation (MATLAB)	115
	Appendix K – Hydraulic VTS spc.....	119
	Appendix L – Airlift VTS spc.....	120
	Bibliography	121

List of Figures

Figure 1: Value chain Nodules mining	15
Figure 2: Cross-section nodule (Retrieved form ISA)	16
Figure 3: Nodule mining Schematic (Courtesy Grid-Arendal)	16
Figure 4: Wave Probability Curve (GSR, 2018)	18
Figure 5: Wind Speed Probability Curve (GSR, 2018)	19
Figure 6: Blue Nodules collector (Blue Nodules, 2020)	20
Figure 7: Diagonal transport (courtesy of Maxime Lesange)	21
Figure 8: Boskalis Dewatering Plant (Chatham Rock Phosphate Limited, 2014)	24
Figure 9: Self Unloading Bulk Carrier (Courtesy of CSL Group)	25
Figure 10: Floating Dredge Hose (Coourtesy of Orientflex)	26
Figure 11: Tandem Offloading (OCIMF, 2018)	26
Figure 12: Offloading Reel (Courtesy of Royal IHC)	26
Figure 13: Bow Loading (Courtesy of OCIMF)	27
Figure 14: COGES	28
Figure 15: MicroURANUS	28
Figure 16: Energy Storage Solutions	29
Figure 19:Deckhouse.....	37
Figure 20: Collector LARS	38
Figure 21: Riser Joints	40
Figure 22: Rack Cross-section	41
Figure 23: Joint storage assembly	42
Figure 24: Booster Station	43
Figure 25: MAN RB-C35 Skid	44
Figure 26: Carousel	45
Figure 27: Assembly Tower	46
Figure 28: Dewatering process	51
Figure 29: dewatering plant.....	52
Figure 30: Cargo Holds	53
Figure 31: Offloading Boom	55
Figure 32: Offloading System	56
Figure 33: Dry Offloading hull form	57
Figure 33: Flowchart wet offloading	57
Figure 34: Offloading Operation	58
Figure 35: Wet Offloading System	59
Figure 37: Wet Offloading hull form	59
Figure 36: Vessel Hull.....	63
Figure 39: Transit ballast.....	64
Figure 40: Mining ballast.....	65
Figure 46: Generic Deck Layout	66

Figure 47: Booster Station Storage	67
Figure 41: Thruster Arrangement	69
Figure 45: Bollard Pull Thrust in function of Propeller Power	69
Figure 42: Hull Resistance	71
Figure 43: Open water diagram (Ka 4-70 Nozzle 19A).....	72
Figure 48: Hydraulic VTS - OP	75
Figure 50: 4 x 7L46DF Engine Room.....	76
Figure 51: Wartsila 7L46Df sfc	77
Figure 52: CO2 Phase Diagram.....	79
Figure 53: LNG cooled CCS (van den Akker, 2017).....	80
Figure 49: Airlift VTS - OP.....	84
Figure 54: COGES sfc (Flatebø, 2012).....	87
Figure 55: COGES General Arrangement	87
Figure 58: SMR General Arrangement.....	90
Figure 61: Alternative mining configuration.....	92
Figure 17: LAES (Vecchi et al., 2021).....	94
Figure 18: Air Phase Diagram (a) & Air Density (b) (Engineering ToolBox, 2018).....	94
Figure 56: LAES (Lee et al., 2017).....	95
Figure 57: T-s Diagram dry air (Lee et al., 2017)	95
Figure 60: Complete vessel design.....	100

List of Tables

Table 1: Vertical transport idea's	21
Table 2: VTS mining effects	34
Table 3: Exhaust Emissions design requirements	35
Table 4: DP Configurations.....	35
Table 5: Sea-States.....	36
Table 6: Deckhouse Properties	37
Table 7: Collector Properties (Blue Nodules, 2017; Hydralift, 1997).....	38
Table 8: Riser Joints Assembly	40
Table 9: Joints rack distribution	41
Table 10: Joint Storage dim.....	42
Table 11: Booster station dim.....	43
Table 12: MAN RB-C35 Properties	44
Table 13: Return Pipe Characteristics	45
Table 14: Carousel Characteristics	45
Table 15: Tower Components.....	47
Table 16: Tower Load Scenarios	48
Table 17: Derrick Tower Properties	49
Table 18: Jumper hose & ROV Properties.....	50
Table 19: Dewatering processess.....	51
Table 20: Dewatering Components	52
Table 21: Cargo Holds Properties.....	53
Table 22: Internal transport System	54
Table 23: Dry Offloading	56
Table 24: Wet Offloading.....	58
Table 25: Wet-/dry-Offloading.....	61
Table 26: Crane Details	62
Table 27: hull Dimensions.....	63
Table 28: Thruster Characteristics	69
Table 29: Thrust power for different sea-states	70
Table 30: Propeller Power Breakdown	70
Table 31: Propeller Cruise properties	72
Table 32: Operating modes Hydraulic VTS	73
Table 33: Wartsila 7L46DF Properties.....	77
Table 34: Wartsila 8L46DF Fuel options	78
Table 35: SBCC Properties.....	80
Table 36: Hydraulic SMR Properties	81
Table 38: Operating modes Airlift VTS.....	83
Table 39: COGES Properties (Flatebø, 2012)	85
Table 40: COGES Fuel options.....	86
Table 42: SMR Properties.....	89
Table 43: Powerplant concepts.....	101
Table 44: Vessel forces results from MATLAB	118

Abbreviations

A&R	Abandonment and Recovery
AHC	Active Heave Compensation
CCS	Carbon Capture and Storage
CCZ	Clarion-Clipperton Zone
COB	Centre of Buoyancy
COG	Centre of Gravity
COGES	Combined Gas Electric and Steam
CWS	Catwalk Shuttle
DCC	Direct Contact Cooler
DP	Dynamic Positioning
DSM	Deep Sea Mining
ECA	Emission Control Area
EEDI	Energy Efficiency Design Index
FPSO	Floating Production, Storage, and Offloading
HFO	Heavy Fuel Oil
HPU	Hydraulic Power unit
HRSG	Heat Recovery Steam Generator
ID	Inner Diameter
IMO	International Maritime Organization
ISA	International Seabed Authority
LAES	Liquid Air Energy Storage a
LARS	Launch and Recovery System
LNG	Liquefied Natural Gas
MARPOL	International Convention for the Prevention of Pollution from Ships
MBR	Maximum Bending Radius
MDO	Marine Diesel Oil
MEPC	Marine Environment Protection Committee

MGO	Marine Gas Oil
NMVOC	Non-Methane Volatile Organic Compounds
O&G	Oil and Gas
OD	Outer Diameter
PCV	Prototype Collector Vehicle
PEMFC	Proton-Exchange Membrane Fuel Cell
PER	Pollutant Emission Ratio
PM	Particulate Matter
PPU	Pneumatic Power Unit
REMP	Regional Environmental Management Plan
SFC	Specific Fuel Consumption
SMS	Seafloor Massive Sulfides
SPE	Specific Pollutant emissions
STS	Ship-to-Ship
TEU	Twenty Foot Equivalent Unit
TRL	Technology Readiness Level
UHC	Unburned Hydro Carbonates
VCG	Vertical Centre of Gravity
VTS	Vertical Transport System

1 Introduction

In the pursuit of finding more and more raw materials to continue making batteries to provide the world of tomorrow with electricity storage. Deepsea mining is becoming a potential alternative to traditional land mining for these minerals.

Currently there are two promising types of deep-sea mining which are becoming financially attractive due to the increase in raw material prices (van Nijen et al., 2019).

The biggest is polymetallic nodules, which are big fields of rocks lying on the seabed in certain areas. These rocks contain high grades of nickel, cobalt, manganese & copper. These rocks can be collected from the sandy seabed.

The other type is seafloor massive sulfide or SMS for short, this occurs when magna comes in touch with seawater and solidifies on the seabed. This is a local phenomenon in volcanic regions and can be mined by excavation.

A third type, which is not yet economically interesting is ferromanganese crust. This is a mineral rich crust on subsea seamounts, but hard to mine due to the high gradients of these seamounts.

In this thesis the focus will be on polymetallic nodules, as it has the strongest case. Due to the vast amount of resources and the scarcity of said materials.

The value chain of these nodules can be roughly shown in Figure 1.

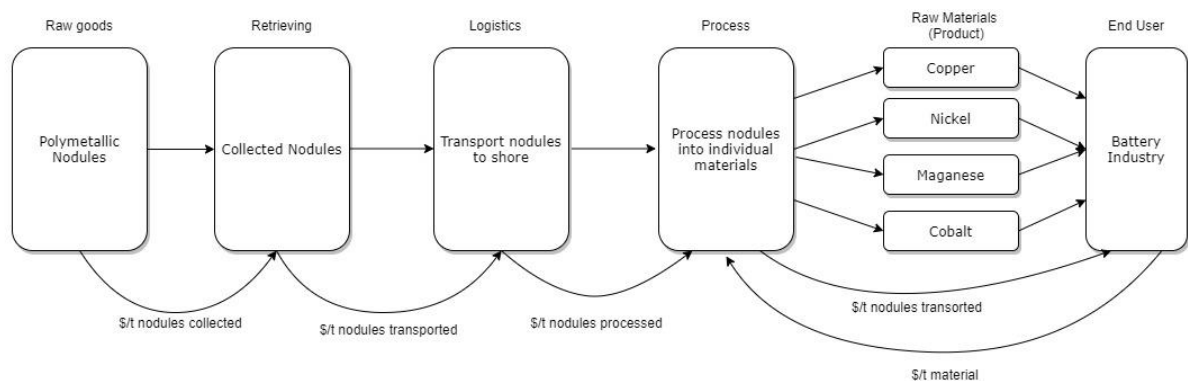


Figure 1: Value chain Nodules mining

The demand of these critical materials for battery production are expected to increase. Materials like cobalt also suffer from limited suppliers, which gives new suppliers a strong bargaining position. This makes Deepsea mining also a geo-political playground, as countries seek to have control over vital resources. Environmentally there is a lot of discussion about nodules, as arguments are made both ways. On one side it's argued nodules are less harmful than traditional open pit mining, and on the other side that the seafloor damage done by the mining is not worth the resources (van Nijen et al., 2019). This are all topics that will define the future of Deepsea mining.

1.1 Polymetallic nodules

Polymetallic nodules are big fields of rocks lying on the seabed in certain areas. These rocks contain high grades of nickel, cobalt, manganese & copper.

Nodules start out as small objects like shark teeth or shells which lay on the seabed. Loose minerals will slowly begin to attach to the object, as it presents a base for minerals to accumulate onto. Over millions of years, this will turn the object into a nodule with multiple build-up layers of minerals around it. Nodules will grow faster on the top, as this side is fully exposed to the seawater, whereas the bottom side is buried in the seabed. A cross-section of a nodules is shown in Figure 2, which shows the layered build-up of metallic sediment around the object in the middle (ISA, 2006).

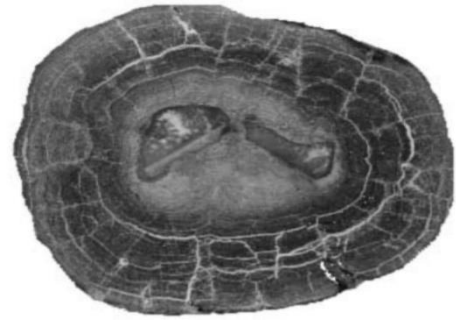


Figure 2: Cross-section nodule (Retrieved from ISA)

A collector tool on the seabed will move over the seabed and collect the top layer of the seabed with the nodules in it. This will then be transported to the sea level to a production support vessel. This vessel will be a FPSO-like structure to filter-out the nodules and store them until a bulk carrier can collect them and transport the nodules to shore.

1.2 Production support vessel

This thesis will look at the design of the production support vessel needed to support the mining operations. Due to the complex nature of a Deepsea mining production vessel, a modular approach will be used to examine the subsystems separately and make it possible to achieve multiple concepts with the different subsystems. Figure 3 shows a basic schematic of a nodule mining operation.

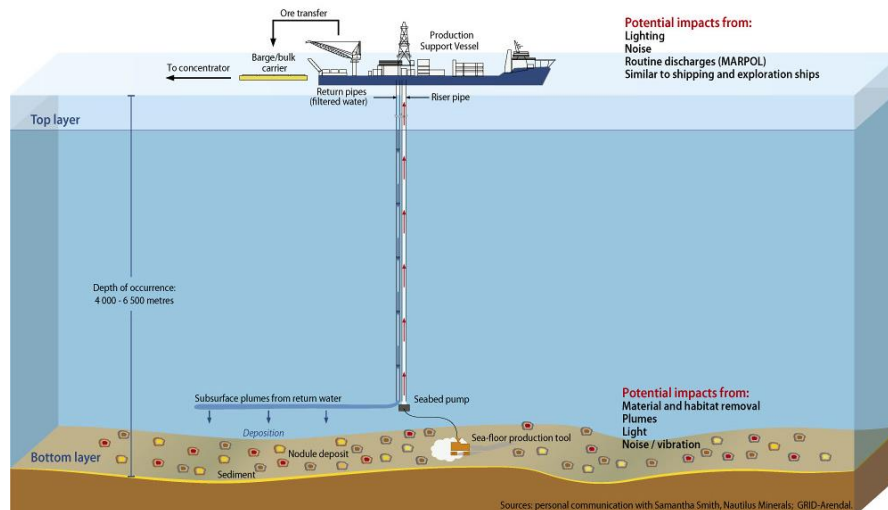


Figure 3: Nodule mining Schematic (Courtesy Grid-Arendal)

The following vessel functions are established:

- Collection: A system which gathers the minerals from the seabed and prepares them for transport to the surface.
- Vertical Transport: A riser system to bring the minerals up through the water column.
- Dewatering: A method to separate the minerals out the seawater
- Storage: A storage solution to store the mined minerals until they can be offloaded
- Offloading: A system to transfer the minerals to a transport vessel.

As the vessel will have to operate in remote areas, independent propulsion and power generation will also be a vessel function.

By examining the weight, volume, and power requirements of each of these subsystems, concepts of a DSM production support vessel can be built up, and a matching power unit can then be selected to achieve a functioning vessel design.

This leads to the following research questions:

Which vessel functions need to be aboard a CCZ DSM production support vessel?

What would a CCZ DSM production support vessel design look like?

What are the required power systems for a CCZ DSM operation and which powerplant concepts are available for independent offshore mining operations?

And the following sub-question:

Which emission regulation can be expected and how can they be met?

2 DSM in the CCZ

Deep sea mining is a relatively novel industry which is currently in its feasibility stage. In this chapter the available background information available about DSM mining in the CCZ relative to this thesis is summed up.

2.1 Location & Environment

The operational area for the production vessel will be the Clarion-Clipperton Zone (CCZ). Which is situated in the Pacific Ocean and is currently the most promising mining zone for nodules with depths ranging between 4000 m and 6000 m (Glover et al., 2016).

The CCZ has been chosen due to its high nodule density at 15 kg/m² together with a relative flat seabed and potato-sized nodules makes it the best mining size currently discovered (by Elaine Baker & Beaudoin, 2013).

The blue nodules research project determined an annual production rate of 2 million tons of nodules per year as a business case. They consider 250 mining days per year with on average 20 hours of activity per day. This results in an hourly production rate of 400 tons nodules per hour (Volkman & Lehnen, 2018). With the nodule abundance of 15 kg/m² in the CCZ, this would result in a mining rate of 9 m²/s and a mined area of 167 km² each year.

The CCZ is subject to El-Nino and the climate is generally not too mild. An environmental study undertaken by Global Sea Mineral Resources gives a good initial look into the conditions at the mining sites. The wave height wind speed, and current velocity over the depth of the water column are all measured.

The wave height probability curve for the Clarion-Clipperton Zone (CCZ) is shown in Figure 4. Which shows that the significant wave height is most likely between 1,5 and 2,5 meters. The wave period for CCZ is between 5 and 8 seconds (GSR, 2018).

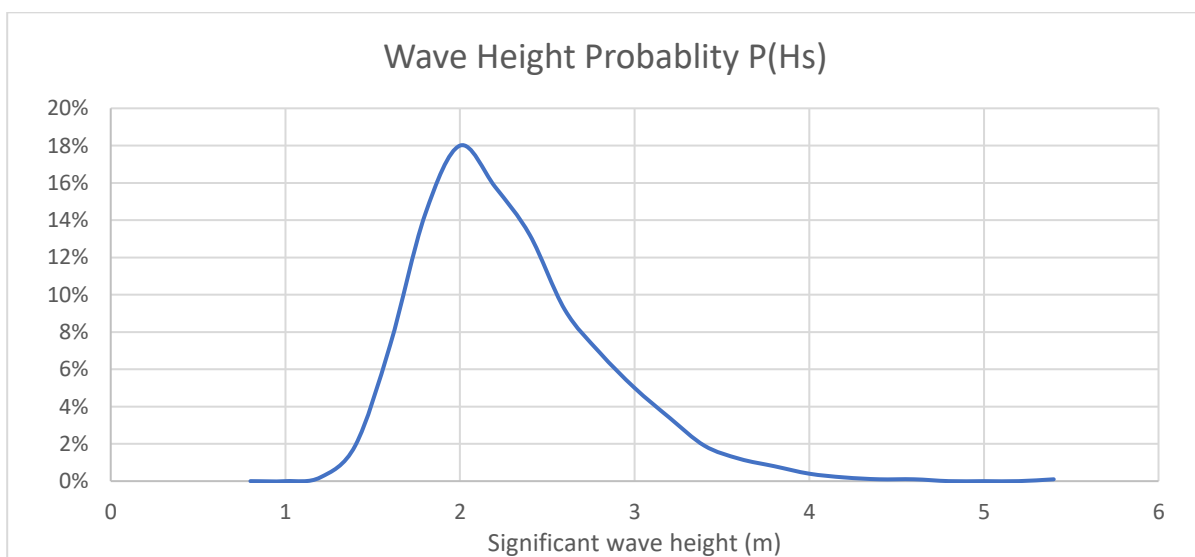


Figure 4: Wave Probability Curve (GSR, 2018)

Defining a design wave height for mining operations is an important design requirement which will influence the vessel's hull, station keeping and operability. The highest waves measured are 5,4 meters and will dictate the survival condition for the vessel.

For the wind speed at the CCZ, the probability curve is shown in Figure 5. The wind speed is shown for each month. Showing the highest wind speeds occur at the end of the year and the conditions are more favorable early in the year and the summer months.

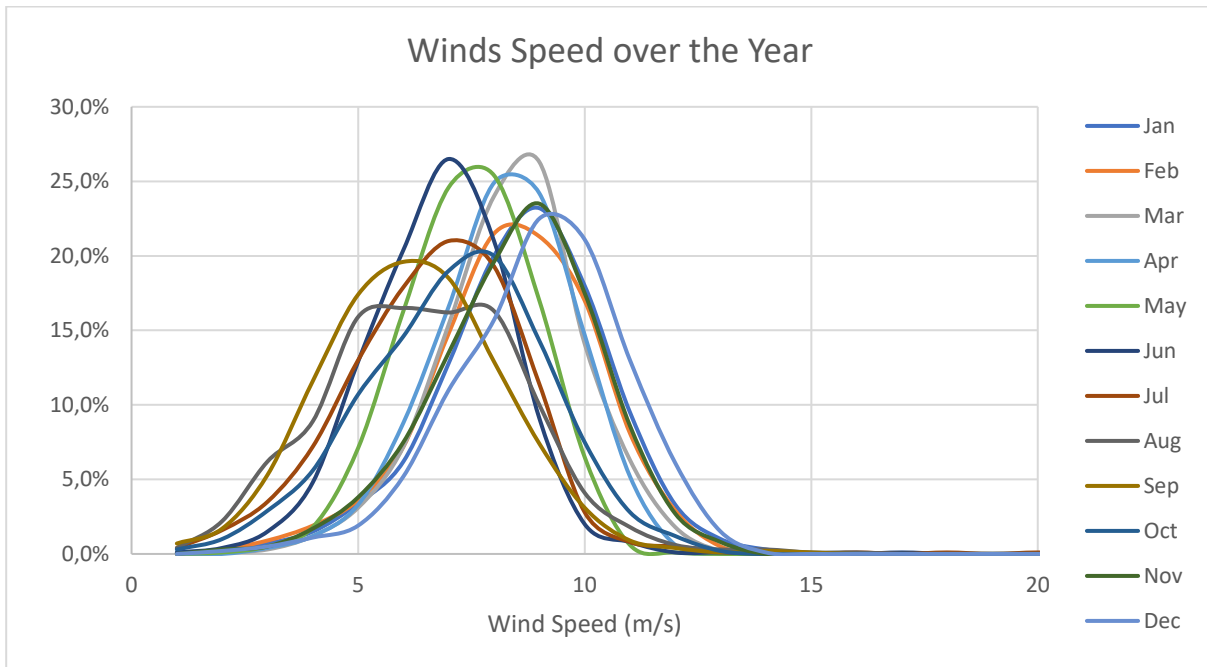


Figure 5: Wind Speed Probability Curve (GSR, 2018)

The maximum measured wind speed is 20 m/s in July. Which shouldn't present any big design restrictions. It will of course still be beneficial to pay some attention to the wind cross area of the vessel to prevent excessive wind forces on the vessel and not induce wind powered yaw moments.

Concerning the current velocities in the CCZ, extensive research has been done over the depth of the water column to analyze riser dynamics and the forces on the collector. For the surface currents, it can be assumed that they generally are around 0,5 m/s (A. Vrij, 2020). With maximums lying around 1,7 m/s (Sun et al., 2018).

2.2 Nodule collector

Full scale production collectors have not been produced yet, but there are some concepts available. Generally, the collectors are expected to be similar to the prototypes that have been trialed the last couple years, but just at a bigger scale.

So, a wider machine with more 1-meter-wide collector heads and larger tracks to accommodate the extra weight. The operating speed for an efficient process is assumed at 0.5 m/s (GSR, 2018). Four set of tracks seem the better solution as this increases the maneuverability of the collector.

The Blue nodules project designed a full-scale machine which has 16 hydraulic collectors of 1 meter wide. Making the machine 16 meters wide and 20 meters long. The vehicle is powered by four tracks and thrusters to prevent pivoting when being deployed. Total power is estimated at 1000 kW (Blue Nodules, 2017). The collector weighs 120 tons in air and has a submerged weight of 20 tons, a basic layout is shown in Figure 6.



Figure 6: Blue Nodules collector (Blue Nodules, 2020)

The Blue Nodules research is based on an annual nodule production of 2 million tons per year. To find the production rate of the collector, the following formula can be used:

$$\text{production rate} = B_{\text{collector}} * v_{\text{collector}} * (\text{nodule abundance}) * \eta_{\text{pick-up}} \quad (1)$$

With the parameters being:

- Width of the collector: adding more collector heads next to each other is the best way to increase production
- Velocity: going faster is better but this reduces the efficiency, as nodules can't be lifted in time before the collector moves further
- Nodule abundance: being in the right area will make all the difference, as so the CCZ is currently favorite at 15 kg/m²

- $\eta_{pick-up}$: the pick-up efficiency of the Coanda-effect collector. This depends on the flow speed through the collector and the collector's speed. Theoretically, 100 % can be achieved. So far pick-up efficiencies are between 87 % and 95 %.

2.3 Vertical Transport System

Once the collector has done its job on the seabed, the loose material has to be transported to the surface. This is a completely new specialization with no existing technology. Looking around at current technologies for inspiration, the riser-system for the oil and gas industry comes to mind and subsea lifting operations with containers.

For some close to shore mining sites, diagonal transport is also considered as a possibility. This would eliminate the need for a production vessel as everything could be done onshore, this concept is visualized in Figure 7 (Maxime Lesage, 2020). While the method does have its advantages it is limited by the horizontal distance between deposit and shore and requires a suitable seabed foundation. So, in this thesis diagonal transport won't be considered due to the remote location of the mining sites.

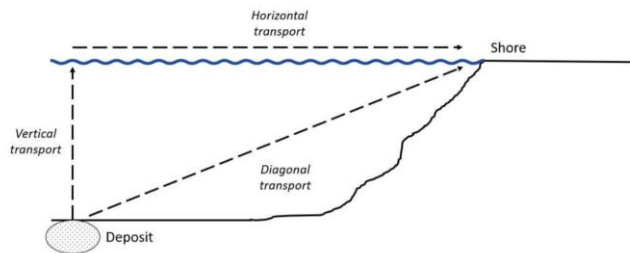
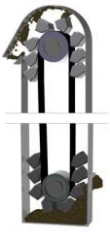


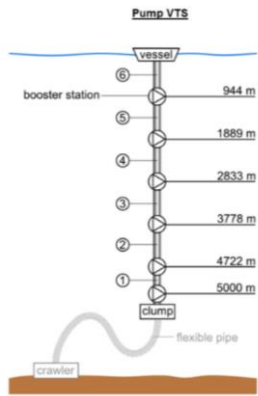
Figure 7: Diagonal transport (courtesy of Maxime Lesange)

Research in this area has led to a various idea's, a summation of Possible solutions is explained in Table 1.

Table 1: Vertical transport idea's

<p>Clamshell grabber</p>  <p>Courtesy Seatools</p>	<p>A giant grab that can pick up the material from the seabed. It's outfitted with thrusters to be able to accurately grab at great depths. It can carry between 10 – 25 m³ in a single grab (Seatools, 2002).</p>
<p>Continuous bucket ladder</p>  <p>Courtesy Feeco International</p>	<p>This process was used for dredging before being replaced by hydraulic systems. This system would be lengthened to achieve the desired depth. The buckets will pick up the material at the bottom and transport it up where it will drop the material as the bucket rotates over the top roller (Tim Matzke, 2021).</p>

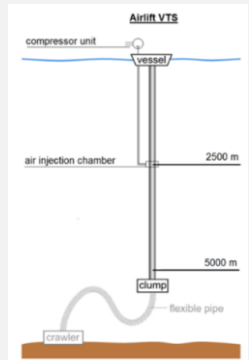
Hydraulic riser



Courtesy Jort van Wijk

the hydraulic riser is an idea based on the oil & gas riser system to bring oil & gas from the seabed to the surface. With the knowledge of dredging this is modified to be able to pump a slurry of mined materials together with water up from the seabed (A. Vrij, 2020; Schulte, 2013a).

Airlift riser



Courtesy Jort van Wijk

Another method using the riser, is to use the upwards force of air bubbles in a (semi-)submerged pipe. By injected air into the riser pipe, a suction-force will be created under the injection point and an upwards force by expanding air. Inserted material at the bottom of the pipe will be “lifted” to the surface (Ma et al., 2017; Schulte, 2013a).

Container hoisting



Courtesy HWFTech

A standardized container can be used to transport material up and down with an AHC crane. The size of the container would depend on the capacity of the crane. For AHC cranes this is up to 1000 tons (MacGregor, 2021).

Container buoyancy lifting



Courtesy Structure-Flex

Containers can also be transported with buoyancy elements. Kind of like a submarine, buoyancy can be added with air to achieve an upwards force to transport the container to the surface.

All these ideas can be useful for a certain task. The clamshell grab is best suited for collecting samples, the container needs very little infrastructure, and the riser can operate continuously.

Taking in mind that the business case for nodule mining would require to mine material at a rate of 400 tons per hour or more, only the riser system remain attractive. Both the hydraulic and airlift riser will be examined.

2.4 Dewatering Process

The nodules will need to be stored onboard before a transport vessel can collect them and transport the nodules to shore. Storing the nodules in a dry state without the slurry water would significantly reduce the required storage and reduce the stability concern of the cargo. This does require the pumped-up slurry to be dewatered into dry nodules and residual water. The efficiency of this process is an important factor in achieving the 2 million ton annually.

2.4.1 Blue nodules proposal

The blue nodules research project suggested to use a three-stage sieving process to dewater the nodules. This would result in a sieving efficiency between 60-98%. A hydro cyclone machine was also considered to filter out smaller nodule parts, this however would also catch the remaining sediment in the water-mix and proved an inefficient process for this case (A. Vrij, 2020; NORI, 2021).

The first sieve's aperture is 10 mm and catches around 38% of the nodules, the second sieve has an aperture of 3 mm and filters out another 49% of the nodules, with the last sieve catching 11% with an aperture of 1 mm (A. Vrij, 2020).

2.4.2 Boskalis Chatham Rise proposal

Boskalis analysis the mining of phosphate nodules at Chatham Rise. This mining location is located between 350 – 450 meters water depth and its proposal utilized modified trailing suction hopper dredgers to mine this site. Aboard the dredger, a dewatering plant would be installed to be able to store the nodules aboard in a dry state. The envisioned dewatering plant is shown in Figure 8.

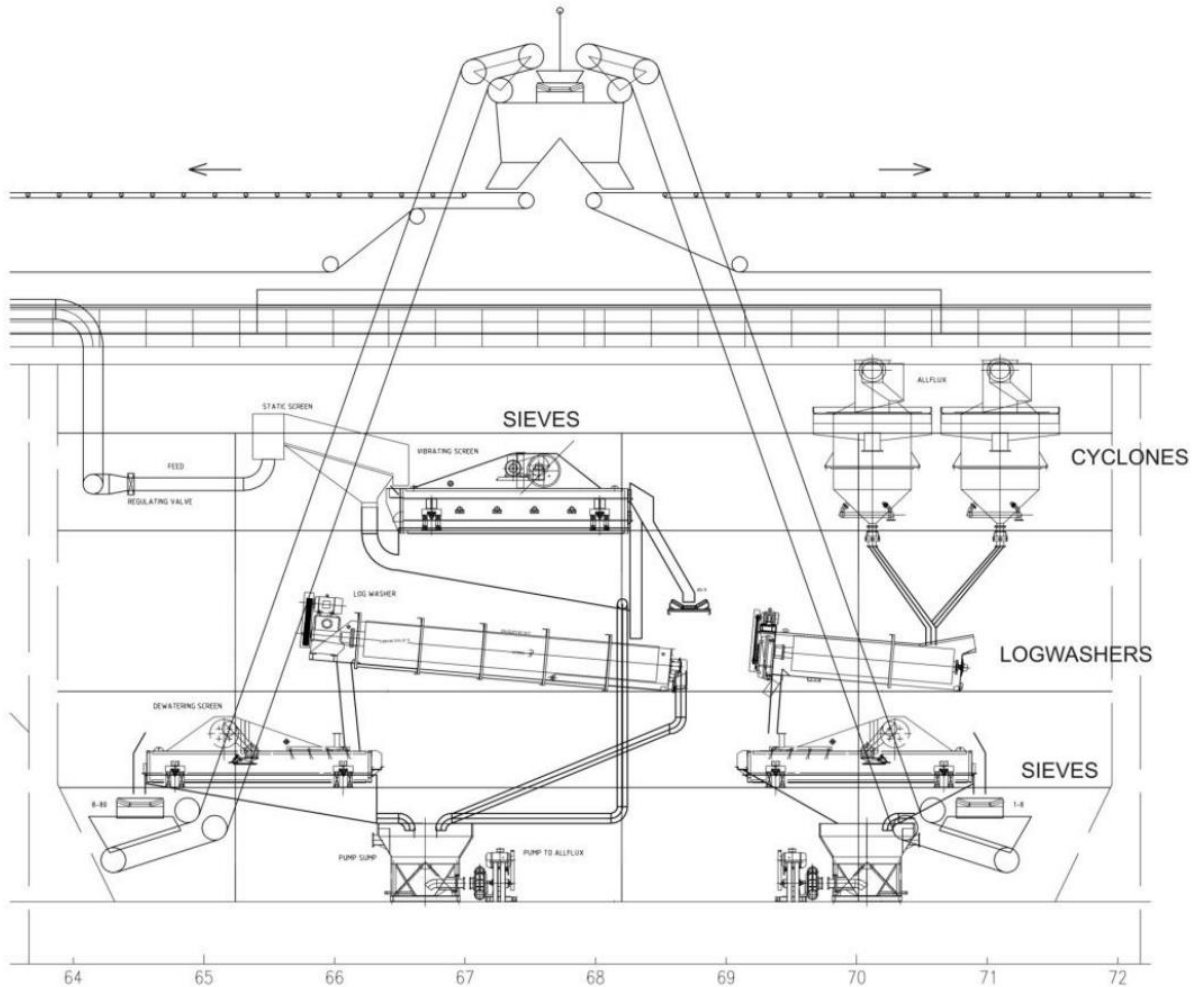


Figure 8: Boskalis Dewatering Plant (Chatham Rock Phosphate Limited, 2014)

The slurry would first be dumped on a dewatering sieve with an 8 mm aperture. After this the remaining water and sediment would be put through a log washer to separate the solids from this water, the solids are then collected by a sieve with a 2 mm aperture. This was found to be a more efficient solution than purely using the sieves.

The water coming out of the logwasher is put through hydrocyclones and then put through a similar setup of logwasher and sieve. This is done to increase the overall efficiency of the system and collect the few solids that aren't collected through the first logwasher process (Chatham Rock Phosphate Limited, 2014).

2.5 Offloading Process

A ship-to-ship transfer method is needed to transport the nodules from the cargo holds to the transport vessel. There are various ideas for this, they can roughly be put into two categories: dry- & wet-offloading.

Wet-offloading means mixing the dry bulk with water to make slurry again which can be pumped to the transport vessel. This does mean another dewatering process is needed once the slurry is pumped to the transport vessel. Dry offloading is transporting the bulk as it is. In this chapter the different solutions will be explained together with the requirements for the bulk carrier for said processes.

2.5.1 Dry Offloading

Worldwide, various self-unloading bulk carriers are in use. They use conveyor belts to unload their holds without needing any port facilities. An example of such a vessel is shown in Figure 9.

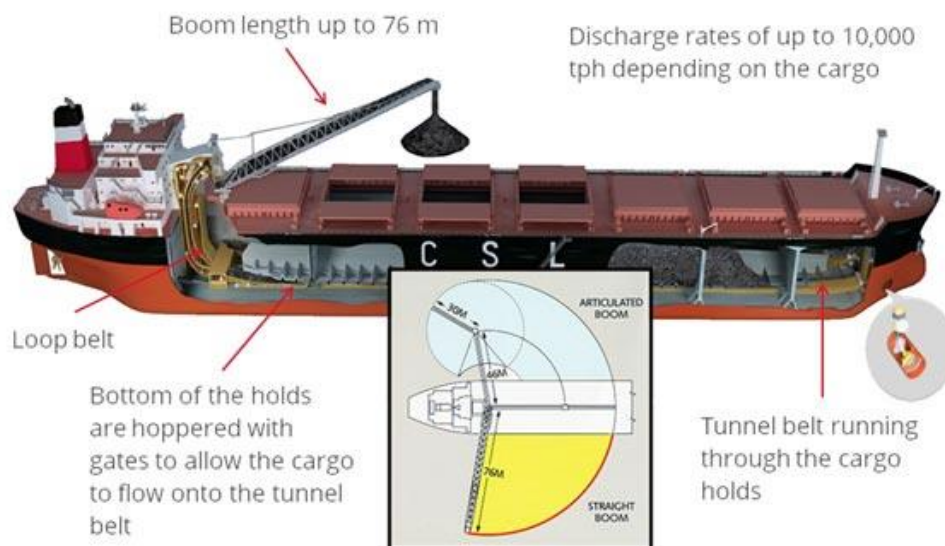


Figure 9: Self Unloading Bulk Carrier (Courtesy of CSL Group)

The vessel is modified with holds that taper inwards to doors on the bottom. Under the doors, a conveyor belt can move material to a central point where it is transported above deck by trapping the material between two conveyor belts. A swinging boom is mounted on deck to dump the material outboards of the vessel. Most of these systems have an unloading rate of 5000 tons per hour, but up to 10,000 tons per hour can be achieved (CSL Group, 2021).

For this method, both vessels need to be side by side. So, the vessels are connected in the same way like with the clamshell grabber. The maximum operating sea conditions for these operations are 2-meter wave height ($H_s = 2 \text{ m}$) during the approach and mooring operations. During the STS transfer, a maximum of 3 meters can be assumed ($H_s = 3 \text{ m}$) (Kristian et al., 2016).

2.5.2 Wet Offloading

Wet offloading is undertaken by connecting the production vessel and bulk carrier with a flexible discharge hose. This method is based on tandem offloading in the oil & gas business and the discharge hose used in dredging.

The first step in this process is to rewater the material by injecting water into the cargo holds. Using a centrifugal pump, the slurry mix can be pumped out of the holds and through the discharge pipe. Such a discharge pipe is flexible hose of roughly 12 meters long and can be up to a meter in diameter (Orientflex, 2021). The pipe can be made floatable, as shown in Figure 10.



Figure 10: Floating Dredge Hose (Courtesy of Orientflex)

2.5.2.1 Tandem offloading

To connect both vessel, tandem offloading used in the O & G industry is a good example. Hereby the two vessels are connected stern to bow by a mooring chain and the flexible hose is suspended or floating in a lazy configuration between both vessels to not induce any vessel forces in the hose. This configuration is shown in Figure 11.

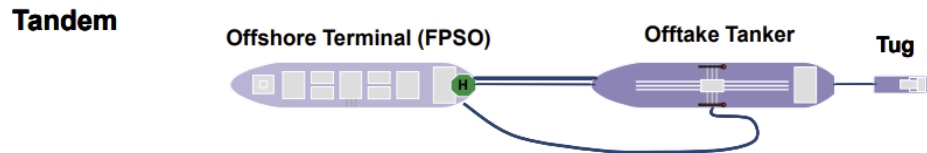


Figure 11: Tandem Offloading (OCIMF, 2018)

This method does require a tug to help the transport vessel to approach and stay in place. The flexible discharge hose can be stored on a reel. An example of a reeled floating discharge hose is shown in Figure 12.



Figure 12: Offloading Reel (Courtesy of Royal IHC)

2.5.2.2 Bow Offloading

Over time various modifications have been made to the tandem offloading method.

Once such innovation, is bow loading. Here the offloading hose is connected to an opening in the bow and the transport vessel is fitted with a Dynamic Positioning (DP) system. This allows for operating in harsh environments and eliminates the need for support vessels like tugs (OCIMF, 2018).

For deep sea mining offloading, a possible dewatering system can be added to the bow modifications.

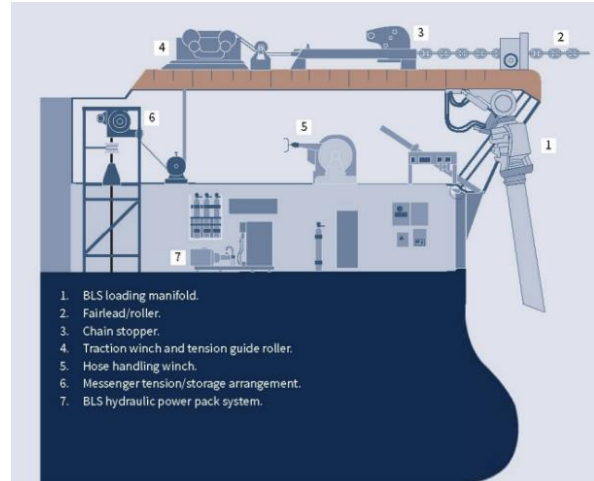


Figure 13: Bow Loading (Courtesy of OCIMF)

With this method, the sea-state thresholds are significantly higher than the other methods and allow approach and mooring operations in waves up to 5,5 meters ($H_s = 5,5 m$). Offloading and disconnect operations can be undertaken in waves of 6 meters ($H_s = 6 m$) (Kristian et al., 2016). This would mean that STS transfer could happen almost all the time in the CCZ, as Figure 4 shows the significant wave height will not exceed 5,4 meters.

2.6 Powerplant

In this thesis, some more complex powerplant options will be discussed as they pose a good solution to the power needs on the vessel. In this part, these plants will be shortly explained to give a general understanding of their working principle and the pros and cons of these plants.

2.6.1 Combined Cycle Gas Plant

Gas turbines are a commonly used in land based powerplant to generate electricity for the grid. They are a reliable source that can burn multiple fuels to generate between 30 and 300 MW's. They are chosen for their reliability and relative low maintenance. The efficiencies are in the order of 35 – 40 % at design condition. The efficiency drops significantly at lower power output, which means gas turbines are mostly used at full power. But they can be turned down, which makes them suitable for controlling the electricity grid.

Using a gas turbine connected to a generator is called a simple cycle powerplant. The hot exhaust gasses of the gas turbine can however be used to generate additional energy and increase the overall efficiency of the powerplant. For this reason, the combined cycle gas plant is commonly found powerplant that uses a heat exchanger to capture the exhaust heat and generate steam to drive a steam turbine to generate additional electricity. Such a configuration is shown in Figure 14. This allows the efficiency of the overall plant to reach 50 – 55 %. While the gas turbine efficiency is very sensitive to the load factor, the heat exchanger and steam turbine can produce a relative constant power output, as the exhaust temperature of the gas turbine remains relatively constant over the power level.

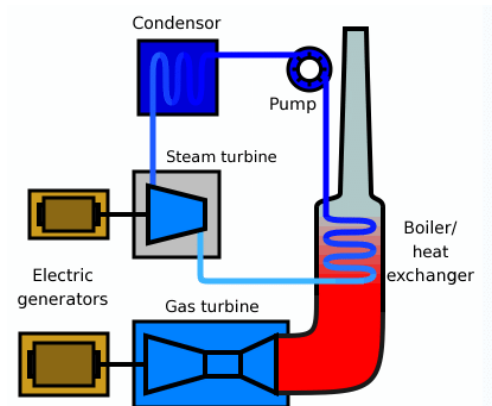


Figure 14: COGES

2.6.2 Small Nuclear Reactors

While nuclear energy has been around for a long time, recently small nuclear reactors or SMR have come more into focus. As, nuclear energy becomes a more understood technology, the technology is getting scaled down to also become a modular solution. With the idea to fit a 30 MWe reactor in a standard forty-foot container (FEU). While this technology is still fresh, it is also being pitched as a zero-emission solution for the maritime sector.

An example of this is the MicroURANUS, which is a custom-made fast neutron spectrum reactor for marine applications. Its small scale allows it to easily fit within a vessel's hull and its thermal capacity of 60 MW makes it about the right scale for application in these kinds of vessels. The reactor vessel and housing are shown in Figure 15.

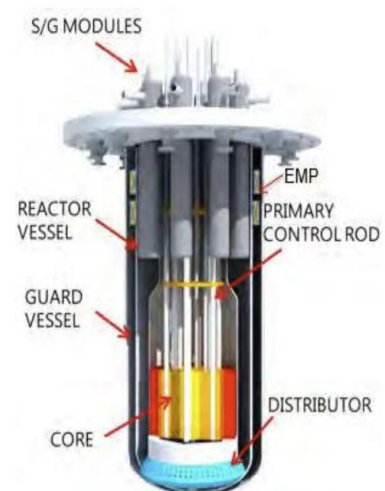


Figure 15: MicroURANUS

While the reactor is primarily protected by the guard vessel, the assembly must be isolated into a containment unit both for radiation and safety considerations. This makes the reactor & containment unit a significant component in weight and size. The main advantage of a nuclear powerplant is however the absence of a fuel tank as the fuel can be stored in the reactor itself and last for its lifetime. The MicroURANUS has a build in steam generator unit to generate the necessary steam to be used in a steam turbine to generate electricity (IAEA, 2020).

A big limitation with nuclear energy is that's its difficult to adjust the load factor, as a nuclear reactor produces a steady rate of heat at its design condition, and this is difficult to reduce. This means that lowering the power output is controlled by removing the excess heat from the reactor, which makes the process inefficient as energy must be put into the process of removing heat. So, it's best to have the powerplant performing between 80 – 100 % load. Conceptually it is believed to be possible to have a reactor put out as low as 20 % load, but it remains unclear how realistic this really is.

2.7 Energy Storage

Just like a land-based energy grid, the electricity grid on a vessel must be balanced at all times so that supply meets demand. This is either achieved by having a powerplant that can easily and efficiently achieve the desired power level or have an energy buffer to handle any peaks.

Energy storage is always a cost-benefit choice as energy storage comes at a price that has to stand in comparison to the running efficiency of the powerplant at certain load factors. Depending on the size and duration of the energy storage, different methods become interesting, Figure 16 shows a number of solutions with this in mind.

Ragone plot

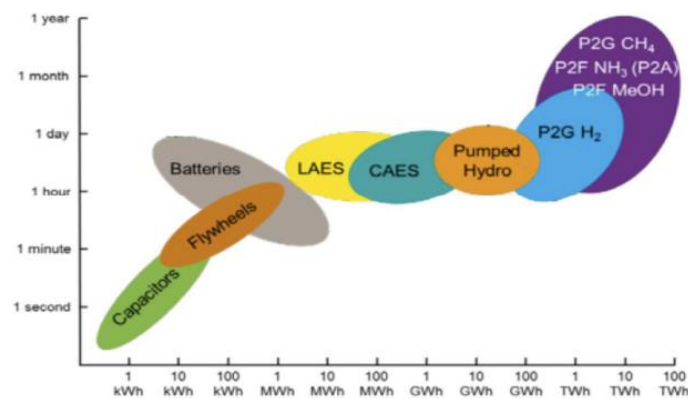


Figure 16: Energy Storage Solutions

In this thesis, flywheels, batteries, and Liquid Air Energy Storage (LAES) will be of consideration.

Flywheels are a small-scale solution where an engine or electric motor must provide varying energy outputs.

Batteries are a well-known solution which store the electric energy directly to ensure a quick capture- and release. They are however relatively expensive and with a high weight, which becomes impractical and expensive above certain power- and endurance levels.

2.8 Regulation

From a regulatory point of view, this chapter explains the exhaust emissions in effect around the world and the specific regulations for a deep-sea mining operation license.

2.8.1 Exhaust emissions

There are a variety of exhaust emissions to be considered, below the currently most contributing ones are listed with their respective legislation.

- CO₂: No regulation except EEDI reference line which is still voluntary and is focusing on transportation of good. So, the emissions are measured in tons of pollutant per ton-mile. The EEDI is calculated as follows:

$$EEDI_{Req} = \frac{1 - X}{100} (a * DWT^{-c}) \left[\frac{g CO_2}{tm} \right] \quad (2)$$

With the factors a and c depending on the vessel type. X is the reduction factor, which will be 30 % from 2030.

The pollutant emission ratio (per) of CO₂ is dependent on the fuel but not the process. So, the only way to reduce the specific pollutant (spe) emission is by increasing the efficiency of the engine. The per values of CO₂ are (IMO, 2018):

$$per_{CO_2} = \begin{cases} MGO = 3\ 206 \\ LFO = 3\ 151 \\ HFO = 3\ 114,4 \\ LPG = 3\ 000 \\ LNG = 2\ 750 \\ Ethanol = 1\ 913 \\ methanol = 1\ 375 \end{cases} \left[\frac{g CO_2}{kg fuel} \right] \quad (3)$$

While regulation on CO₂ is currently not nailed down, the general approach of the IMO is that CO₂ should reduce by 50 % in 2050 compared to the level in 2008 (imo, 2018).

Alternative fuels like ethanol and methanol cause a significant drop in CO₂ but are not considered in this thesis as they are not commonly available and a market for these fuels doesn't exist as it does with HFO, MGO, LNG.

- SO_x: emission control dictates that the Sulphur content in exhaust may not exceed 0,5%. For the EU this is further restricted to 0,1%. The SO_xspe [g/kWh] can be determined relative easily by multiplying the Sulphur content in the fuel by a factor 20 (Fontelle et al., 2019).

$$spe_{SO_x} \leq 2 \frac{g}{kWh} \quad (4)$$

- NO_x emissions are mostly tightly controlled. With the IMO governing a Tier 1,2, and 3 policy which gives a spe reference line based on engine speed. With Tier 3 being the strictest and enforced in specific emission control areas (ECA's). It can be reasonably expected that in the future this Tier 3 will become more the norm than the exception and more areas will fall under its control. The NO_x limit formula goes as follows:

$$spe_{NO_x} \leq \begin{cases} 3.4 & (n_e < 130) \\ 9n_e^{-0.2} & (130 < n_e < 2000) \\ 2 & (2000 < n_e) \end{cases} \left[\frac{g}{kWh} \right] \quad (5)$$

With n_e the engine speed in rpm (Fontelle et al., 2019).

- UHC emissions stands for unburned hydrocarbons. These are emissions related to incomplete combustion inside the engine. The consists of methane and non-methane volatile organic compounds (NMVOC). The methane proportion is generally around 2% of UHC (Fontelle et al., 2019). UHC emissions are significantly lower than the before mentioned emissions and generally improve over time as engine become more efficient. Regulation therefor is pretty much non-existent for UHC.
- CO is another emission related to incomplete combustion, which has no legislation.
- Particulate matter emission or PM for short, consists of several components including but not limited to carbonaceous substances, inorganics salt, organic compounds, and metals. They have a strong impact on air quality, climate change and human health such as cardiopulmonary disease and lung cancer. PM is indirectly regulated through the SO_x and as so has the following limitation (Fontelle et al., 2019):

$$spe_{PM} \leq 2 \frac{g}{kWh} \quad (6)$$

2.8.2 Mining License

Currently the International Seabed Authority (ISA) has granted 19 exploration licenses for nodule locations in international waters (Yue et al., 2021).

2.8.2.1 *Exploration license*

For current testing mission, exploration licenses and a Regional Environmental Management Plan (REMP) are of effect. They don't have emission regulation, but the REMP of the CCZ includes nine Areas of Particular Environment Interest (APEI) in which mining is forbidden (ISA, 2011).

2.8.2.2 *Exploitation license*

The ISA has published a draft of the regulations for exploitation of seabed resources, they do not yet go in depth on specifics, but set out the main goals for the regulations. They aim at preserving the marine environment both on the seabed and in the water column. They also specify the role the sponsoring state that puts in the proposals has, as at their discretion, additional regulations can be added (ISA, 2019). So far, these additional regulations have been in line with current IMO regulations.

A rest product from the dewatering process will off course be the water. This water will still contain elements that can pass through the dewatering process, this means the water will not be clean seawater. As the water comes from the seabed, it will have other properties than seawater at the surface. For this reason, the ISA is considering legislation to make sure the pumped-up seawater is also returned to the place it belongs and minimize environmental impacts from releasing this water at the sea-level. It's yet unclear at which depth the water will need to be returned, current designs suggest a depth of 1200 meters (NORI, 2021).

In the DSM field, the guidelines on underwater noise by the IMO's Marine Environment Protection Committee (MEPC) have been followed as much as possible. They aim to reduce underwater noise to address adverse impacts on marine life. The guidelines specify certain vessel design considerations on the propellers, hull form, and onboard machinery to reduce the vibrations and noise levels (IMO, 2014).

3 Design Requirements

With the knowledge accumulated in the previous chapter, the design requirements for the vessel can be set up. They are displayed in the table below.

Design Requirements			Comments
Yearly production	2 000 000	t/ year	Most feasible scale ¹
Hourly production	400	t/h	¹
Cruise speed	14	knts	
Max. Mining depth	6 000	m	Max depth in CCZ ¹
Collector speed	0,5	m/s	As determined in 2.2 ²
Nodule storage	67 000	t	Storage for 9 days ¹
Offloading rate	4 000	t/h	Offloading in a half day ¹
Hs max. mining	3,4	m	$(P < 3,4 m) = 97 \%$ ²
Hs max. Offloading	3	m	$(P < 3 m) = 92 \%$ ³
Hs max. Survival	5,4	m	$(P < 5,4 m) = 100 \%$ ²
Cruise range	10 000	Nm	Cross every ocean
Mining endurance	30	Days	Bunker after 1 month mining ¹
Nodule density	2500	Kg/m ³	¹
Water density	1025	Kg/m ³	
Return water density	1100	Kg/m ³	Water density after dewatering ¹
Max. Length	400	m	Suezmax
Max. Width	77,5	m	
Max. Depth	20,1	m	
Max. Height	68	m	

The vessel's build year is expected to be around 2030 with an operational lifetime of around 20 years. The build year is determined based on current estimates as to when the industry has matured.

¹ (A. Vrij, 2020)

² (GSR, 2018)

³ (Kristian et al., 2016)

For the various system aboard, the following assumptions are made:

- Nodule collector:
 - Coanda-effect collector
 - > 95 % pick-up efficiency
 - Stored and launched from production vessel
- Vertical transport system:
 - Oil & gas type riser system
 - 4000 – 6000 m water depth
 - Stored and assembled on board
- Dewatering:
 - > 95 % efficiency
 - On board processing
- Nodule storage:
 - Onboard
 - In a dry state

For the vertical transport system (VTS) of the vessel, the hydraulic- and airlift concept will both be examined as mentioned before. This also yields a second sub question for the research:

What are the differences in powerplant and vessel between the hydraulic and airlift riser concept?

3.1 VTS Differences

As discussed in the previous section, the main difference in the operational profile between both VTS concepts is the maintenance downtime. The airlift system has less maintenance occurrences over the year as it is a simpler system with less components. The maintenance occurrences with the airlift system also have a shorter duration, as the systems are easily accessible onboard and don't require the disassembly of the riser system.

As can be seen in Table 2, this leads to more days a year spend mining. In total it is assumed that 15 more mining days are achievable with the airlift system. This will increase the amount of collected nodules per year, and as such an increase in revenues. This is displayed in Table 2. The sales value of the nodules is taken \$ 649 per ton, which is an average estimate based on 2017 numbers (Volkman et al., 2018)

Table 2: VTS mining effects

	Hydraulic VTS	Airlift VTS
Mining days	233 days	248 days
Nodules	2,24 mil. Tons	2,38 mil. Tons
Revenue	\$ 1 452 mil.	\$ 1 545 mil.

So, the 6 % more mining days a year yields an increase in revenue of \$ 97 million.

3.2 Vessel Size

The maximum dimensions of the vessel are based on the Suezmax threshold. A big motivator for this is the maintenance of the vessel which will have to be undertaken in a drydock from time to time. With very few drydocks larger than Suezmax existing in the world, Suezmax is chosen as a maximum to ensure there are drydocks available for the vessel around the world.

3.3 Emission

For the emission regulations, the most stringent current regulations are taken as design requirements. This is to ensure the vessel will meet any future emissions regulations, as it is assumed that mining licenses could come with these emissions regulations and that mining sites could become ECA's. This is summarized in Table 2.

Table 3: Exhaust Emissions design requirements

Emission	Threshold	Notes
CO ₂	-	Aim for 50 % reduction from 2008
SO _x	2 g/kWh	Fuel sulfur content < 0,1 %
NO _x	2,5 – 2,8 g/kWh	390 < rpm < 600
UHC	-	Better fuel efficiency
CO	-	-
Particle Emission	2 g/kWh	Indirectly by SO _x limit

This thesis will also examine to which extent a zero-emission scenario is feasible and how this can be achieved with the required endurance of 30 days of offshore mining. The endurance of 30 days is chosen to allow for long offshore independent operations as well as being able to have a reserve in case of storms, when the vessel must survive at sea for some time. With the CCZ being a very remote area with long lead times of over a week to get supplies to, this means the vessel needs the flexibility to overcome any setbacks and continue independent operations.

3.4 Dynamic Position System

When the production vessel is mining at the mining site, it will have to keep station above the collector to ensure the riser and jumper hose stay in the vicinity of the collector. Due to the water depth of 4000 – 6000 meters and the continuously moving operation, a mooring system is unfeasible, and a Dynamic Positioning (DP) system will be required. There are three kinds of DP configuration, listed in Table 3.

Table 4: DP Configurations

DPS-1 (Non-redundant)	Automatic and manual position and heading control under specified maximum environmental conditions.
DPS-2 (Master/slave redundancy)	Automatic and manual position and heading control under specified maximum environmental conditions, during and following any single fault excluding loss of a compartment. (Two independent computer systems).

DPS-3 (Modular redundancy & Majority voting)	Automatic and manual position and heading control under specified maximum environmental conditions, during and following any single fault including loss of a compartment due to fire or flood. (At least two independent computer systems with a separate back-up system separated by A60 class division).
---	---

DP-2 is mandatory in these kinds of operations due to the involvement of personnel and the added potential hazards this imposes. The main design choice will as so be between a DP-2 and DP-3 configuration. Hereby the big difference is that DP-3 requires two engine rooms separated by a watertight wall, to ensure operability in the case of a floated engine room.

In case of total loss of power whereby the DP system would fail, an emergency scenario needs to be thought out to keep the vessel and personnel out of any harm. A possible solution could be:

- Jumper hose emergency disconnect @ collector
- Collector umbilical emergency disconnect with buoy for recovery

With this emergency concept, a DP-2 configuration would sufficient, as no dangerous situation with potential hazards for personnel or environment are created. With this in mind, DP-2 will be chosen as the base scenario for the vessel design.

For the offloading, two vessels will be within the 500-meter safety zone of each-other. This will require a risk assessment to determine if one or both vessels will need to be fitted with a DP-3 system. But this is out of the scope of this thesis. If a powerplant can be configured into a DP-3 system, this will be mentioned.

3.5 Sea-states

The sea-states for the different operating modes displayed in Table 32 are based on the design criteria of the vessel. With mining to continue up to significant wave height of 3,4 meters. The values for each sea-state are shown in Table 4.

Table 5: Sea-States

Sea-state	Wave-Height (H_s)		Wind speed (v_w)		Current (v_c)
	Lower	Upper	Lower	Upper	
Mild (71 %)	0 m	2,4 m	0 m/s	9 m/s	0,431 m/s
High (26 %)	2,4 m	3,4 m	9 m/s	11 m/s	0,5 m/s
Extreme (3 %)	3,4 m	5,4 m	11 m/s	20 m/s	1,5 m/s

For the maximum mining condition, a wave height of 3,4 meters is chosen. This would ensure that there is a 97 % probability that mining can happen. This wave height is also similar to drillships, which can operate in wave heights of 3 – 3,2 meters (van der Stoep & Peters, 1997). To match the probability of 97 % chosen for the waves, the wind design condition for mining is taken at 11 m/s.

4 Vessel blocks

Building on the knowledge collected in the previous chapters, the production support vessel can be split into various design blocks which can be designed separately with their own power needs, mass, and volume. By building these blocks up individually, they can later be placed together based on their function, mass, and volume to achieve a suitable ship design which can offer good functionality and mass distribution.

For each block, an energy flow diagram is created and can be found in Appendix E – Energy Flow Diagram

4.1 Accommodation

The accommodation block is assumed to be of the same scale as current design of drillships. This is done for the sake of simplicity and the simple fact that there is a lack of knowledge on the personnel needs of the operations.

This design consists of 9 decks in total, with 4 of those located in the hull itself and the remaining 5 making up the deckhouse. This configuration offer room for between 200 – 230 personnel (Maersk Drilling, 2021). The deckhouse is shown in Figure 17.

The properties of the deckhouse are shown in Table 5. The weight of the deckhouse is estimated based on system-based ship design (Kai Levander, 2012).

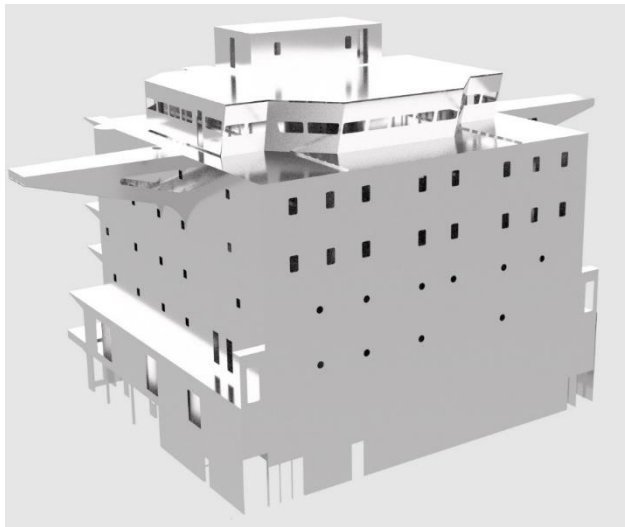


Figure 17: Deckhouse

$$W_{ss} = 0.09 * L * B * H = 1258.56 \text{ t} \quad (7)$$

Table 6: Deckhouse Properties

Dimensions	Weight	Deckspace	Power
23m x 32m x 19m	≈ 1300 t	736 m ²	3 000 kW

For the envisioned endurance of 30 days, the freshwater tank can be calculated.

$$\left\{ \begin{array}{l} V_{water} = 0,25 \frac{m^3}{man * day} * 230 \text{ man} * 30 \text{ days} = 1725 \text{ m}^3 \\ W_{water} = 1725 \text{ t} \end{array} \right. \quad (8)$$

4.2 Collector

The production support vessel will carry two collectors aboard. One for the mining operation and one spare to minimize any possible maintenance downtime on the collector vehicles.

This configuration is chosen, as launching the collector through the moonpool is determined unfeasible. Due to the abundance of machinery needed around the moonpool and the two pipes traveling through the moonpool, there is not enough space left over to launch any sized collector. The moonpool and its associated machinery will be discussed in detail in 4.3.5. This means that the collector will be lowered over-stern or over-board.

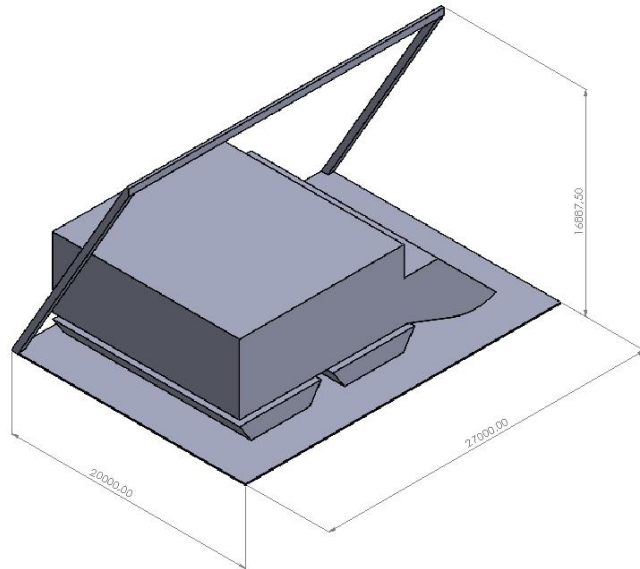


Figure 18: Collector LARS

The collector launch and recovery (LARS) platform with the collector is visualized in Figure 18. The collector is launched with an A-Frame, which is outfitted with a snubber to guide the collector through the splash-zone.

Once the collector is below the splash-zone, the snubber disconnects, and it's lowered to the seabed by its umbilical. The umbilical is stored on an active heave compensated (AHC) winch, to ensure a smooth touchdown on the seabed. The properties of the LARS and collector are displayed in Table 6 (A. Vrij, 2020; Hydralift, 1997; NORI, 2021; Palfinger Marin, 2021).

Table 7: Collector Properties (Blue Nodules, 2017; Hydralift, 1997)

	Dry Weight	Submerged Weight	Deck space	Power
A-frame	195 t			300 kW (Hydraulic)
Collector	120 t	24 t	352 m ² (22m x 16 m)	1 000 kW
AHC-Winch	≈ 10 t			1 000 kW
	≈ 325 t (COG _z = 4 m)	Overboard: COG _y = 14m	540 m ² (27m x 20m)	

When the A-frame is deployed with the collector, it will be positioned 14 meters overboard. The center of gravity will shift 24 meters from the stationary resting point.

The three components all need their power at different times, meaning that only 1000 kW is required.

The collector is lowered at 0,5 m/s and the whole deployment last around 3 hours.

4.3 Vertical Transport

Once the collector vehicle has done its job in collecting the nodules from the seabed, they need to be transported to the surface. This is achieved by a riser built out of joints that is vertically suspended from the vessel. Having a suspended riser allows the vessel to move around freely, this way the vessel can be put in "DP – follow target" mode and follow the path of the collector at the seabed.

The mining area on which this thesis is focused, the CCZ, is between 5 000 and 6 000 meters deep. So, this means a riser is needed of the roughly the same depth to make the mining operation possible. The riser will hang around 100 meters above the seabed to allow the collector to move around freely without the riser being in the way. A flexible hose will be required to connect riser and collector together.

In this section two different options of vertical transport will be explained. In the collector the nodules will be mixed with seawater to create a slurry which consists of 12 % nodules and 88 % water on a weight basis. The first option will be to transport the slurry through the riser by using a series of centrifugal pumps which increase the pressure in stages to achieve the necessary pump head to overcome the pressure in the pipe. The second option makes use of the airlift-principle. Where compressed air is injected into the pipe to create an upwards three-phase flow.

Next to the riser pipe, a return pipe will also be required to return water from the slurry back to the layer of seawater where it was retrieved from. The legislation about this is still being drawn up, but for this thesis it will be assumed that the requirements will be to deposit the water back to the seabed. This way the vessel will be capable to adhere to the stringent regulations.

For the return pipe, a flexible pipe is chosen. This significantly reduced the weight and volume of the stored pipe. The flexible pipe can be mounted on the fixed riser to keep it in place.

4.3.1 Riser storage (Shaffer / Schlumberger)

For the vertical transport a riser will be assembled, either with an airlift or hydraulic solution. The riser is an assembly of 22,9-meter-long riser joints with an inner diameter of 49,5 cm (19,5 inch) (NOV, 2018). The riser joints have buoyancy elements fitted around them as visualized in Figure 19. These buoyancy elements reduce the submerged weight of the riser assembly to reduce the top tension load on the vessel. With the increase of the hydrostatic force over the depth, the buoyancy elements are adjusted for compression.

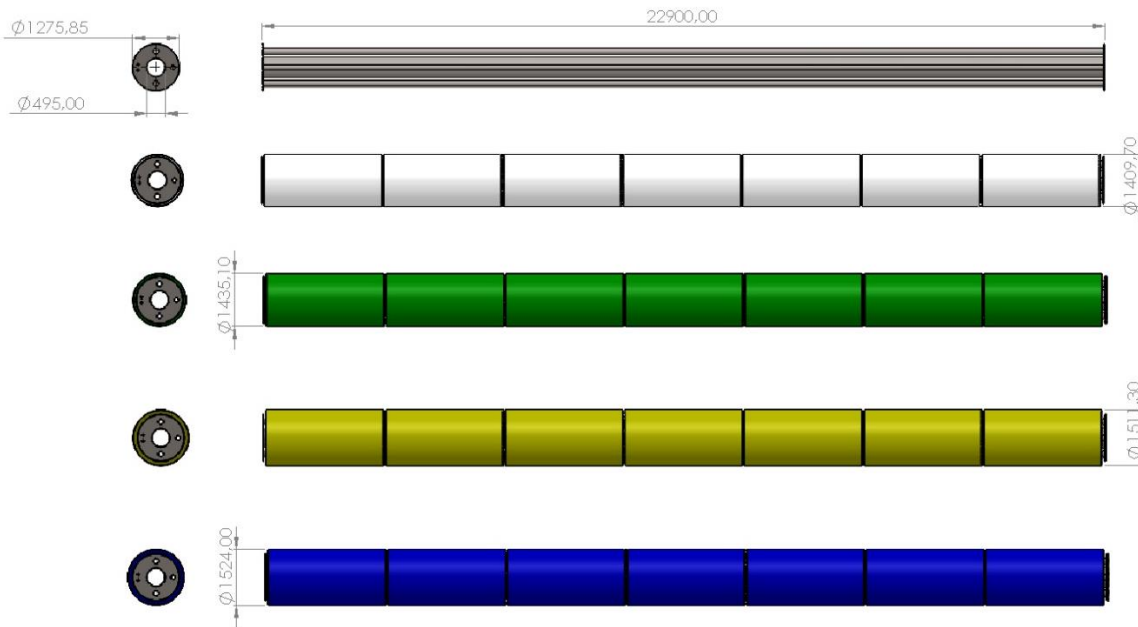


Figure 19: Riser Joints

Figure 19 shows the bare riser joint above with four joints with different buoyancy elements strapped to them. To assemble a 6000-meter riser pipe, the required joints with buoyancy are displayed in Table 7 (Brekke et al., 2005).

Table 8: Riser Joints Assembly

Depth	# Joints	Dim.	Dry weight	Submerged weight
Type 1 0 – 1000 m	44x Riser	Ø 1,41 m 22,9 m	26 t	0,546 t
Type 2 1000 – 1500 m	21x Riser	Ø 1,44 m 22,9 m	27,3 t	0,355 t
Type 3 1500 – 2300 m	35x Riser	Ø 1,51 m 22,9 m	30,3 t	0,636 t
Type 4 2300 – 5000 m	162x Riser	Ø 1,52 m 22,9 m	32 t	3,168 t
Total	262		7962 t	567 t

The disassembled joints are stored on deck close to the derrick tower. Due to the varying diameters of the buoyancy elements and the assembly order, the joints are stored based on this. A riser joint rack is created that can store 36 joints with type 1 or 2 buoyancy elements or 32 joints with type 3 or 4. This is displayed in Figure 20.

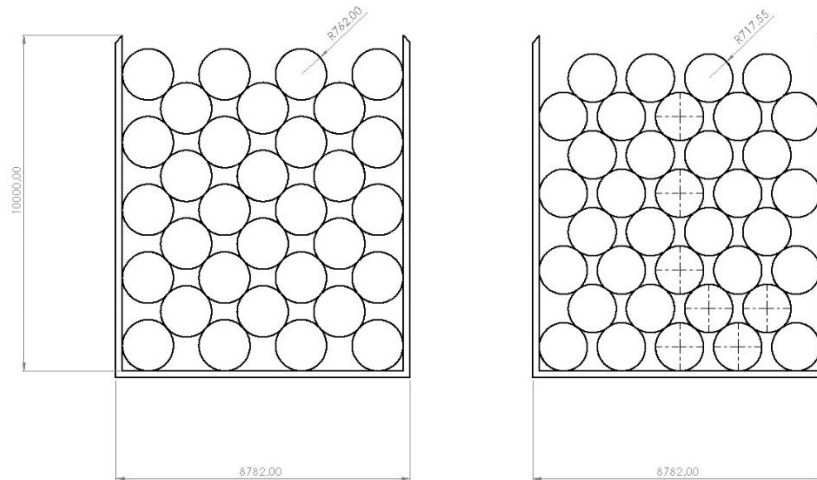


Figure 20: Rack Cross-section

Now to arrange the 271 joints over eight racks, a distribution is made in Table 8.

Table 9: Joints rack distribution

	Rack 1	Rack 2	Rack 3	Rack 4	Rack 5	Rack 6	Rack 7	Rack 8
Type 1 0 – 1000 m	36x	8x						
Type 2 1000 – 1500 m		21x						
Type 3 1500 – 2300 m			32x	3x				
Type 4 2300 – 5000 m		5x		29x	32x	32x	32x	32x
Rack Weight	≈ 15 t							
Joints weight	936 t	1022 t	970 t	1019 t	1024 t			
Total Weight	951 t	1037 t	985 t	1034 t	1039 t			
Rack Dim.	L = 25 m, B = 8,78 m, H = 10 m							
Deck Area	220 m ²							
Deck load	≈ 20 t/m ²							

To transport the joints between the storage area and the derrick tower for assembly. A gantry crane is used to pick the joints from the racks and place them on a catwalk shuttle that moves the joint to the derrick tower. Based on the configuration seen in drillships, four racks can be put side by side with the catwalk shuttle in the middle and the gantry crane moving overhead. This assembly is depicted in Figure 21.

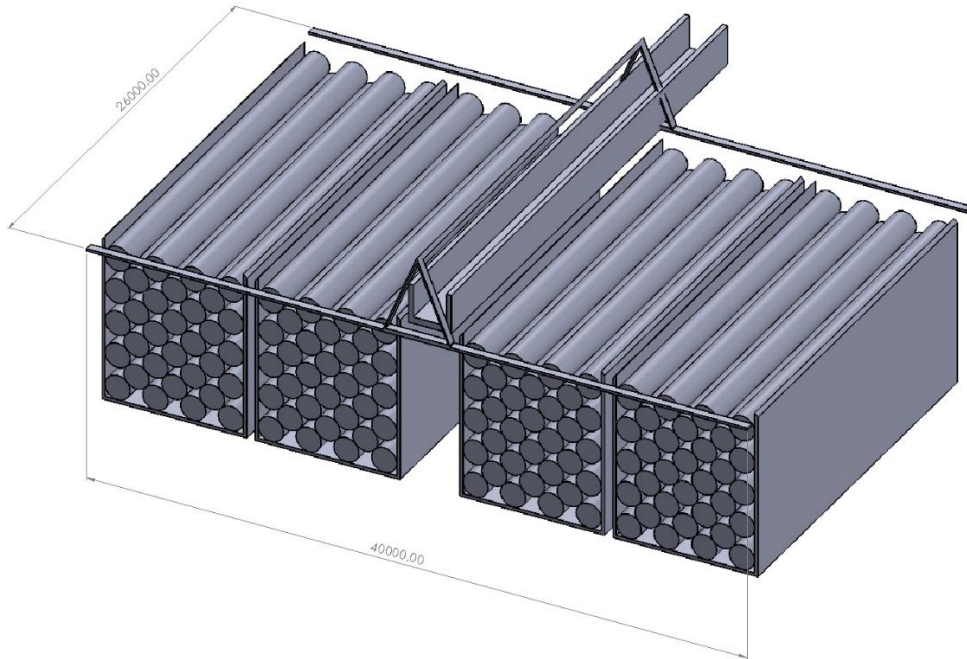


Figure 21: Joint storage assembly

With the required eight racks, that means that two of these assemblies will be able to store all the required riser joints. The properties of this assembly are shown in Table 9.

Table 10: Joint Storage dim.

	Lightweight	Deadweight	Deck space	Power
Racks	15 t	951 – 1039 t	220 m ²	
Gantry Crane	100 t	100 – 140 t	40 m ²	100 kW
Catwalk shuttle	40 t	40 – 80 t	85 m ²	75 kW (Hydraulic)
Total	200 t (COG_z = 11 m)	≈ 4300 t (COG_z = 5,2 m)	1040 m² (26m x 40m) (H = 15 m)	175 kW

4.3.2 Hydraulic Transport

For hydraulic transport, a total of six booster station needs to be fitted into the riser. A booster station consists of two centrifugal slurry pumps. A Modified joint with the integrated pumps is displayed in Figure 22. The booster stations are 15 meters long. This means that four less joints are needed in the riser assembly. The electrical power supply for the pumps can be rooted through the auxiliary lines integrated in the joints. The properties for a booster station are displayed in Table 10 (A. Vrij, 2020; WARMAN, 2009).



Figure 22: Booster Station

Table 11: Booster station dim.

Dim.	Dry Weight	Submerged Weight	Deck Space	Power
15 m Ø 2,5 m	56 t	≈ 52 t	45 m ² (15m x 3m)	1 200 kW (2x 600 kW)

In total, the six booster stations require 7,2 MW of power. Due to their asymmetrical design, they need to be stored separately. They should be stored relatively close to the derrick tower, so that an on-deck crane can transport the booster stations for the storage area to the derrick tower.

4.3.3 Airlift Transport

For airlift, the riser modifications are minimal. A joint need to be modified to have an injection point into the pipe and an airline can be integrated into one of the auxiliary lines on the riser joints. This means that this specific riser joint has the same properties as the other riser joints and can also be stored in the racks.

A compressor is however needed on deck to compress the ambient air to 250 bars, so that it can be injected up to a water depth of 2500 meter, or roughly halfway on the riser.

To achieve a stable system, a volumetric gas flux rate of 5 m/s is needed (Schulte, 2013b). For the given riser system with an inner diameter of 49,5 cm (19,5 inch), the volumetric flow can be calculated using the following formula:

$$Q_{G,atm} = J_{G,atm} * A_{pipe} = 5 \frac{m}{s} * 0,193 m^2 = 0,96 \frac{m^3}{s} = 3468 \frac{m^3}{h} \quad (9)$$

A barrel type centrifugal compressor is chosen. This compressor is suitable for compressing atmospheric air and is used in similar concepts as Compressed Air Energy Storage (CAES). The barrel also allows the high pressure and flow rate needed in this application.

The MAN RB-C35 is such a compressor that can achieve a flow up to 6000 Am³/h with a 0,9 m diameter barrel with a length of 1,6 m (MAN Diesel & Turbo, 2022).

The compressor assembly is shown in Figure 23, and consists of the barrel compressor with its auxiliary systems and can be driven by an electric motor, gas turbine or steam turbine.

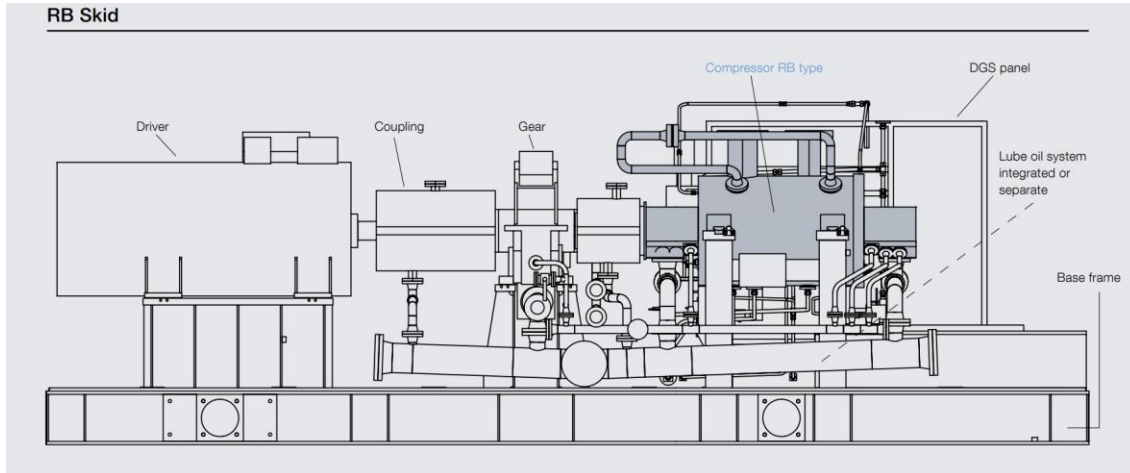


Figure 23: MAN RB-C35 Skid

The properties of the compressor assembly are shown in Table 11.

Table 12: MAN RB-C35 Properties

Dim.	Weight	Deck Space	Power	speed
10m x 4m x 4m	100 t	40 m ²	30 MW $\left(6000 \frac{Am^3}{h} @160 bar\right)$	< 20 000 rpm ⁴

When the compressor is running at the required 3468 m³/h at 250 bar, it is assumed it requires 22,5 MW of power.

4.3.4 Return pipe

In the dewatering process, the slurry flow of 1333,33 m³/h is split into 160 m³/h of nodules and 1173,33 m³/h of residual water. This water must be returned underwater to a depth specified by current regulations. The regulations are not yet put in stone, and it can be assumed that it will be anywhere between 1 200 meters and 6 000 meters.

As these regulations are yet unsure and can change depending on mining site. It will be assumed that the requirement is “back to the seabed”. So, the return riser has to be able to extent the full 6 000 meters. This will make the vessel future-proof for any stricter future regulations and the vessel can still be outfitted with the minimal 1 200-meter return pipe.

⁴ (Baker Hughes, 2022)

The density of the return water can be assumed at $1\,100\text{ kg/m}^3$ (A. Vrij, 2020) with a flow of $0,33\text{ m}^3/\text{s}$. The aim is to let gravity do the work of returning this water back to the seabed. A pipe diameter will have to be chosen to allow for the gravity on the return water to overcome the pipe friction loss. The gravity pressure on the return water is:

$$p_g = (\rho - \rho_{sw})gH \quad (10)$$

The friction pressure loss in the pipe is:

$$\Delta p_{loss,tur} = \frac{1}{2}\rho\lambda\frac{L}{D}v^2 \quad (11)$$

With the pipe friction factor:

$$\lambda = \left(-1.8 * \log \left[\frac{6.9}{Re} + \left(\frac{Ro}{3.7} \right)^{1.11} \right] \right)^{-2} \quad (12)$$

The flow in the pipe will be turbulent, so the pipe friction factor will be dominated by the pipe roughness factor (Ro), which depends on the pipe diameter and the wall roughness ($k = 0,025$). For a gravity flow to exist within the pipe, the following needs to be true:

$$p_g = \Delta p_{loss,tur} \quad (13)$$

A pipe diameter of 12 inch (305 mm) is chosen, which leads to a flow speed of 4,67 m/s in the pipe, and gives the required equilibrium:

$$p_g = \Delta p_{loss,tur} \quad (14)$$

The flexible pipe characteristics are shown in Table 12.

Due to the flexibility of the pipe, it can be stored on a carousel with a minimum radius of 5 meters to adhere to the maximum mending radius (MBR). The carousel is shown in Figure 24, with its characteristics displayed in Table 13 (Drammen Offshore Leasing, 2022).

Table 13: Return Pipe Characteristics

Flexible Pipe	
ID	12 inch (305 mm)
OD	17 inch (432 mm)
MBR	5 m
Dry weight	190 kg/m (1 140 t)
Wet weight	117 kg/m (704 t)

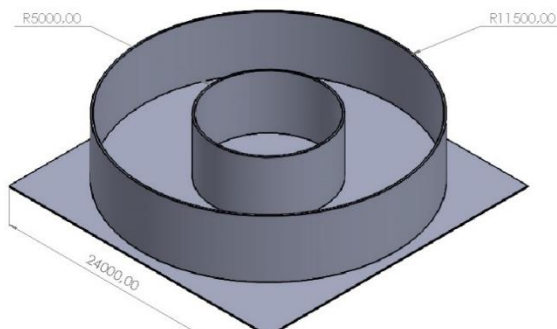


Figure 24: Carousel

Table 14: Carousel Characteristics

Carousel	
Dim.	24 m x 24 m x 6 m
ID	10 m
OD	23 m
Dry weight	350 t
Deadweight	1 490 t
Power	2x 86 kW
Max. speed	1 884 m/h

4.3.5 Assembly Tower

An assembly tower houses all the equipment needed to assemble and disassemble the riser-joints and the return pipe. The tower is situated between both holes through which the pipes travel. This design requires a moonpool of 25,6 m by 12,5 m. The tower on top of the moonpool cut-out is shown in Figure 25. The “drill floor” is situated 8 meters above the deck to be level with the catwalk shuttle, as discussed in 0. This also allows working in the moonpool to fit the riser end and auxiliary lines.

The tower itself will be 40 meter high, as this is enough to vertically assemble to 22,9 m joint. The reel-lay wheel is mounted above to allow for the MBR of 5 meters.

The tower will have a footprint of 27 meters by 20 meters.

The power components needed to assemble and disassemble the riser with the tower are listed in Table 14.

The riser dynamics, when the riser is fully deployed with the return pipe, will not be analysis in this thesis, as it falls outside the scope. So, it will be assumed that the dynamics are within check and that the riser tensioner will be able to dampen the forces to within acceptable limits at higher sea-states.

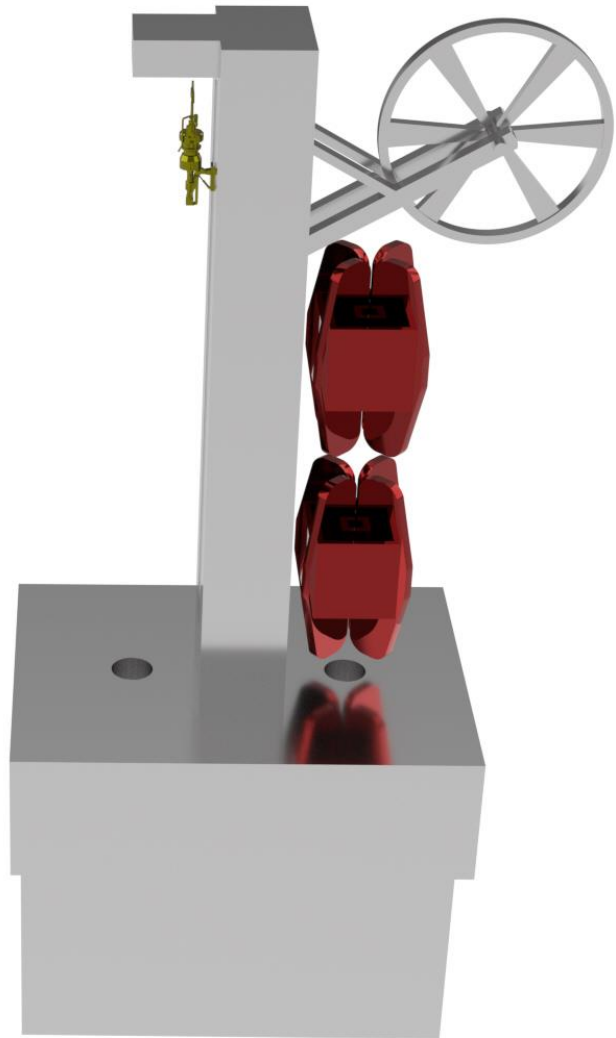


Figure 25: Assembly Tower

Table 15: Tower Components

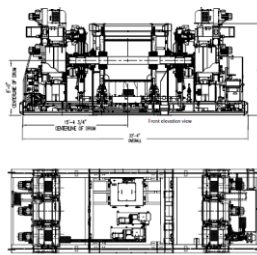
Top Drive



The top drive moves along a set of rails up and down to pick-up the joints from the catwalk shuttle and raise them vertically. After a new joint is connected, the top drive lowers the riser, so that a new joint can be attached. This means the top drive needs to be able to carry the weight of the entire submerged riser.

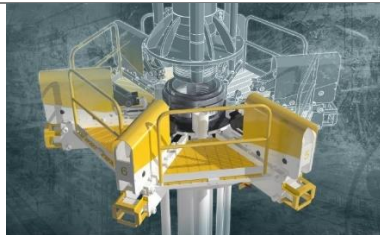
Drawworks

AHD-1000



The drawworks are a set of winches that connect to the top drive. They are positioned on the drillfloor outside the derrick. The drawworks can be modified to active heave compensating winches to smoothen the tension loads in the riser during higher sea states.

Riser Spider

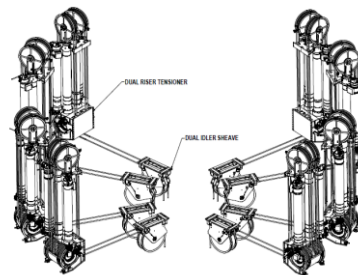


@ KYU Design

The spider is a machine for connected the riser joints together. the spider holds the assembled riser in place and connects or disconnects the joint. The spider is integrated in the drillfloor and is operated hydraulically.

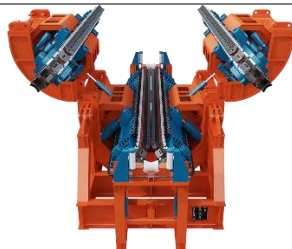
Riser Tensioner

Wireline Riser Tensioner (WRT)



A riser tensioner system is an AHC system to hold the riser in place once fully assembled. The wire tensioners are operated by pneumatic cylinders that damp out the vessel's heave motion.

Flex-lay track Tensioner



@ MDL

To lower and rise the flexible return pipe a track tensioner is used. 4 tracks positioned diagonally grip the pipe under a constant pressure to keep it in place. By moving the tracks, the pipe can be lowered or risen.

Top Wheel	 <p data-bbox="560 312 699 342">@ Huisman</p>	A wheel drive is mounted on the top of the tower to guide the flexible return pipe vertically through the tower. The pipe can be guided from a carousel to the wheel.
A&R Winch	 <p data-bbox="544 556 711 588">@ MacGregor</p>	An Abandonment and recovery winch is placed on deck to connect to the end of the flexible return pipe. The A&R winch is used to lower and rise the pipe through the assembly tower without needing the tensioners.

Table 16: Tower Load Scenarios

	Weight	Max. Load	Power
Hydraulic Riser = 900 t			
Top Drive	18,14 t	910 t	860 kW
Drawworks	94,18 t	907 t	5 200 kW
Spider	≈ 15 t	1000 t	100 kW <i>(Hydraulic)</i>
Tensioner	≈ 100 t	1008 t	1 000 kW <i>(Pneumatic)</i>
Airlift Riser = 600 t			
Top Drive	18,14 t	910 t	860 kW
Drawworks	90,92 t	680 t	4 300 kW
Spider	≈ 15 t	1000 t	100 kW <i>(Hydraulic)</i>
Tensioner	≈ 100 t	720 t	600 kW <i>(Pneumatic)</i>
Return Pipe = 704 t			
Tensioner (2x)	290 t	400 t	1 500 kW
A&R Winch	150 t	650 t (dynamic)	2 660 kW
Drive Wheel	≈ 15 t		130 kW

The weight of the hydraulic riser is significantly heavier due to the added booster stations. This causes a significant increase in the power required to assemble the riser. Table 16 shows the weight and power of the complete dual-derrick tower with all the necessary systems. A breakdown of this power balance can be found in Appendix A – Riser Assembly Power Breakdown.

Table 17: Derrick Tower Properties

	Lightweight	Lightweight + Suspended Riser's	Deck Space	Power
Hydraulic	1 500 t (COG _z = 19 m)	3 200 t (COG _z = 13 m)	540 m ² (27 m x 20 m)	14 142 kW
Airlift	1 500 t (COG _z = 19 m)	2 900 t (COG _z = 13,7 m)	540 m ² (27 m x 20 m)	12 842 kW

This includes the following weight components not listed before (NOV, 2018; Romas Marine, 2022):

- Hydraulics pack: 9 t (1 TEU)
- Pneumatics pack: 10 t (1 TEU)
- Tensioner power unit: 10 t (1 TEU)
- Tensioner Control unit: 10 t (1 TEU)
- Derrick tower steel framework: 200 t
- Drillfloor with integrated spiders: 100 t
- Moonpool Housing: 150 t

With this installation it is expected that a new riser joint is added every 3 minutes. Installing the booster stations or airlift injection point is expected to take 15 minutes (A. Vrij, 2020). This means the hydraulic riser is assembled in roughly 14 hours, and the airlift riser in around 11 hours.

For the flexible return pipe, the deployment speed is limited by the tensioners. For deployment they can reach a speed of 1800 m/h, resulting in a deployment time of 3,5 hours. For recovery the speed is limited to 1320 m/h, resulting in a procedure lasting 4,5 hours (IMECA, 2016).

4.3.6 Energy Dynamics

To assemble and disassemble the riser, return pipe and collector requires a significant amount of power for around 15 hours. Some components like the ROV, deck crane, A&R winch, only need to be used for short times. Components like the catwalk, riser spider, and drawworks work in fixed intervals with adding a new joint to the riser. This makes it very difficult to quantify the energy variations, and some of these variations are cancelled out by the hydraulic-, and pneumatic-power units. This means that the main variable is the drawworks.

The drawworks hoisting and lowering the riser joints has a consistent fluctuation in requiring peak energy to hoist the joint and requires braking to lower the joint back down. This braking energy can be stored in an energy carrier to be used again for the hoisting to achieve a more constant grid load.

The drawworks have 4 300 kW or 5 200 kW of installed power based on an airlift or hydraulic VTS. Installing a riser joint takes 3 minutes as explained in 4.3.5. This can be split up into 1 minute of connecting the top drive and hoisting the joint, 1 minute of connecting the joint to the riser with the spider, and 1 minute of lowering and disconnecting the top drive. This means that roughly 1 minute of energy storage is needed in this case:

$$\begin{cases} E_{airlift} = 4\,300 \text{ kW} * \frac{60 \text{ s}}{3600 \frac{\text{s}}{\text{h}}} \approx 72 \text{ kWh} \\ E_{hydraulic} = 5\,200 \text{ kW} * \frac{60 \text{ s}}{3600 \frac{\text{s}}{\text{h}}} \approx 87 \text{ kWh} \end{cases} \quad (41)$$

4.3.7 Jumper Hose & ROV

At the bottom of the riser a jumper hose is connected between the riser and collector vehicle. This flexible hose measures 400 – 600 meters and is stored on a reel aboard the vessel. The hose is fitted with several buoyancy elements to ensure an S-shape so that the collector can move freely around below the jumper hose.

At the start of the riser assembly, the jumper hose is thrown overboard and connected to the riser bottom end in the moonpool. The jumper hose will stay buoyant during this operation due to the buoyancy elements, until it is forced underwater as the riser extends deep enough.

When the riser is fully assembled, the jumper hose needs to be connected to the collector vehicle. For this operation an ROV is needed.

The details of both components are shown in Table 17 (MDL, 2022; QUASAR, 2022).

Table 18: Jumper hose & ROV Properties

	Weight	Deck Space	Power
	3,5 t	7 m ² (3,5 m x 2 m)	250 kW
	150 t (COG _z = 5 m)	144 m ² (12m x 12 m)	170 kW (Hydraulic)

Both components will need to be positioned on starboard or portside of the vessel to allow for overboard deployment. The jumper hose reel should be positioned in relative vicinity of the moonpool to allow for connecting the jumper hose to the riser.

The following support system will be needed for both components to function (MDL, 2022; QUASAR, 2022):

- Reel drive control unit: 4 t (5m x 2.4m)
- Reel drive spares container: 6 t (3m x 2.3m)
- ROV control unit: ≈ 5 t (1 TEU)

4.4 Dewatering

For the dewatering of the nodules, the proposal for the phosphate nodule mining project at Chatham Rise is used as a prime inspiration (Chatham Rock Phosphate Limited, 2014). This mining site consist of smaller nodules sizes then the CCZ, so this concept filters to smaller grain sizes then required for the CCZ. This means that the dewatering plant is well adequate for the concept in this thesis and is also capable of mining area's with smaller nodule sizes.

The dewatering process is visualized in Figure 26. The dewatering processes are explained in Table 19.

Table 19: Dewatering processes

1	10mm Dewatering screen	The nodule-water slurry is put through a 10mm mesh to filter out the big nodules.
2	Logwasher	A logwasher separates solids from the waterflow that fell through the dewatering screen.
3	3mm Vibrating Screen	A Vibrating screen collects the solids that come out of the logwasher.
4	Hydrocyclone	The waterflow coming out of the logwasher is put through a hydrocyclone that uses gravity to separate the heavier solids from the water.
5	Logwasher	A second logwasher removes any liquid from the hydrocyclone outflow.
6	1mm Vibrating screen	A smaller second vibrating screen collects the solids out of the logwasher.

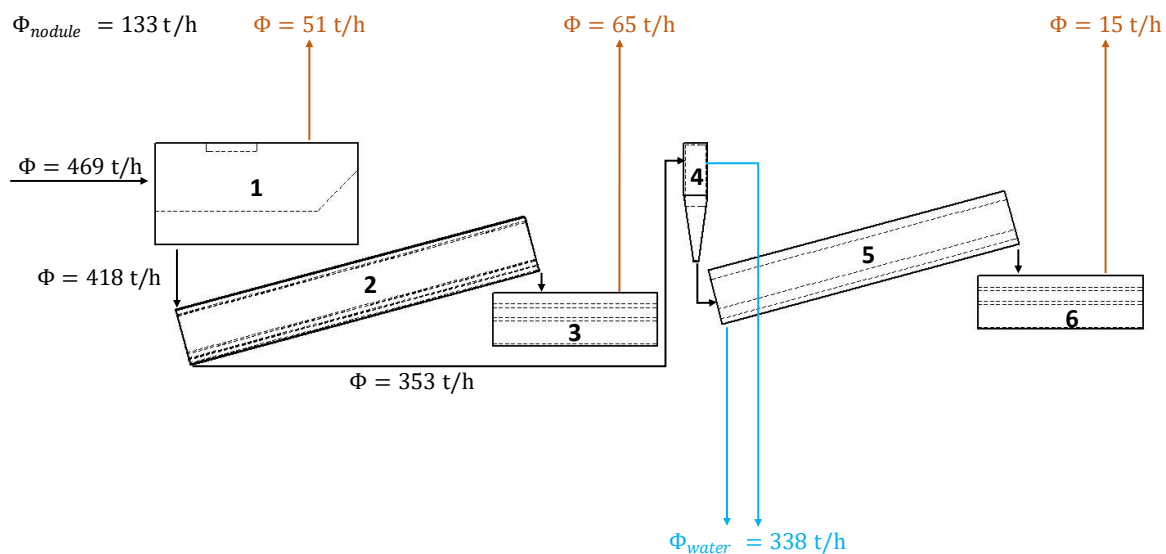


Figure 26: Dewatering process

This assembly consists of two hydrocyclones to be able to handle an inflow of 533 t/h of slurry. So, for a slurry flow of 1600 t/h consisting of 400 t/h of nodules, three of these assemblies are needed. The details of the components are displayed in Table 19 (McLanahan, 2022b, 2022a, 2022c; Mclanahan, 2022).

Table 20: Dewatering Components

	#	Weight	Dimensions			Power [kW]	
			Length	Width	Height		
Dewatering Screen (10 mm)		3x	5 t	6 m	2,5 m	3 m	24 kW
Logwasher Big		3x	20 t	10,7 m	1,8 m	1,65 m	150 kW
Vibrating Screen (3 mm)		3x	8,5 t	4,9 m	2,3 m	1,6 m	30 kW
Hydrocyclone		6x	2 t	∅ 0.7 m		3,5 m	50 kW
Logwasher Small		3x	15 t	9,1 m	1,8 m	1,65 m	60 kW
Vibrating Screen (1 mm)		3x	8,5 t	4,9 m	2,3 m	1,6 m	30 kW
Total			450 t (COG_z = 4,5m)	35 m	15 m	10 m	1 382 kW

The total weight of the dewatering plant includes 200 kW of circulation pumps and the 250-t weighing superstructure, which houses the whole installation. The complete installation is depicted in Figure 27.

To transport the dewatered nodule to the cargo holds, conveyor belts will be used.

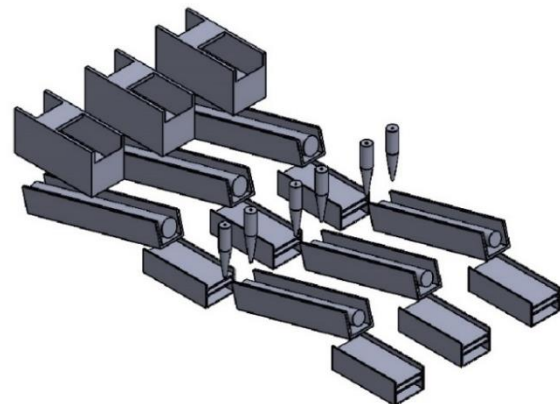


Figure 27: dewatering plant

4.5 Nodule Storage

The dewatered nodules need to be stored onboard until they can be unloaded to a transport vessel. The storage requirement of 9 days equals 67 000 tons of nodules, which requires 45 000 m³ of storage capacity. The 9 days of storage are determined based on the remote location of the CCZ, which requires the transport vessel to sail for a week to reach it from a nearby port.

This capacity is achieved by 10 storage holds. Arranged in five rows of two wide in the hull of the vessel. Two of these cargo holds are visualized in Figure 28.

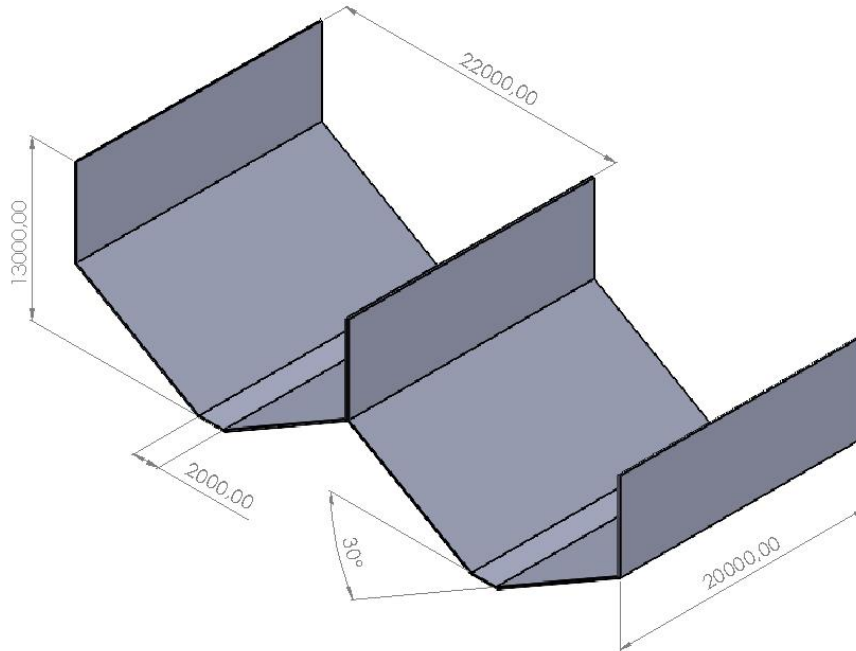


Figure 28: Cargo Holds

The cargo holds will be open on the top, so that conveyor belts can dump the nodules in the holds. The bottom 4,5 meters of the holds is tapered in to allow for self-unloading of the hulls through a set of doors located in the bottom of the cargo holds. The complete properties of the cargo holds are written down in Table 20.

Table 21: Cargo Holds Properties

	Length	Width	Height	Volume	Lightweight	Deadweight
1 Cargo Hold	20 m	22 m	13 m (4,5 m Tapered in)	4 565 m ³ (A = 228 m ²)	169 t (COG _z = 4,7 m)	6 869 t (COG _z = 7,6 m)
All Cargo Holds	100 m	44 m	13 m	45 650 m ³	1 620 t (COG _z = 4,7 m)	68 690 t (COG _z = 7,6 m)

The holds are split in two over the width to increase the stability of the ship and the offloading speed by having two parallel sets of offloading doors. A headroom of 2 meters above the holds is advanced to account for internal transport.

4.6 Internal transport

To transport the dry nodules throughout the vessel, conveyor belts are used. The weight and power requirements of a conveyor belt system can be quite easily calculated with simple physics.

To allow easy scaling of the conveyor belts if the design requires this, the weight and power are calculated per running meter.

For the internal transport, a throughput of 400 t/h is required. This equals 111,11 kg/s. For the conveyor speed, 2 m/s is assumed, and the conveyor width is chosen at 0,8 meters.

The weight per running meter on the conveyor belt can now be calculated (Mike Gawinski, 2020):

$$W_{nodules} = \frac{111,11 \frac{kg}{s}}{2 \frac{m}{s}} = 55,55 \frac{kg}{m} \quad (15)$$

The weight of the conveyor belt itself is:

$$W_{conveyor} = B * t_{rubber} * \rho_{rubber} = 0.8 m * 0,05 m * 1360 \frac{kg}{m^3} = 54,5 \frac{kg}{m} \quad (16)$$

Now the total weight on the conveyor belt equals:

$$W_{total} = W_{nodules} + W_{conveyor} = 110,05 \frac{kg}{m} \quad (17)$$

This is the weight that the roller of the conveyor will need to displace. This can be converted in power by using the friction coefficient of the system (C_f) and the gravitational constant. The friction coefficient for a standard conveyor belt can be taken at 0,5.

$$P = W_{total} * C_f * g = 0,54 \frac{kW}{m} \quad (18)$$

The weight of the empty conveyor belt system can be assumed at 154,5 kg/m.

For a conveyor belt system to travel between the dewatering station and all the cargo holds, it's expected that 295 meters of conveyor belt is needed. The properties of the internal transport system are shown in Table 21.

Table 22: Internal transport System

Dimensions	Lightweight	Deadweight	Power
295 m x 1 m x 1 m	46 t	78 t	160 kW

4.7 Offloading

The two different offloading methods discussed before are examined. These are dry-offloading with a conveyor belt for ship-to-ship transport, and wet-offloading with a water-nodules slurry through a floating hose. The two methods are compared in this section, to select one of the two concepts for the production support vessel.

4.7.1 Dry Offloading

One offloading option is dry offloading. This makes use of self-unloaders seen in bulk carriers. A conveyor belt is placed underneath the cargo holds, by opening the doors in the cargo holds, the nodules can be dumped onto this conveyor belt and transported to the self-unloader. The nodules are transported above deck by trapping the nodules between two conveyor belts. Above deck the nodules are dumped onto a swinging boom with a conveyor belt.

For the DSM production support vessel, the offloading rate is chosen at 4000 t/h. The offloading boom for this design is shown in Figure 29. The boom uses a 3-meter-wide conveyor belt and measures 76 meters long. The boom can be raised up to 18° from its horizontal positions and can swing 95° to either side.

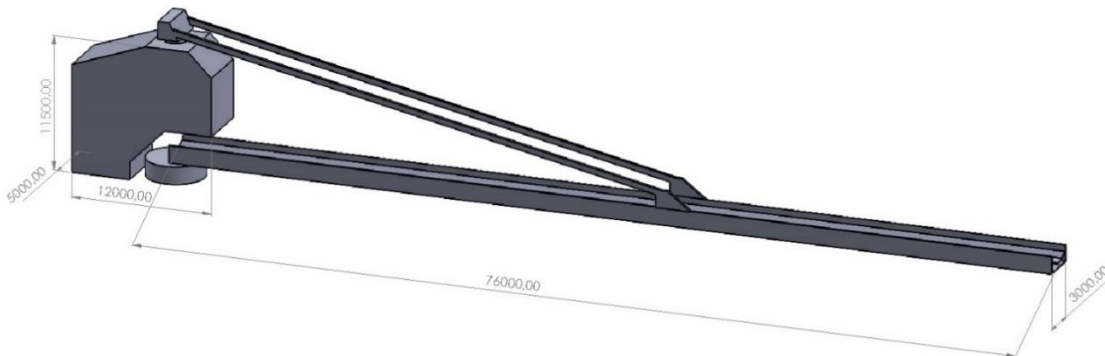


Figure 29: Offloading Boom

This system is limited by the vessel's roll, as any roll will cause significant movement of the end of the boom. A chute can be fitted to the end of the boom to allow more accurate dumping and reduce dust.

The properties of the offloading system are displayed in Table 22. The offloading operation will last around 12 h – 17 h.

Table 23: Dry Offloading

	Lightweight	Deadweight	Deckspace	Power
Housing	≈ 100 t	≈ 100 t	60 m ² (12m x 5m)	≈ 50 kW
Boom	≈ 50 t	92 t	400 m ² (80m x 5m)	600 kW
Vertical Conveyor	23 t	34 t	25 m ² (5m x 5m) (H = 20 m)	250 kW
Cargo Hold Doors	6.5 t		8,4 m ² (3,5 m x 2,4 m)	132 kW (HPU)
Horizontal Conveyor	150 t	234 t		1 000 kW
Total	330 t	460 t	400 m² (Overboard boom: 60 m²)	2 050 kW

An overview of how this system will work is displayed in Figure 30.

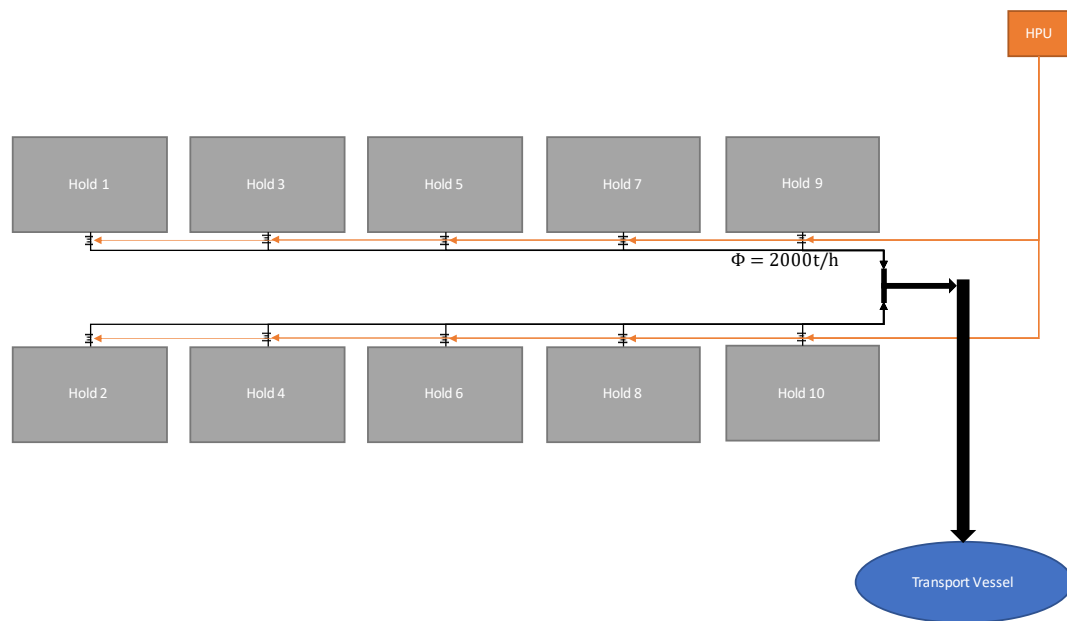


Figure 30: Offloading System

The bottom doors in the holds are hydraulically operation by a hydraulic power unit (HPU). The opening of the doors can be controlled in interval to manage the flowrate out of each of the holds. This way stability of the vessel can be kept in check during the offloading process.

A sketch of the complete system is shown in Figure 31.

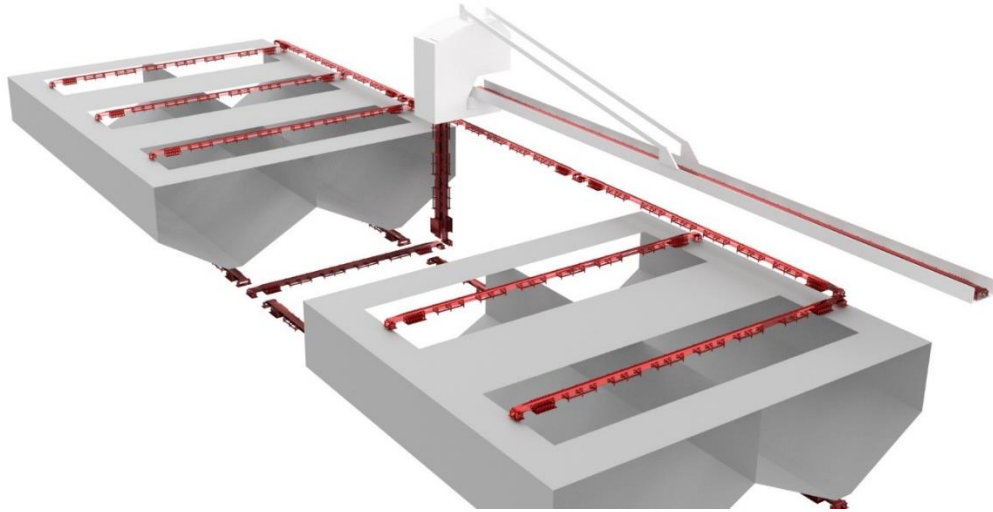


Figure 31: Dry Offloading hull form

The conveyor belts underneath the holds require 1.5 meters of headroom. The vertical transport in the hull is fitted into a 5 meter by 5 meter “chimney” going the entire height of the hull.

4.7.2 Wet Offloading

A second offloading solution is wet offloading. Hereby the dry nodules are rewatered, and this liquid slurry is pumped out of the cargo holds to the transport vessel. On the transport vessel the nodules are dewatered again. Because the dewatered water cannot be pumped into the sea, it must be pumped back aboard the production support vessel to either be reused or dumped through the return pipe.

For the required offloading rate of 4000 t/h of dry nodules, the flowchart is given in Figure 32.

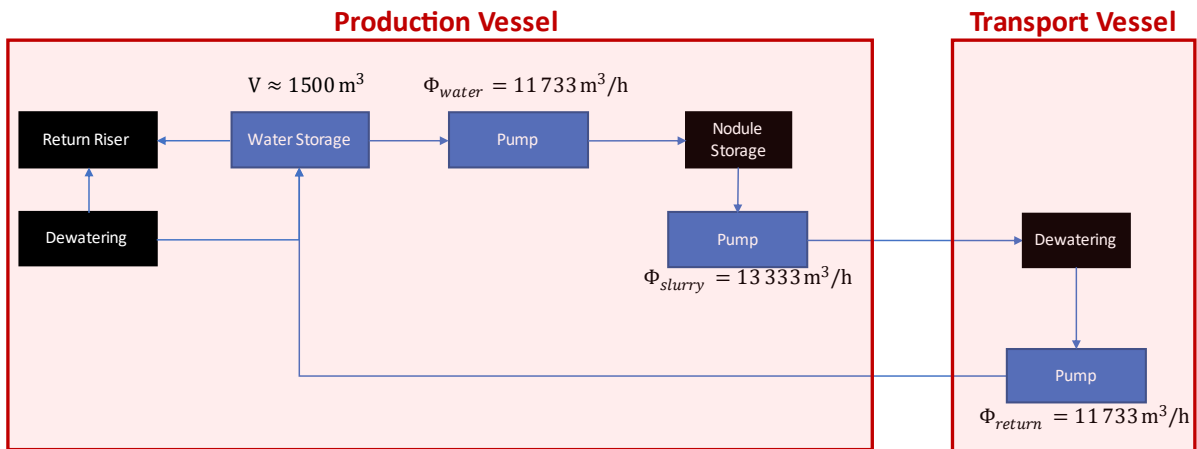


Figure 32: Flowchart wet offloading

In total, three pumping stations are needed and a dewatering plant. The dewatering plant is identical to the one described in 4.4, except its throughput is 10 times higher.

A practical overview of the offloading operation is shown in Figure 33. A mooring chain connection is made between both vessels and four hoses connect both vessels to pump the slurry over and return the water from the dewatering plant.

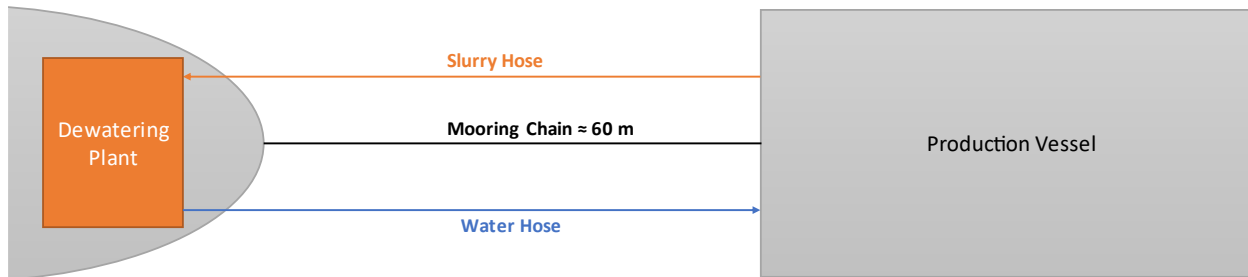


Figure 33: Offloading Operation

Both hoses have an inner diameter of 0,8 meter, which will result in a flow rate of 7,37 m/s in the slurry hose and 6,48 m/s in the water hose. This ensures the flow speed is high enough to prevent the nodules from accumulating on the bottom of the hose.

The power components for the offloading process are listed in Table 23 (IHC Merwede, 2022; Keppel, 2015; MDL, 2022; Warman, 2009).

Table 24: Wet Offloading

	#	Deckspace	Weight	Power
Hose Reel	2	144 m ² (12 m x 12 m)	150 t	132 kW (HPU)
Mooring Winch	1	21,3 m ² (5,6 m x 3,8 m)	≈ 15 t	480 kW
Rewatering pump	2	12 m ² (4 m x 3 m)	20 t	850 kW
Slurry pump	2	12 m ² (4 m x 3 m)	20 t	850 kW
Dredge Valves	22	/ (0,5 m x 1 m x 4 m)	3,3 t	35 kW (HPU)
Total		360 m² (12m x 30 m)	395 t	4 047 kW

The pumps in Table 24 are all identical and have a maximum flowrate of 7500 m³/h with a head of 43 meters and a pipe diameter of 55 cm (Warman, 2009). The dewatering plant and return pump are assumed to be part of the transport vessel and powered by its own powerplant.

The offloading operation will last around 12 h – 17 h.

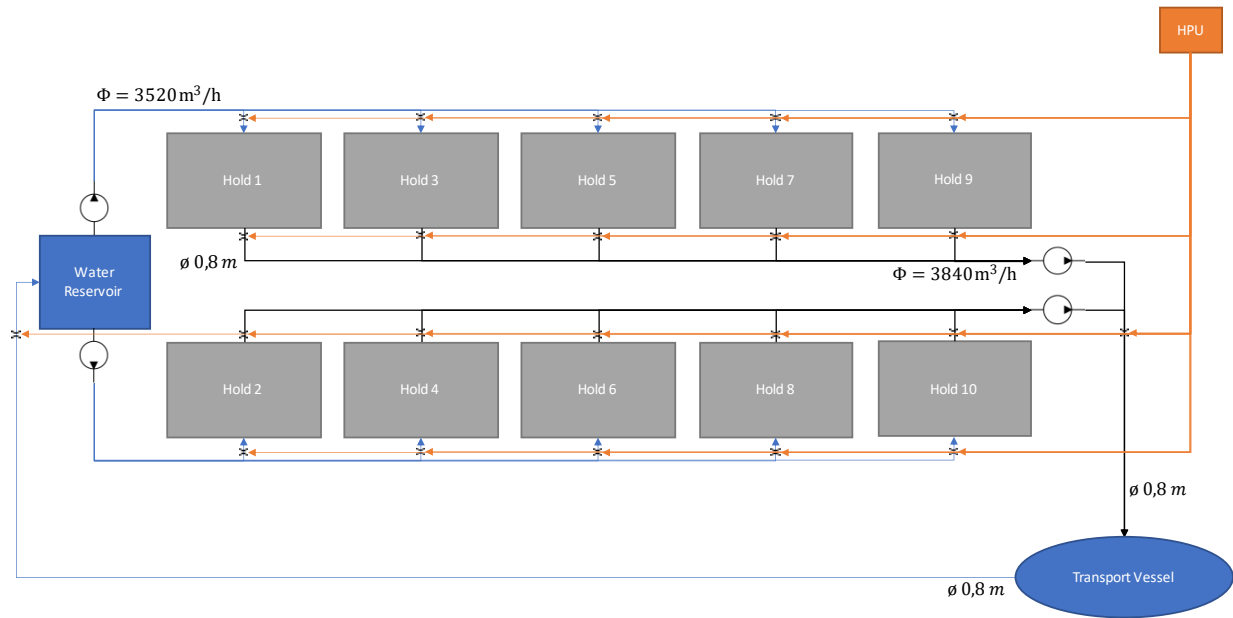


Figure 34: Wet Offloading System

To offloading the nodules by means of rewatering and pumping to the transport vessel through a flexible hose, the following layout is created, as seen in Figure 35.

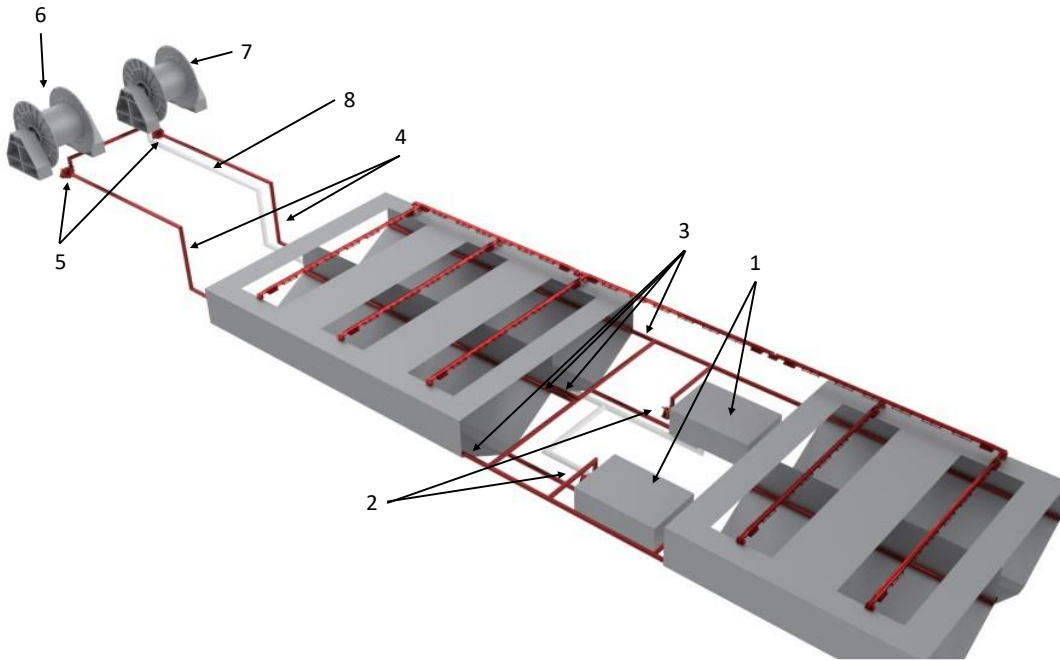


Figure 35: Wet Offloading hull form

The system consists of the following components:

1. Slurry water reservoir tanks (2x 750 m³) are placed on either side of the moonpool.
2. Slurry water circulation pumps.
3. Water injection pipes in the nodule cargo holds; inject the water into the holds by means of waterjets aimed at the doors in the bottom of the holds.
4. Two parallel slurry pipes, going underneath the holds transport the slurry from the holds to the stern of the vessel.
5. Slurry circulation pumps.
6. Flexible hose reel.
7. Return flexible hose reel.
8. The return water is pumped through a pipe going underneath the cargo holds back to the reservoir tanks.

For this method, 1.5 meters of clearance is required between the top of the double hull and the bottom of the cargo holds to house the piping. In the stern, the piping has to be guided around the engine room and fuel tanks.

4.7.3 Offloading selection

Looking at both offloading methods, they both have their pros and cons. For a few key performance indicators, the considerations are shown in Table 25 (Kristian et al., 2016).

Table 25: Wet-/dry-Offloading

	Wet	Dry
Power	4 047 kW Pumps require more power	2 050 kW Conveyor belt not that power intensive
Under cargo hold clearance	< 1 meter Only a pipe with valves needed	1,5 meters Suspended conveyor belt and adjustable cargo holds doors with room for maintenance
Cargo holds modification	Water jets needed to rewater and 2x 750 m ³ water tanks needed for the rewatering	Adjustable doors in the bottom
Vertical transport	$NSPH_{req} > 20$ m	Complex system with two sets of conveyor belts which requires significant space
Deck space	360 m ² 2x Reel drive & mooring winch	400 m ² 76m conveyor boom with housing
Sea-state	Approach & Mooring: $H_s < 4,5$ m Offloading & Disconnect: $H_s < 5$ m	Approach & Mooring: $H_s < 2$ m Offloading & Disconnect: $H_s < 3$ m
Bulk Carrier modifications	Tug or DP2 / DP3 required during operation & a dewatering plant and internal transport system	Tug or DP2 / DP3 required during operation
Ship-to-ship distance	50 – 100 meters (Stern to bow)	0 – 50 meters (side-to-side)

The main advantage of wet offloading is its operational window, with offloading up to a significant wave height of 5 meters. While dry offloading is only allowed until 3 meters.

Wet offloading does however come with a big disadvantage, that the bulk carrier needs to be extensively upgraded to accommodate a very large dewatering plant and must be able to move the dewatered nodules to its cargo holds. A modular solution for the dewatering process will mostly solve this but looks unfeasible due to the immense size of the dewatering plant. Which must dewater the slurry at 10 times the rate of the dewatering plant onboard the production support vessel ($\dot{m}_{offloading} = 10 * \dot{m}_{mining}$). Lower efficiency dewatering process could reduce both the power and deck space requirements but will reduce the overall revenue of the operation as well. This means, a custom-made bulk carrier is required for this process, significantly increasing the cost of this approach.

While dry offloading has a narrower operating window, it can be assumed there is room for improvement here. The offloading boom is 76 meters long and when mounted on the side of the production vessel it allows for 50 meters of clearance between both vessels. The end of the offloading boom can also be fitted with a flexible hose to allow the boom to heave without interrupting the dumping of nodules in the cargo hold.

With this room for improvement in the operability of dry offloading together with only a Dynamic positioning system modification needed for the bulk carrier, the dry offloading method is the more attractive solution. So, for these reasons the dry offloading method will be selected for the worked-out concepts in this thesis.

It can however be noted that the selected offloading method will have a minimal effect on the design as the two concepts require roughly the same space and the required power is rather insignificant compared to the whole vessel. So, redesigned for wet offloading shouldn't pose any significant design challenges.

4.8 Onboard cranes

Multiple cranes will be placed across the deck on the vessel. These cranes will be required to handle certain tasks in the deployment – and recovery of the riser, return pipe and collector. They will also serve for maintenance tasks on the various components and take in supplies for supply ships.

Table 26: Crane Details

For these reasons, one lattice boom crane with a wide outreach is chosen to take in supplies and be able to move cargo between vessels. Furthermore, a number of knuckle-boom cranes are installed for maintenance and other tasks on deck. The details of both cranes are displayed in Table 26 (NOV, 2022; NOV LH, 2018; Offshore Crane, 2022).

	Lattice boom Crane (OC3550L)	Knuckle-Boom crane (OC3932K)
		
SWL	150 t (@ 14m)	85 t (@ 18,5 m)
Outreach	8 m – 70 m	7,3 m – 42 m
Weight	135 t	145 t
Power	2x 350 kW	500 kW
Deckspace	27 m ² (5,2 m x 5,2 m)	27 m ² (5,2 m x 5,2 m)

5 Vessel Design

Chapter 4 has defined the vessel functions into systems with their own mass, volume, and power requirements. In this chapter these systems will be assembled in an efficient way based on their weight and volume to achieve a compact vessel with a low center of gravity to ensure good stability offshore in the conditions of the CCZ.

5.1 Hull Design

Based on the design blocks defined, a hull can now be defined to house the necessary systems. This hull is shown in Figure 36.

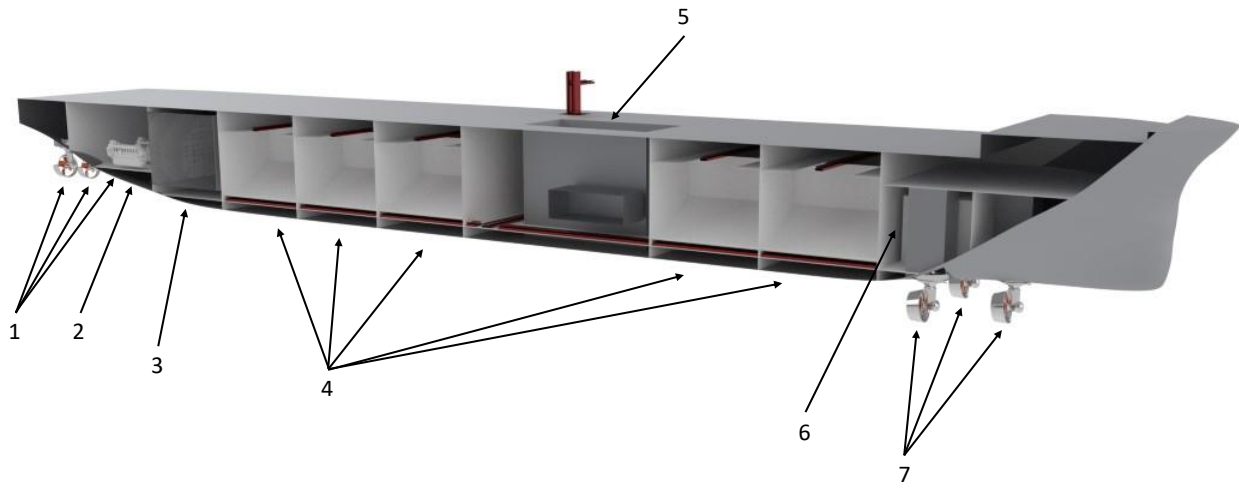


Figure 36: Vessel Hull

The vessel has a double hull which measures 2 meters high on the bottom and 1,75 meters wide on the sides. the accommodation module will be situated at the front as with a drillship, with the fuel tank and engine room situated at the aft of the vessel. The main dimensions of the hull are displayed in Table 27.

Table 27: hull Dimensions

The general arrangement is summed up as follows:

1. 3x Azimuth aft propulsion/DP
2. Engine Room
3. Fuel Tank
4. 10x Nodules cargo holds
5. Moonpool
6. Retractable azimuth housing
1. 3x Azimuth bow for DP

Hull		
Loa	246.88	m
Lwl	239.47	m
Lpp	238.92	m
B	47.5	m
D	20	m
T_design	13	m
Cb	0.7894	
Δ	116786	m ³
COB_x	120.96	m
COB_y	0	m
COB_z	6.925	m

5.2 Stability

To ensure the hull offers a stable platform that can withstand extreme sea-states, the static stability of the hull will be estimated. Two scenarios' will be considered:

5.2.1 Transit scenario

In this mode the vessel is top heavy with all the mining equipment dissembled on deck and the nodule cargo holds empty. Ballast tanks in the double hull are available to ensure sufficient draft and stability in this case.

The ballast configuration for this case is shown in Figure 37. The forward part of the double hull [1][2] is filled. This is to combat the trim instilled by the stern-heavy deck equipment. The dewatering tanks [3] situated on both sides of the moonpool are also filled with ballast. Other tanks of concern are the freshwater tank [4] and black water tank [5].

This results in a displacement of 62 818 tons and a draft of 7,4 meters with a block coefficient of 0,73. The center of buoyancy of the hull is now:

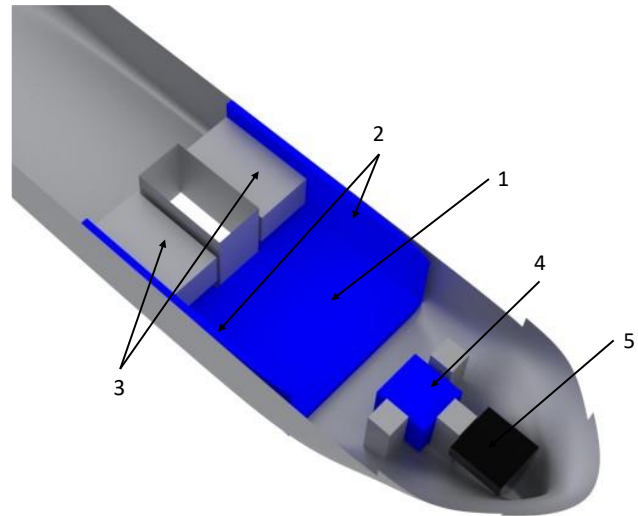


Figure 37: Transit ballast

$$COB = \begin{cases} x = 123,7 \text{ m} \\ y = 0 \text{ m} \\ z = 3,9 \text{ m (KB)} \end{cases} \quad (19)$$

For static stability, the metacentric height can be calculated as follows:

$$GM = BM + KB - KG \quad (20)$$

The BM distance can be calculated as follows:

$$BM = \frac{I_T}{\Delta} = \frac{1\,578\,680 \text{ m}^4}{61\,286 \text{ m}^3} = 25,74 \text{ m} \quad (21)$$

Hereby the waterplane moment of inertia around its centerline is divided by the vessel's displacement in the load condition. The moment of inertia is estimated by using Simpson's first rule.

The Centre of gravity from the keel is estimated based on all the weights and their location on board. This led to the following:

$$COG = \begin{cases} x = 122,81 \text{ m} \\ y = 0 \text{ m} \\ z = 13,48 \text{ m (KG)} \end{cases} \quad (22)$$

This gives the following metacentric height:

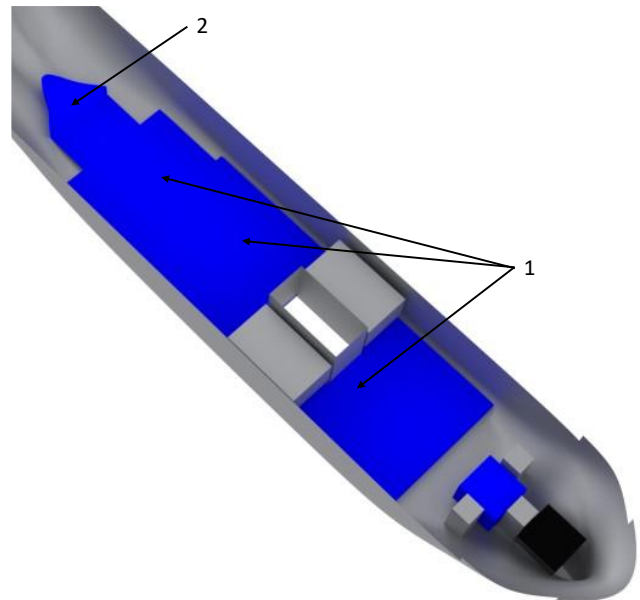
$$GM = 16,18 \text{ m} \quad (23)$$

With the very large BM due to the relatively large beam ($\frac{L}{B} = 4,85$), a stable vessel is ensured with a high metacentric height.

5.2.2 Mining scenario

During mining, the heavy mining equipment is deployed and get rids of a lot of heavy equipment on deck. In the hull, the nodule cargo holds are being filled with nodule, which means a lot of heavy weight is situated low in the vessel's hull. This will result in a heavy vessel which will be around its design draft.

The ballast configuration is shown in Figure 38. Which focusses around filling the bottom double hull [1] to improve the center of gravity, to ensure a stable working platform. With the heavy deck equipment on the stern deployed, the center of gravity moves forward. To combat this, the stern ballast tank [2] if filled to cancel out any trim.



The vessel now has a displacement of 117 863 tons with a draft of 12,8 meters and a block coefficient of 0,79. The center of buoyancy now is:

Figure 38: Mining ballast

$$COB = \begin{cases} x = 121,05 \text{ m} \\ y = 0 \text{ m} \\ z = 6,82 \text{ m (KB)} \end{cases} \quad (24)$$

The same calculations as in the previous section are used to calculate the metacentric height for this load case. This yields the following results:

$$BM = \frac{1\ 800\ 400 \text{ m}^4}{114\ 988 \text{ m}^3} = 15,69 \text{ m} \quad (25)$$

$$COG = \begin{cases} x = 121,88 \text{ m} \\ y = 0 \text{ m} \\ z = 11,58 \text{ m (KG)} \end{cases} \quad (26)$$

Which gives the following metacentric height:

$$GM = 10,93 \text{ m} \quad (27)$$

Similar to the transit condition, with the mining condition, the stability of the vessel is ensured with its large beam yielding a high BM and consequently a high metacentric height.

Analyzing both the considered load conditions, it is obvious ship stability is well ensured with the large beam. Longitudinally the center of gravity and center of buoyancy are in each other vicinity (≈ 1 m) in both load cases.

5.3 Deck layout

With the vessel's hull figured out, it's time to go above deck and create a deck layout with all the systems which will be placed on deck. A generic layout is shown in Figure 39.

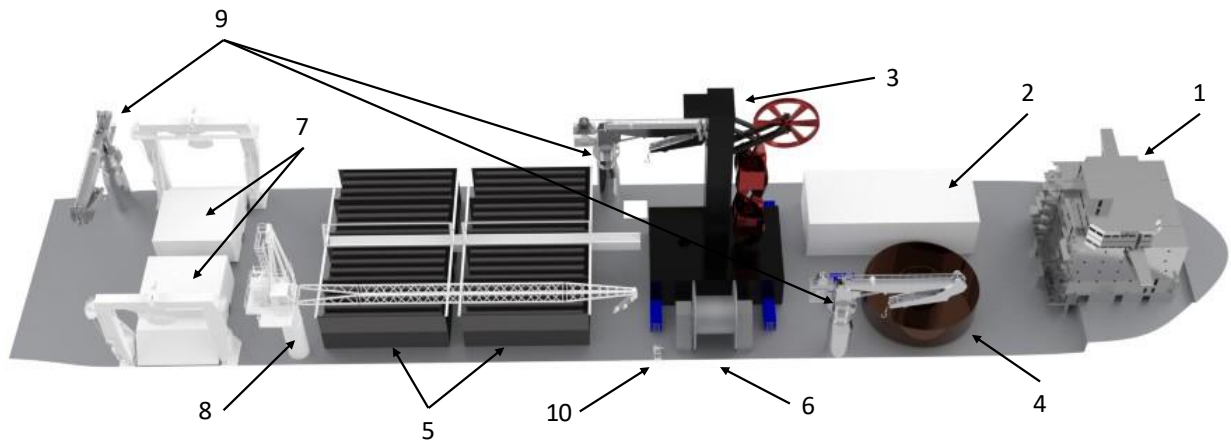


Figure 39: Generic Deck Layout

The deck follows the boundaries of the hull and as so measures 47,5 meters in width. Measured from the aft plane, the deck is 204 meters long. With the remaining length being dedicated to the deckhouse and bow. The moonpool is situated centerline 128,5 meters from the aft with the assembly tower over it. The moonpool measures 25,6 meters in length and 12,5 meters in width.

The layout in Figure 39 is as follows:

1. Deckhouse
2. Dewatering plant
3. Riser assembly tower
4. Flexible return pipe carousel
5. Riser joint storage
6. Jumper hose reel
7. Collector storage and A-frame for LARS
8. 150 t Lattice crane (70m)
9. 84 t Knuckle-Boom crane (42m)
10. ROV

A complete overview of the deck layout including dimensions, can be found in Appendix F – Deck Layout. It also shows the outreach of the deck cranes with a circle of their maximum outreach.

For the hydraulic riser system, the six-booster station which have the centrifugal slurry pumps integrated, will need to be stored on deck. Due to their asymmetric design, they can't be stored in the riser joint storage racks and will need a separate storage rack with a deck crane capable of lifting the booster stations from this rack to the assembly tower.

For this reason, the booster stations are stored between the joint storage and the assembly tower in two racks, which both contain three booster joints. The knuckle-boom crane on portside of the vessel can handle the booster stations. This is depicted in Figure 40.

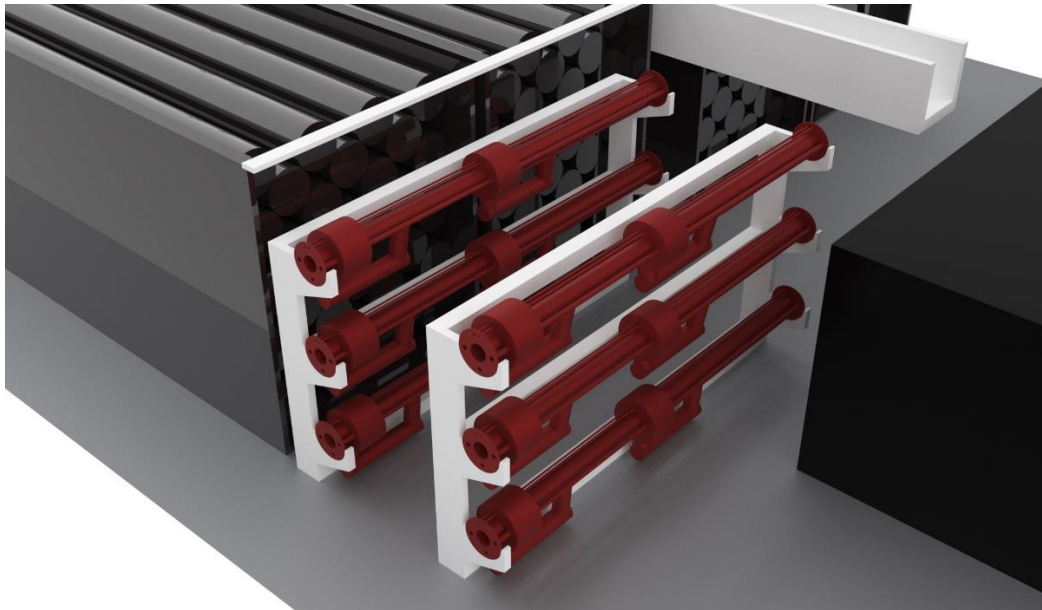


Figure 40: Booster Station Storage

The airlift system doesn't require any additional deck equipment, as the tubing and the injection point for the airlift systems are worked away in the riser joints, which can be stored in the joint storage racks.

5.4 Propulsion

With the hull being defined, a thruster configuration can be matched to achieve the DP – capabilities that are required of the vessel. As well as making sure the vessel can sail on its own power.

5.4.1 DP Vessel Force estimation

To be able to select the right propulsion for the vessel to perform in DP-mode, the forces on the vessel in DP-mode are estimated. This will be done for the different sea-states which were defined.

The vessel forces can be divided into waves, wind, and current.

- Wave force

The force created by the waves slamming into the vessel are estimated with the Froude-Krylov wave force. This is done by integrating the pressure of the wave over the applicable hull-surface:

$$\bar{F}_{wave} = \iint (p * \bar{n}) dS \quad (33)$$

- Wind force

The wind force on the vessel can be estimated with the following set of formulas (IsherWood, 1972):

$$\begin{cases} F_{wind_x} = \frac{1}{2} \rho_{air} C_X(\alpha_{wind}) A_T v_{wind}^2 \\ F_{wind_y} = \frac{1}{2} \rho_{air} C_Y(\alpha_{wind}) A_L v_{wind}^2 \\ M_{wind_z} = \frac{1}{2} \rho_{air} C_M(\alpha_{wind}) A_L L v_{wind}^2 \end{cases} \quad (38)$$

- Current force

For the current forces on the vessel's hull, the following formulas can be used (Remery & van Oortmerssen, 1973):

$$\begin{cases} F_{current_x} = \frac{0.075}{(\log(Rn) - 2)^2} * \frac{1}{2} \rho v_{current}^2 * \cos(\alpha_{current}) * |\cos(\alpha_{current})| * S \\ F_{current_y} = \frac{1}{2} \rho C_Y(\alpha_{current}) A_{LS} v_{current}^2 \\ M_{current_z} = \frac{1}{2} \rho C_M(\alpha_{current}) A_{LS} L v_{current}^2 \end{cases} \quad (39)$$

These forces were calculated with the help of MATLAB, of which the script is shown in Appendix J – DP Vessel force Calculation (MATLAB) Appendix J – DP Vessel force Calculation (MATLAB). The results from the MATLAB script can also be found in Table 42 in the Appendix. The maximum load condition is when waves, currents, and wind is longitudinally loaded on the hull. In this case, a force of 3 198 kN is exerted onto the hull. This is the maximum force the DP-system must be able to withstand.

5.4.2 Thruster layout

To achieve the required thrust of 3 198 kN defined in the previous section, a total of six azimuth thrusters are chosen. Three azimuth thrusters of 6,5 MW will be placed at the stern of the vessel to function as the main propulsion. Three further 5,5 MW azimuth thrusters are mounted in the bow to complete the thruster arrangement. These three forward thrusters will be retractable as they are for DP-purposes only and will be retracted during cruising to negate the drag they would induce. This arrangement is shown Figure 41.



Figure 41: Thruster Arrangement

This is an identical configuration to that of a drillship, as the hull and DP-requirements are very similar. The chosen thrusters and their characteristics are shown in

Table 28: Thruster Characteristics

	WST-65U	WST-55RU
P_p	6 500 kW	5 500 kW
D_p	4,2 m	3,9 m
W_{dry}	132 t	133 t
Dim.	4 m x 4 m x 7,2 m	6 m x 6 m x 20 m
Thrust	1 039 kN	896 kN

Table 28 (Marine Solutions, 2017; Wärtsilä, 2017).

By matching the thrust from the thrusters to the vessel forces, the power requirements can be read out. This is shown in Figure 42.

The extreme – Y condition is not shown, as no DP is required in this condition.

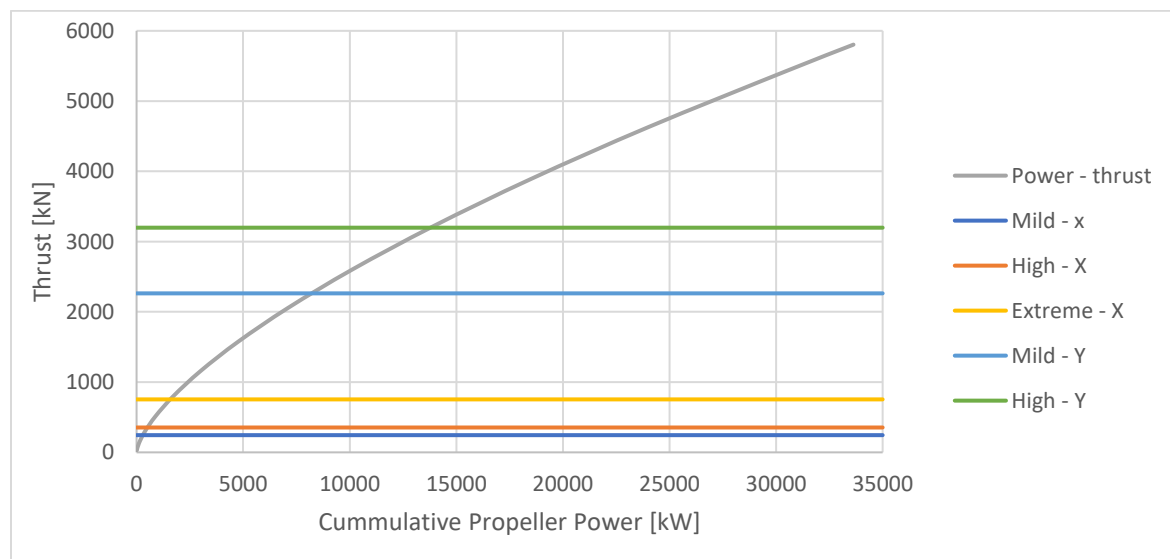


Figure 42: Bollard Pull Thrust in function of Propeller Power

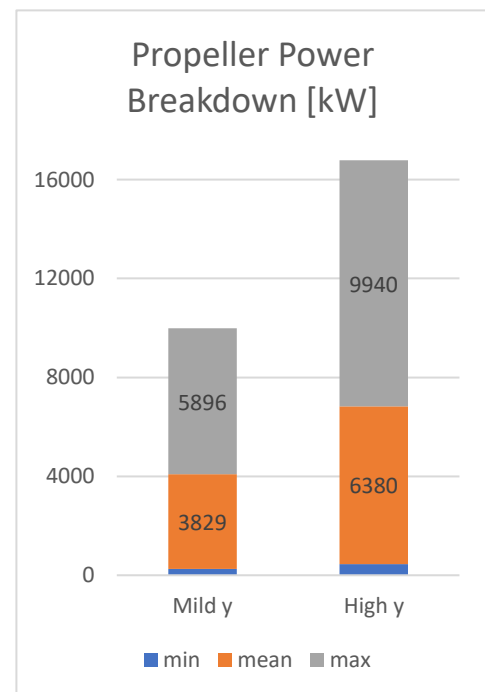
Reading out the power values, they are displayed in **Error! Reference source not found.** The extreme condition is left blank, as the vessel will face head waves to survive as best as possible.

Table 29: Thrust power for different sea-states

	Mild		High		Extreme	
	X	Y	X	Y	X	Y
Force [kN]	245	2 263	354	3 198	754	8 410
Power [kW]	292	8 209	508	13 790	1 579	-

So, this shows that the power requirement of the DP-system will be somewhere between 292 kW and 13 790 kW. This power level is calculated as a time average of the wave load, which in reality is a varying load over time. As the wave equation used in the Froude-Krilov method is time and space dependent. So, lets break this maximum power up in a mean value and an amplitude to get a clearer image of the power levels over time. This is shown for the two longitudinal load cases in Table 30, as these are the two highest load cases. From the waves in the CCZ, it is known they generally have a period of 5 – 8 seconds.

Table 30: Propeller Power Breakdown



This shows that the DP-system requires a mean power of up to 6 MW but can require up to 10 MW of additional peak power to deal with wave impacts.

This dynamic behavior requires the powerplant to do the same. This would require the powerplant to output an extra 10 MW with 5 – 8 second intervals. As not every powerplant is suited for this, an energy storage solution is added in-between. This way the time averaged power levels can be taken as the power requirements of the DP system.

A battery energy storage is chosen as it's well suited for these short peaks with it's instant response time. The size of the battery is chosen at one minute of exposure to the 10 MW. This is to ensure the battery can sustain several peaks and has a safety margin. This yields the following size:

$$E_{DP} = P_{DP} * t_{DP} = 10\,000\text{ kW} * \frac{60\text{ s}}{3600 \frac{\text{s}}{\text{h}}} \approx 170\text{ kWh} \quad (40)$$

So, the maximum power requirement of the DP-system is 13,8 MW with a 170 kWh battery.

5.4.3 Cruise speed

To sail to and from the mining site, the vessel will be powered by the three aft azimuth thrusters. In this section, the maximum cruising speed of this thruster configuration will be determined. To ensure the vessel can sail from and to the mining site in a reasonable time, the design requirement is to achieve a cruise speed of 14 knots.

The hull resistance is estimated by using the Holtrop & Mennen resistance calculation. The results for the hull resistance are shown in Figure 43.

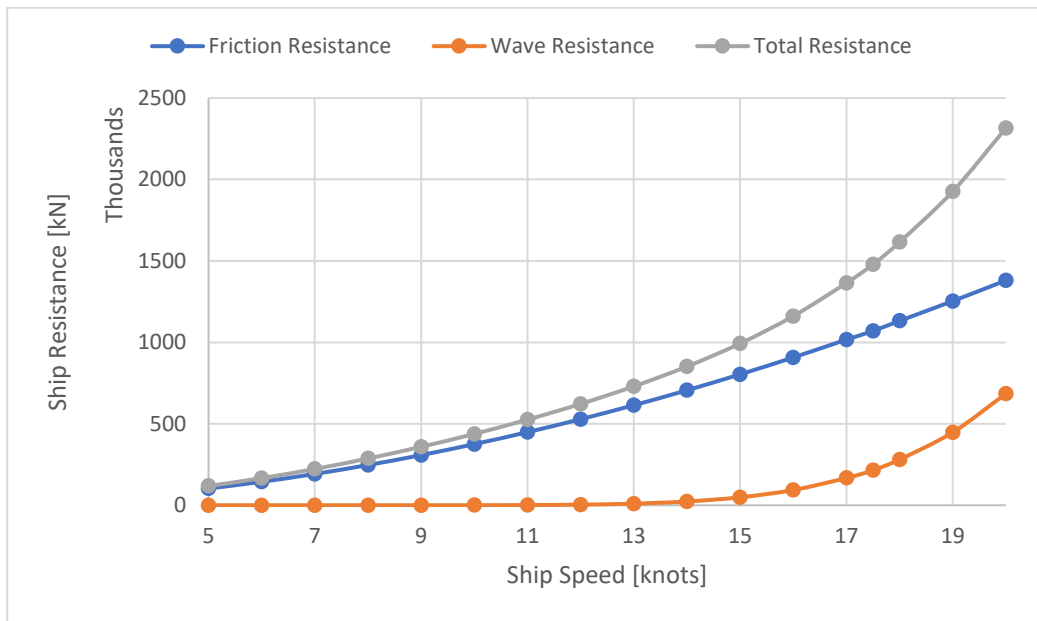


Figure 43: Hull Resistance

The graph shows that the total resistance is dominated by friction resistance until about 15 knots and that after that wave resistance start to play a significant role. This is great, as the design requirement of 14 knots should be more easily achieved.

To check the maximal attainable ship speed with the three 6,5 MW aft propellers, let's calculate the achievable thrust. The thrust for each propeller can be calculated from the ship resistance:

$$T = \frac{P_T}{v_a} = \frac{P_E}{k_p * v_a * \eta_H} = \frac{R_T * v_s}{k_p * v_a * \eta_H} \quad (28)$$

This can now be used to calculate a K_t curve for the ship:

$$K_{T,ship}(J) = C_7 J^2 = \frac{C_8}{\rho D_p^2} J^2 = \frac{T}{\rho v_a^2 D_p^2} J^2 \quad (30)$$

Now the K_t curve of the ship can be put in the open-water diagram of the propeller. The Ka-4 70 propeller is chosen with nozzle 19A, as it is a very common propeller for these applications. A D/P ratio of 1.2 is chosen, which offers a good compromise for the low-speed cruising and DP functionality. The open water diagram of this is shown in Figure 44.

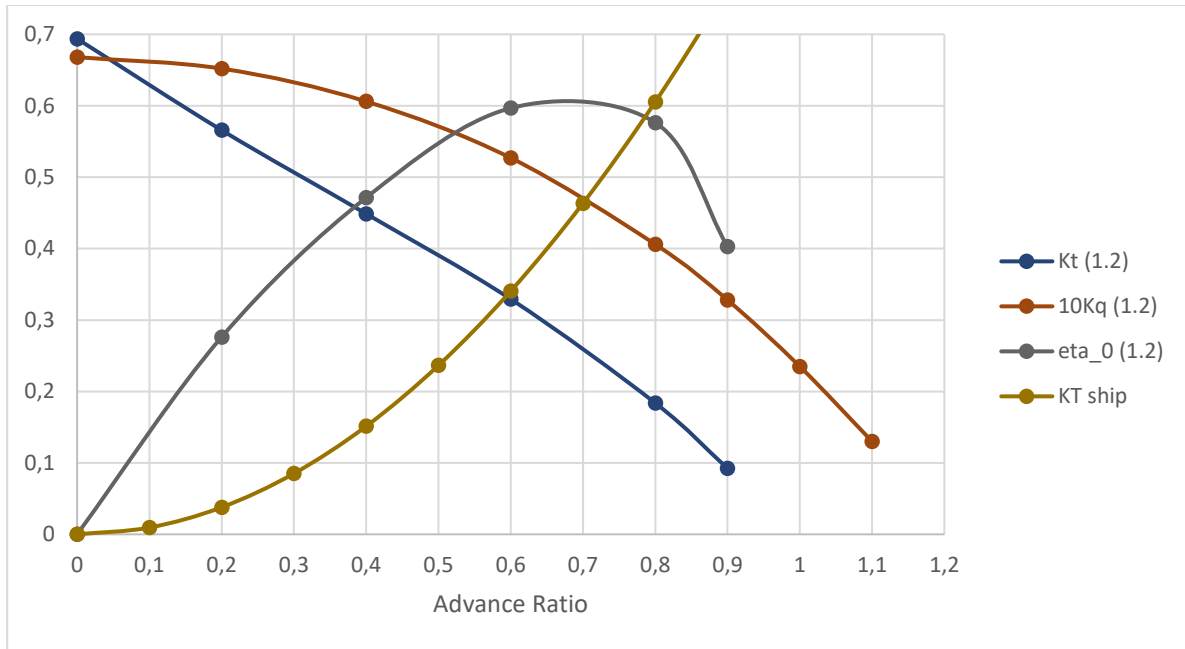


Figure 44: Open water diagram (Ka 4-70 Nozzle 19A)

The intersection point between both K_t curves can be found and the resulting advance ratio. With this the propeller speed can be derived:

$$n_p = \frac{v_a}{D_p * J} \quad [rps] \quad (31)$$

With this the propeller torque and power can be calculated:

$$\begin{cases} M_p = \frac{K_q \rho n_p^2 D_p^5}{\eta_R} \\ P_p = 2\pi n_p M_p \end{cases} \quad (32)$$

Now finding the maximum vessel speed for the chosen azimuth thrusters are displayed in Table 31.

Table 31: Propeller Cruise properties

3x 6,5 MW WST-65U Azimuth Thrusters		
Ship Speed	17,5	Knots
Ship Resistance	1 478	kN
Propeller P/D	1,2	
Advance Ratio	0,59	
Open water Efficiency	59	%
Relative Rotative Efficiency	95	%
Propeller Speed	143	rpm
Propeller Thrust	597	kN
Propeller Torque	428	kNm
Propeller Power	6 396	kW
Transmission Efficiency	97	%
Required Power	18 613	kW

6 Hydraulic VTS – Powerplants

With the vessel design complete, a complete picture of the requirements of the powerplant can be set up. In this chapter the DSM vessel with a hydraulic riser will be examined to achieve a powerplant concept.

6.1 Operational profile

The different operating modes of the DSM production support vessel are displayed in Table 32 with the relative times spend in each mode. The time distribution is based on the Blue Nodules research (Blue Nodules, 2017).

Table 32: Operating modes Hydraulic VTS

Operating Mode	Sea-state	Description	Time
Transit	Mild	Roughly 20 days a year the vessel is cruising between a nearby port and the mining site. This will mainly be due to maintenance.	5 %
DP 1	Mild	The vessel stays in DP mode when it's offshore but not mining due to weather or maintenance related downtime.	4 %
DP 2	High	Same as "DP 1" but in a heavier sea-state.	1 %
LARS 1	Mild	(dis)assembling the riser and collector systems at the mining location.	2 %
LARS 2	High	Same as "LARS 1" but in a heavier sea-state.	2 %
Assembled Standby	Mild	Staying in DP-mode at the mining location with riser and collector deployed but not mining due to any downtime.	4 %
Mining 1	Mild	Mining nodules at 1 knots.	45 %
Mining 2	High	Same as "Mining 1" but in a heavier sea-state.	19 %
Offloading 1	Mild	Offloading the nodules to a transport vessel and continue mining at 1 knots.	4 %
Offloading 2	High	Same as "Offloading 1" but in a heavier sea-state.	2 %
Survival	Extreme	Staying offshore at the mining site during a storm/hurricane. There are 40 extreme weather days a year in the CCZ.	7 %
Harbor	-	Staying in a nearby harbor for maintenance or other purposes.	4 %

The table shows the number of days per year percentage wise.

The vessel is expected to have around 35 days of offshore downtime in total, due to maintenance of the systems. This will be mostly due to problems with the vertical hydraulic transport, as the system is expected to clog-up during operations and a pump-failure requires the redeployment of the entire riser system (A. Vrij, 2020). The downtime is distributed over DP 1, DP 2, and "Assembled Standby".

The available mining days can be categorized in three groups based on the sea-state. The calm sea-state 1 occurs 71 % of the time, with the higher sea-state 2 occurring 26 % of the time. There is a 3 % change

the sea-state exceeds the mining conditions and the vessel must go into survival mode. To be safe, it is assumed this occurs 25 days a year.

The Launch and recovery of the mining equipment is expected to occur 16 times a year, as the system must be recovery when the sea-state exceeds the design conditions and for maintenance purposes roughly every three months. This process takes roughly one day as explained in 4.3.5.

The offloading process happens every 7th mining day based on the storage capacity of the vessel and takes between 14 – 17 hours as explained in 4.7.

The remaining of the year is spent in transit mode between harbor and mining site for maintenance that is required to be done in the harbor.

For each of the operating modes, the power requirement is calculated, this is shown in Figure 45.

With 70 % of the time spend mining, this will be the focus for the powerplant and define the installed power aboard the vessel. The main power consumers aboard are the thrusters, vertical transport system, and the launch and recovery system. Certain modes like the offloading on LARS operating modes are only used for a limited amount of time. This means it can be considered to make use of energy storage aboard to deal with these power peaks.

The minimum required power is 27,5 MW for the mining 2 operating mode and a maximum power of 29,5 MW is required for the offloading and mining process. The lowest operating mode is in the harbor, when only 3 MW is required for the accommodation unit. With the minimum offshore power being 11,5 MW in dynamic positioning.

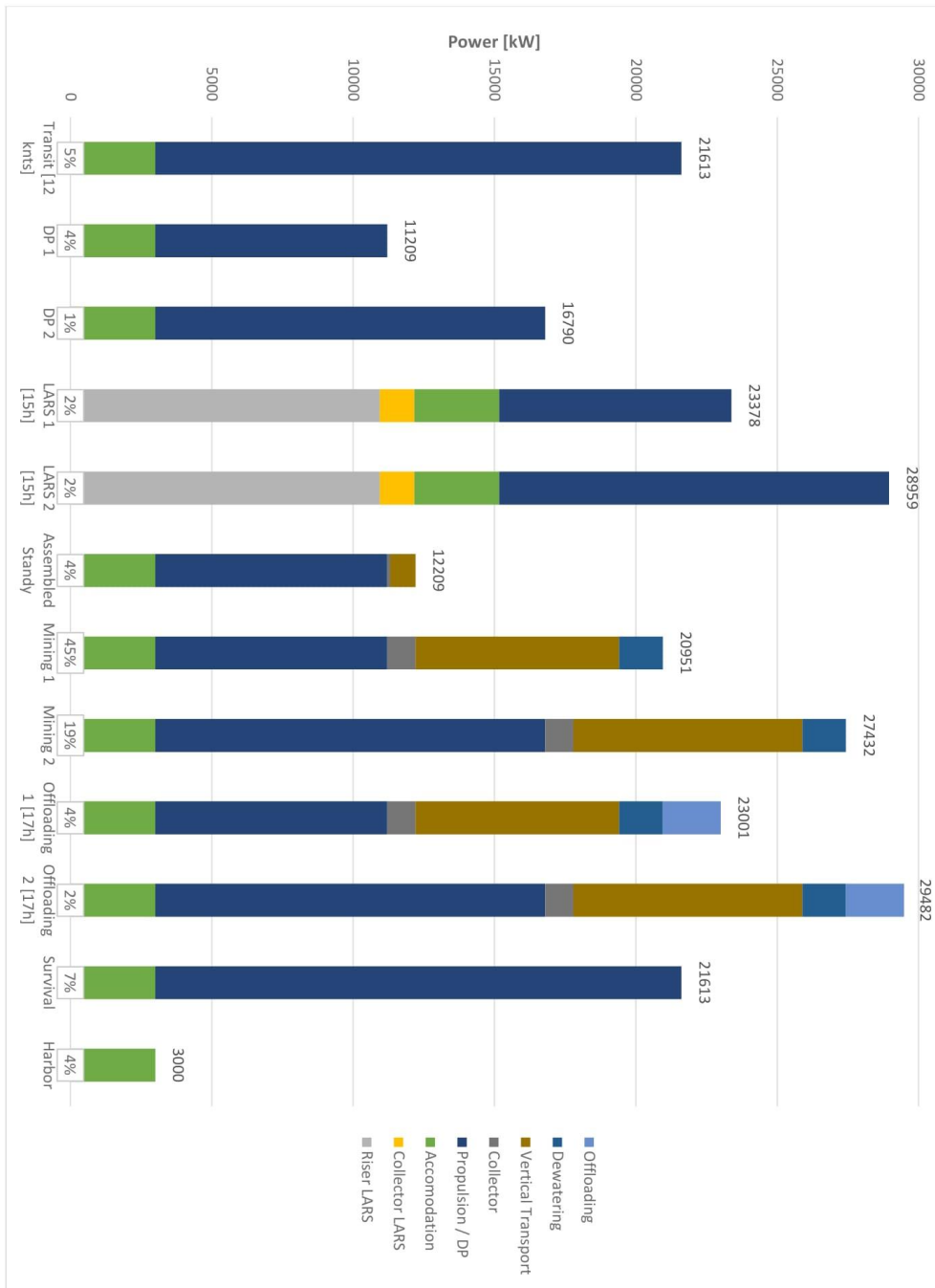


Figure 45: Hydraulic VTS - OP

6.2 Powerplant concept – Diesel Generators

A well known marine powerplant is the internal combustion engine. Which offers a robust solution which can run on a number of widely available fossil fuels. In this case four Wartsila 7L46DF Dual fuel engines are installed to generate up to 32 MW in total. Four engines are chosen for the redundancy they offer, and it allows to possibility to switch one or two engines off in lower power modes, to run the powerplant more efficiently. Dual fuel engines are chosen, as they offer a more versatile emissions compliance. This makes the powerplant more futureproof by allowing the use of LNG for lower overall emissions.

The engine room is depicted in Figure 46 and is situated in the stern of the hull. The engine room which houses the four engines [1] measures 25 meters in length.

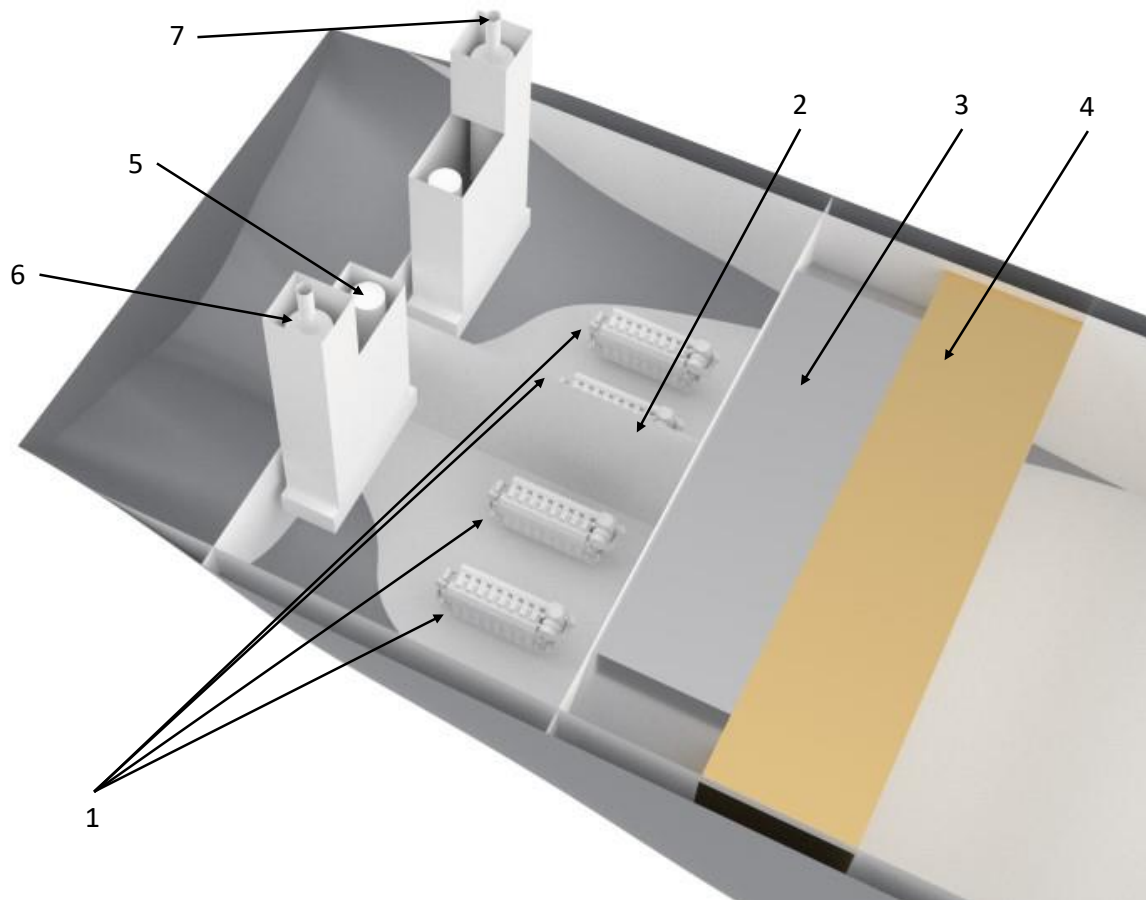


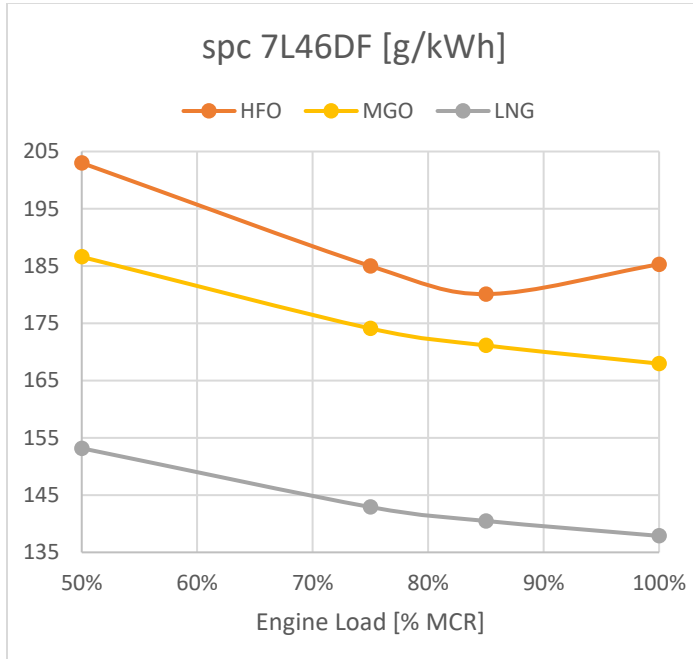
Figure 46: 4 x 7L46DF Engine Room

As seen in the drawing, the four engines can be separated into two engine rooms by a watertight frame [2]. This makes the vessel DP3 compliant. This offers additional redundancy and can be implemented as the four engines mean that only the watertight frame is needed.

The engine properties are shown in Table 33.

The specific fuel consumption of this engine over its power range is shown in Figure 47.

Table 33: Wartsila 7L46DF Properties



Wartsila 7L46DF		
Length	9,8	m
Width	3,2	m
Height	4,9	m
Weight	124	t
P_B	8 015	kW
N_e	390 – 600	Rpm
Airflow	12,9	Kg/s
Exhaust flow	12,8	Kg/s
Exhaust temp.	365	°C
Lube oil. Sfc	1 – 3.5	g/kWh

Figure 47: Wartsila 7L46DF sfc

The CAPEX of this powerplant can be estimated by the specific cost of \$ 250 / kW, yielding a total cost of \$ 8,01 million (Frederico et al., 2005).

The fuel tank [3] is situated in front of the engine room and is constructed in the shape of a heptagon to allow for the narrowing hull towards the stern and allow for a strong construction, to also be able to carry LNG. Its dimensions depend on the fuel used. The different fuels are compared in Table 34.

A more detailed overview of the fuel consumption in its different power modes can be found in Appendix K – Hydraulic VTS spc.

Table 34: Wärtsilä 8L46DF Fuel options

		HFO	MGO	LNG
Fuel Price (04/2022)	\$ / t	840	1 140	1 800
		Fuel Tank		
Fuel tank volume	m ³	3 639	3 829	6 170
Fuel tank length	m	5,7	6	9,6
		Specific Fuel Consumption		
Mining sfc	g/kWh	193	175	143
Average sfc	g/kWh	193	177	144
		OPEX		
Bunkering Cost	k\$	2 965	3 667	4 720
Annual Fuel Cost	k\$	32 986	41 034	52 907
		Emissions		
CO₂	g/kWh	655,7	618,8	433,4
NO_x	g/kWh	12,3	11,7	0,8
SO_x	g/kWh	4,0	0,4	0
PM	g/kWh	1,2	0,2	0
CO	g/kWh	0,7	0,7	1,5
UHC	g/kWh	0,3	0,3	0,1

As can be seen, the chosen fuel has a big impact on the fuel tank dimensions, annual operational expenditure and the emissions. LNG is the “cleanest” fuel but is required to be stored under pressure and cooled, requiring a bigger fuel tank. The OPEX of LNG is also 40 % higher than that of HFO. In all cases however, CO₂ is still a big problem that can’t be ignored. With HFO and MGO emitting over 100 000 tons of CO₂ annually and LNG emitting roughly 80 000 tons per year.

6.2.1 Energy Storage

As has been discussed for the power systems aboard, some of them have dynamic energy demand over time. The DP-system requires up to 10 MW of additional power over 5 – 8 seconds of time. The riser LARS requires 5 MW of additional power over 1 minute of time. This means that within a minute the energy requirement can vary by up to 15 MW.

For the varying load factor, an energy storage solution is installed, as the diesel generators can’t throttle up fast enough to meet these energy peaks. It also allows the diesel generators to run more efficiently at their design rpm. A 1 MWh energy storage solution with a maximum output of 15 MW is chosen, to allow enough reserve to power the DP-system and riser LARS for a couple minutes.

For this size, the best solutions are flywheels or battery storage, as explained in 2.7. A battery is prioritized over a flywheel as it is better suited for irregular peaks and is a more flexible solution. A battery can however not perform as many full charge/discharge cycles. So, the storage is chosen significantly bigger than required to allow the State of Charge of the battery to stay between 20 % and 80 %.

Based on current batterie technology, the energy density can be taken at 350 Wh/l and a specific weight of 175 Wh/kg (Kortlever, 2021). This gives the battery a weight of 6 tons and a volume of 3 m³.

6.2.2 CO₂ – Reduction

With the CO₂ exhaust emissions still being a big polluter, which can't really be reduced as it is an inherent consequence of burning fuel, there are some solutions to capture the CO₂ from the exhaust and store it. This technology is called Carbon Capture and Storage or CCS for short. For some land-based power plants, like gas turbines, this is currently being done. Capturing the CO₂ does however require additional energy and a storage solution is needed.

With carbon dioxide only having a density of 1,87 kg/m³, storing it at atmospheric conditions would be unfeasible. It can however be cooled and compressed to achieve higher densities; the phase diagram of CO₂ is shown in Figure 48.

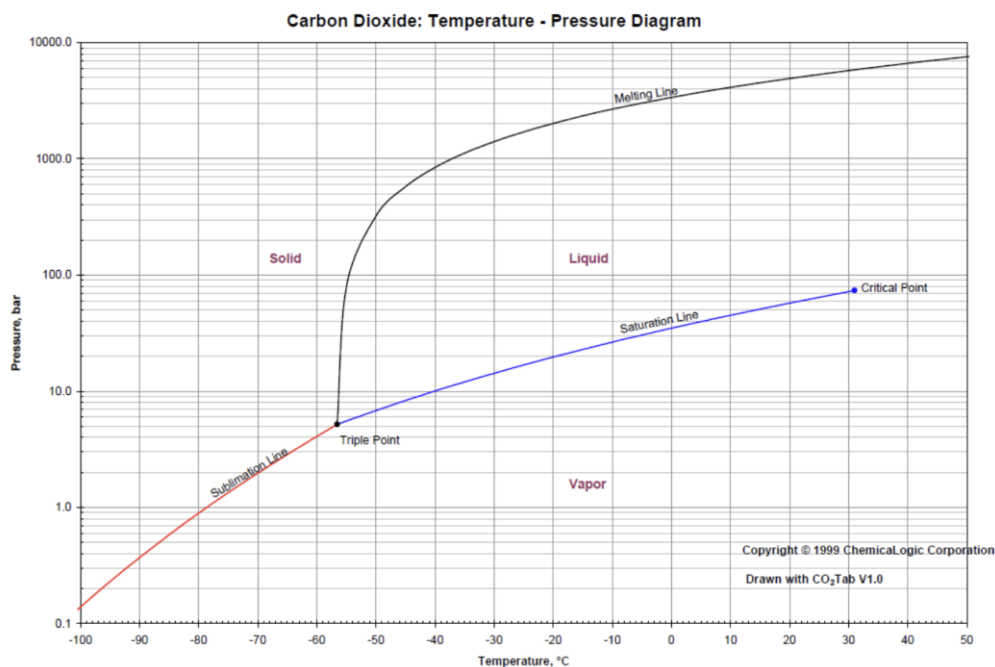


Figure 48: CO₂ Phase Diagram

The triple point of CO₂ is 5,18 bar at -56,6 °C. So, at atmospheric conditions it's a gas, and it will need to be pressurized to its liquid phase or cooled to its solid phase. The solid phase is considered impractical as it's less easy to transport, store, and unload it.

A promising solution to achieve this without requiring an additional cold source, is to use the cold from the stored LNG to cool compressed carbon dioxide into its liquid form. The complete process of capture and storage is visualized in Figure 49.

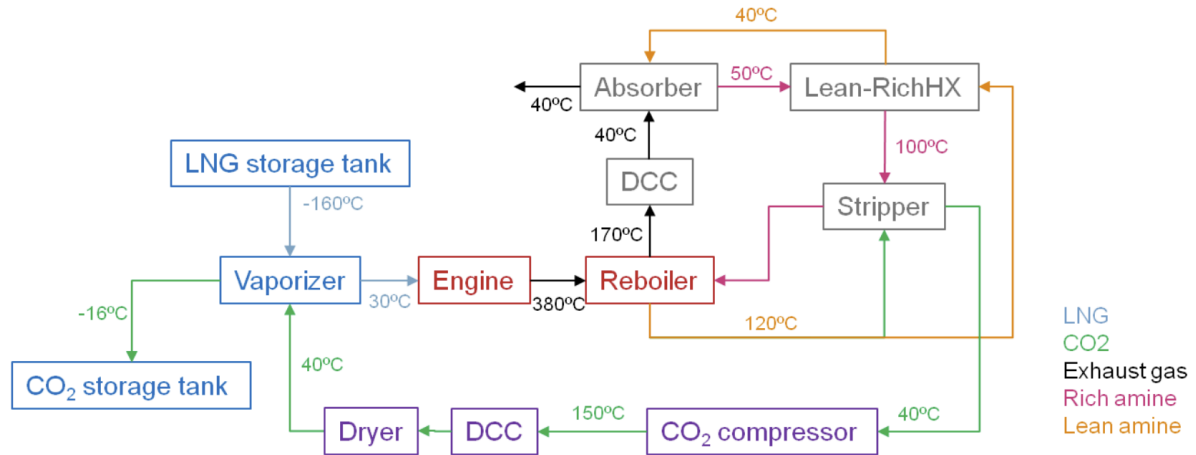


Figure 49: LNG cooled CCS (van den Akker, 2017)

While this concept was worked out for 8000 DWT general cargo vessel, a later study scaled this solution for the large crane vessel “Sleipnir”, which is powered by four engine rooms consisting of three 8 MW DF engines. As this vessel has very similar engines and exhaust flow, the concept for the “Sleipnir” can be relatively easily implemented on this study. The conceptual design is similar to the process depicted in Figure 49 and the worked-out concept can be found in Appendix H – Sleipnir LNG-fueled Ship Based Carbon Capture.

This system would have a capture rate of 80 %. This means that the new carbon dioxide exhaust emissions of the vessel are:

$$per_{CO_2} = 20\% * 2750 \frac{g CO_2}{kg LNG} = 550 \frac{g CO_2}{kg LNG} \quad (44)$$

$$spe_{CO_2} = 20\% * 433,4 \frac{g CO_2}{kWh} = 86,7 \frac{g CO_2}{kWh} \quad (45)$$

The CO₂ will be compressed to 20 bar and then cooled to – 20 °C into its liquid phase. This yields a density of 1032 kg/m³. For the fuel tank of 2 622 tons of LNG, this means 5768 tons of CO₂ is captured and needs to be stored on board in the tank depicted in Figure 46 [4]. The main components of the system are shown in Table 35 (Ros et al., 2022; van den Akker, 2017).

Table 35: SBCC Properties

	Diameter	Height	Weight
Direct Contact Cooler (DCC)	3,03 m	2 m	≈ 3 t
Absorber [5]	2,95 m	7 m	≈ 6 t
Stripper [6]	2,27 m	7 m	≈ 7 t
Heat Exchanger	2 m	6 m	≈ 20 t

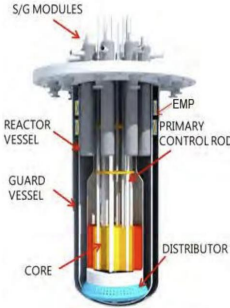
To ensure the DP3 functionality, the two engine rooms both have their own capture plant. The whole operation of capturing and compression requires 1 MW of power, so for both engine rooms this is 2 MW. In the current powerplant configuration there is enough headroom for this additional power.

6.3 Powerplant Concept – SMR

With just over 70 % of the operational time spend in high power modes during the mining process, nuclear energy is a good alternative to provide vast amounts of energy on the vessel. While no custom solution exists for this application, the small modular reactor (SMR) discussing in the literature can be scaled up to suit the powerplant concept. The MicroURANUS is scaled up roughly 50 % to accommodate the larger core and necessary steam generator to generate the additional 30 MW's of thermal power.

The powerplant components are listed in Table 36. They consist of the nuclear reactor, a containment building, and a steam turbine with generator to generate 30 MW of electrical power. The containment building is a reinforced concrete box filled with water, which functions as the last barrier to contain radiation and radioactive substances. The water acts as a biological shield for the radiation and the walls of the building are 800 mm thick to block remaining radiation (IAEA, 2020).

Table 36: Hydraulic SMR Properties

30 MW SMR									
MicroURANUS			Containment Building			Steam Turbine			
									
Diameter	4	m	Length	15	m	Length	16	m	
Height	9	m	Width	15	m	Width	3,4	m	
			Height	17,5	m	Height	5	m	
Weight	250	t	Weight⁵	≈2 700	t	Weight	105	t	
P_thermal	90	MW				P_B	30	MW	
Lifetime	40	years				P_{max}	140	Bar	
						T_{max}	540	°C	
						N_{max}	12 000	Rpm	
						Efficiency	33	%	

With the reactor being fueled for 40 years of operations, meaning that no refueling is needed during the lifetime of the vessel. This means that this concept doesn't have any refueling cost. The CAPEX of the plant is difficult to determine but can be estimate by the installed power. With an SMR estimated at around \$ 2 901 / kW, this yields a total cost of \$ 87,03 million (Mihelčič et al., 2020). For the steam turbine, \$ 500 / kW can be taken as a reference, yielding a cost of \$ 15 million (Alex Dopico, 2020). This makes the total cost of the powerplant at around \$ 102 million.

⁵ 0,8 m thick reinforced concrete (IAEA, 2020)

6.3.1 Dynamic Performance

The heat created by fission inside the reactor is transferred to water to create steam. These steam generators are placed within the reactor vessel. The steam turbine then transfers this thermal energy into mechanical energy and subsequently into electrical energy. To control the electrical energy output, the heat rate in the reactor must be controlled. The surplus of heat can also be discharged by the steam, but this requires an additional heat exchanger to get rid of this excess heat.

Control rods can be inserted into the reactor core to block fission from happening. The further the rods are pushed down into the reactor core, the less room for fission to occur and the lower the heat output of the reactor is. This must be done in a slow and controlled manner to ensure a stable fission reaction in the reactor. When the control rods are pushed down too far the temperature inside the reactor falls too much, resulting in the reactor shutting down. This means there is a minimum power level to ensure a stable fission reaction. This minimum is not known for this reactor but looking at nuclear reactors overall, a minimum of 15 % can be assumed (Preston, 2013).

7 Airlift VTS – Powerplants

The second DSM production support vessel concept focusses around the airlift riser system. Which is analysis for its benefits of being lower in maintenance and downtime, which should offer a higher yearly production rate of about 6 %. In this chapter the powerplant concept for this riser system are explained.

The operational profile is shown in Table 37. The main difference compared to the hydraulic system lies in the downtime of the system. With all moving system above deck any problem can be quickly resolved and the compressor is expected to have a negligible downtime. This results in 15 more mining days over the year, which are distributed over “mining 1” and “mining 2” operating modes.

Table 37: Operating modes Airlift VTS

Operating Mode	Sea-state	Description	Time
Transit	Mild	Roughly 20 days a year the vessel is cruising between a nearby port and the mining site. This will mainly be due to maintenance.	5 %
DP 1	Mild	The vessel stays in DP mode when it's offshore but not mining due to weather or maintenance related downtime.	4 %
DP 2	High	Same as “DP 1” but in a heavier sea-state.	1 %
LARS 1	Mild	(dis)assembling the riser and collector systems at the mining location.	2 %
LARS 2	High	Same as “LARS 1” but in a heavier sea-state.	2 %
Assembled Standby	Mild	Staying in DP-mode at the mining location with riser and collector deployed but not mining due to any downtime.	2 %
Mining 1	Mild	Mining nodules at 1 knots.	47 %
Mining 2	High	Same as “Mining 1” but in a heavier sea-state.	21 %
Offloading 1	Mild	Offloading the nodules to a transport vessel and continue mining at 1 knots.	4 %
Offloading 2	High	Same as “Offloading 1” but in a heavier sea-state.	2 %
Survival	Extreme	Staying offshore at the mining site during a storm/hurricane. There are 40 extreme weather days a year in the CCZ.	7 %
Harbor	/	Staying in a nearby harbor for maintenance or other purposes.	4 %

For the airlift concept, the difference mainly lies in the mining operating modes. Here the compressor requires 22,5 MW of power, this can clearly be seen in Figure 50. This makes the four mining modes significantly higher than other modes. With a required power of 42,6 MW for mining and a peak load of 44,7 MW during offloading operations.

The other modes are very similar to the hydraulic concept, except for 4 % more mining time due to the airlift system requires less maintenance.

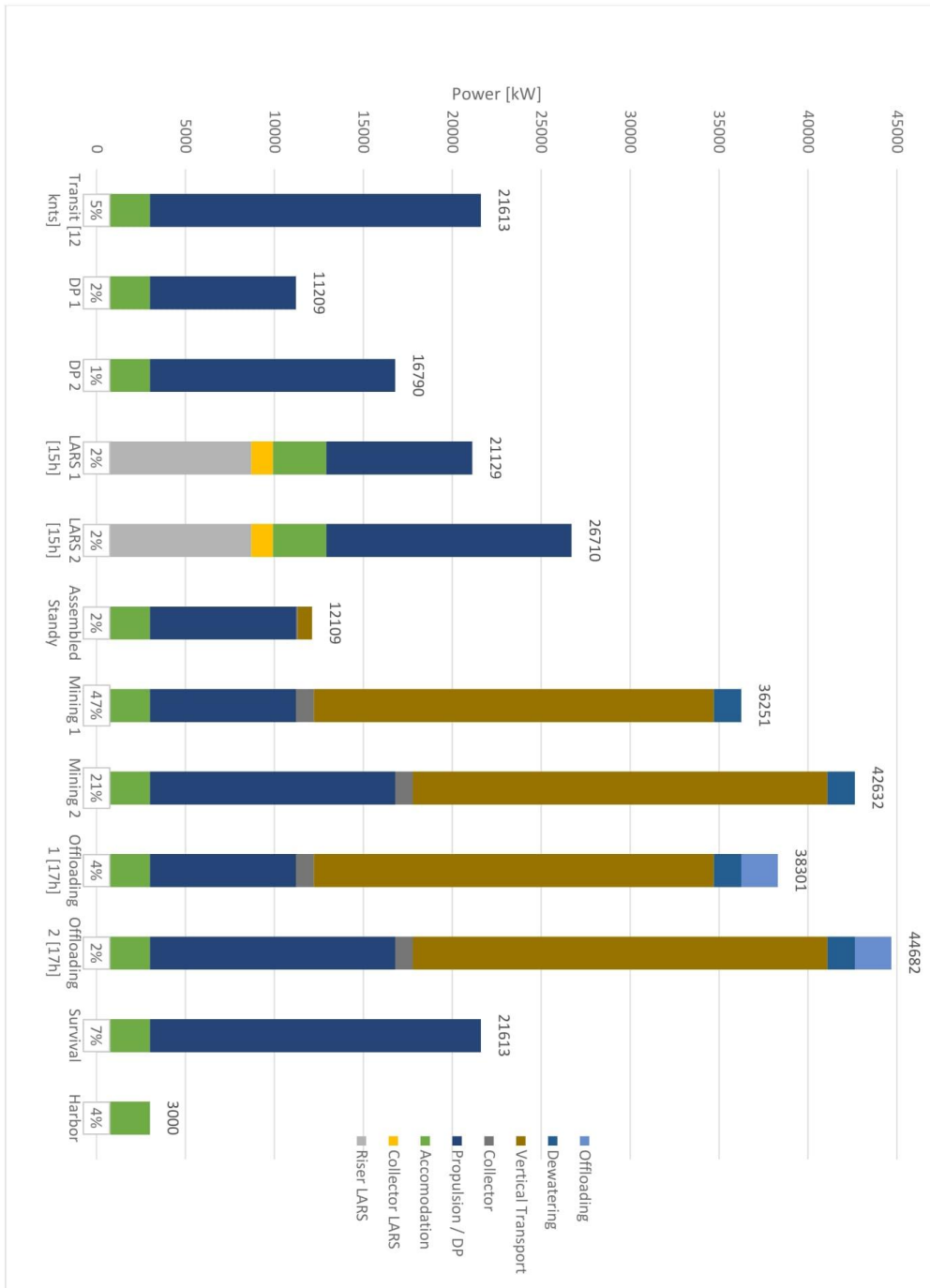


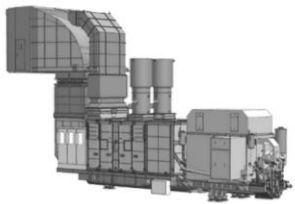
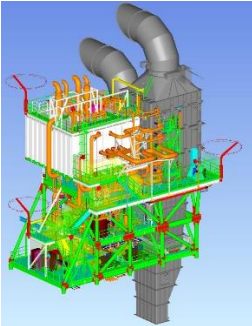
Figure 50: Airlift VTS - OP

7.1 Powerplant Concept – COGES

For the airlift concept, a similar concept to the hydraulic concept can be used. With a set of diesel generators to achieve the necessary power. This would in effect be a scaled-up solution with five Wartsila 8L46DF engines instead of three. The bigger power requirement does however also open up new options.

The compressor is the biggest power consumer aboard with 22,5 MW needed to power it. This can be achieved with a large electric motor, but direct drive may be a more suitable solution. The compressor can be driven by a gas turbine or steam turbine. This makes a Combined Gas – Electric Steam (COGES) powerplant an attractive option. A corresponding power plant to the required power level required is shown in Table 38.

Table 38: COGES Properties (Flatebø, 2012)

42,3 MW COGES								
Gas Turbine: LM2500 G4			HRSG			Steam Turbine		
								
Length	16	m	Length	20	m	Length	16	m
Width	3,4	m	Width	10	m	Width	3,4	m
Height	5	m	Height	20	m	Height	5	m
Weight	220	t	Weight	140	t	Weight	105	t
P_B	32 600	kW				P_B	10 800	kW
N_e	3000	Rpm				P_{steam}	24	Bar
Airflow	90	Kg/s	Steam flow	11	Kg/s	T_{steam}	470	°C
Exhaust flow	90	Kg/s						
Exhaust temp.	526	°C						
Efficiency	38,3	%	Efficiency	69	%	Efficiency	30,1	%

A detailed schematic of this powerplant is shown in Appendix D – COGES Plant Schematic

The gas turbine can provide a maximum of 32,6 MW and the steam turbine can add an extra 10,8 MW to that to achieve a total power of 42,3 MW. The cost of this COGES plant can be estimated at \$ 32,67 million based on its size and configuration (ONSITE SYCOM Energy Corporation, 2000).

The fuel options for the COGES plant are shown in Table 39. A DF engine is added as reference to show the differences between both options.

Table 39: COGES Fuel options

		HFO	MGO		LNG	
		DF	DF	COGES	DF	COGES
Fuel Price (04/2022)	\$/t	840	1 140		1 800	
		Fuel Tank				
Fuel tank volume	m ³	5 653	6 116	5 867	9 933	9 532
Fuel tank length	m	8,8	9,5	9,2	15,5	14,9
		Specific Fuel Consumption				
Mining sfc	g/kWh	181	170	163	140	134
Average sfc	g/kWh	187	174	185	143	150
		OPEX				
Bunkering Cost	k\$	4 606	5 857	5 618	7 699	7 292
Annual Fuel Cost	k\$	48 650	61 635	60 843	79 922	78 497
		Emissions				
CO₂	g/kWh	630,6	606,1	598,3	426,9	419
NO_x	g/kWh	11,8	11,5	0	0,7	0
SO_x	g/kWh	3,9	0,3	0	0	0
PM	g/kWh	1,1	0,2	0,1	0	0
CO	g/kWh	0,7	0,7	0	1,5	0
UHC	g/kWh	0,3	0,3	0,1	0,1	0,1

As can be seen, the main advantage of the COGES plant is its high efficiency at fuel load. This results in the mining sfc being significantly lower than the DF engine option. Conforming that the COGES plant yields and overall better efficiency, but the average sfc shows that it is important to keep the plant running at its optimum to ensure this efficiency. This can also be seen in the fuel consumption over the power load, depicted in Figure 51.

A more detailed overview of the fuel consumption in its different power modes can be found in Appendix L – Airlift VTS spc.

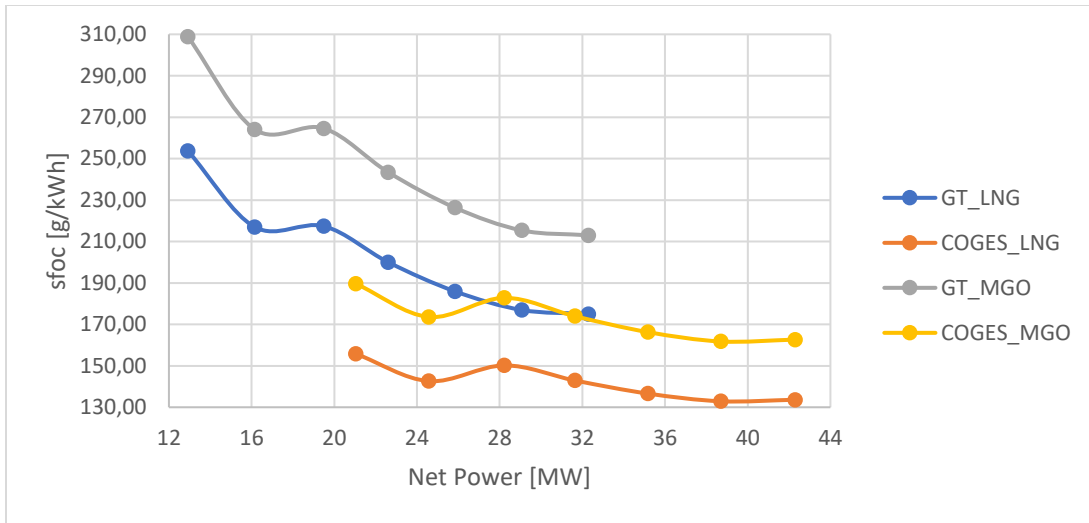


Figure 51: COGES sfc (Flatebø, 2012)

This shows that an energy storage solution for this powerplant would be quite advantageous to improve the running at high efficiencies. The arrangement of this powerplant is shown in Figure 52. With the gas turbine [1], compressor [2], HRSG [3], and the steam turbine [4].

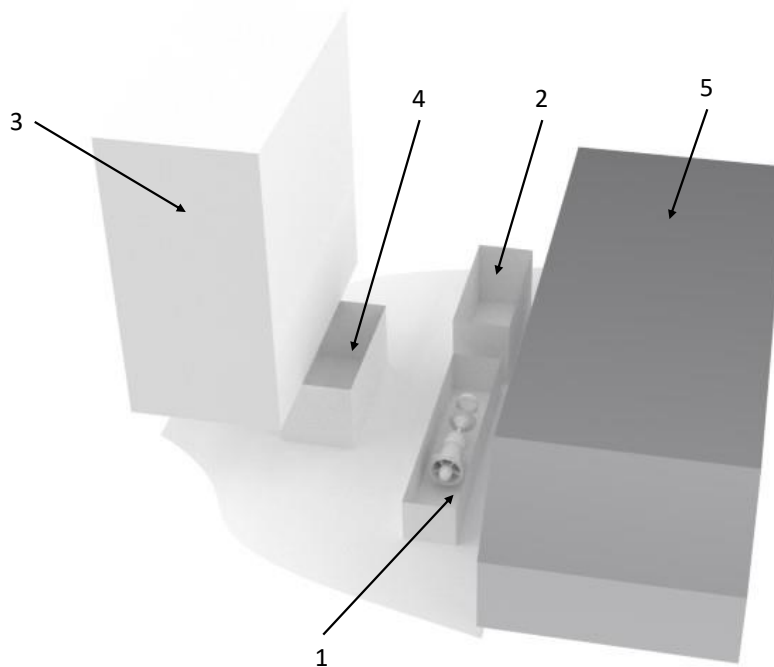


Figure 52: COGES General Arrangement

As fuel LNG is chosen as it offers the best environmental consideration as seen with the DF engine in the previous powerplant concept. The LNG tank [5] measures 15 meters long. The LNG also offers cold work which can once again be used for liquid CO₂ storage.

7.1.1 Energy Storage

Similar to the hydraulic transport, a 1 MWh battery is added for similar reasons to deal with sudden energy peaks. As the dynamic energy draw is similar.

7.1.2 CO₂ – Reduction

With this powerplant still emitting a substantial amount of CO₂ despite its efficiency, a similar carbon capture and storage solution as with the hydraulic transport can be used. With LNG also used as fuel in this case, the setup is identical and only has to be scaled to have the required storage capacity. This would result in a CO₂ tank of 10 795 m³. This is a very large tank which would measure over 16 meters in length, that can't be fitted inside the chosen hull, so hull modifications would be required to achieve this. This shows that CCS is less suited for bigger powerplants with larger fuel tanks.

With the powerplant efficiency and the LNG as fuel, the emissions are already significantly reduced and further reduction with CCS would require substantial changes to the vessels hull.

7.2 Powerplant Concept – SMR

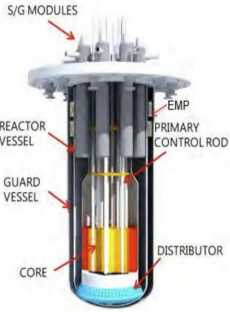
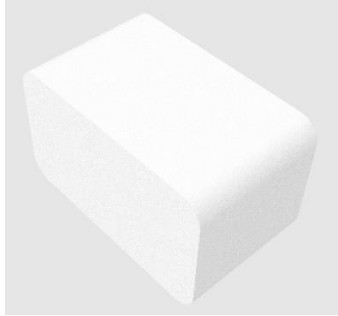
With the airlift system running close to full power for more than 70 % of the time, another solution is nuclear energy. This however has social-political considerations as well as technical ones, in this thesis only the technical size will be discussed.

As solution for this concept, two 60 MWt MicroURANUS reactors are chosen, as they offer the required power and are a custom-made marine solution which meets the demands of offshore operations and are well within bounds to fit inside the vessel's hull together with the containment unit. The containment unit is a concrete box shaped around the two reactors. The box is filled with water, to reduce the radiation.

The two reactors have integrated steam generators that produce the required steam for the steam turbines. Each reactor powers a 20 MWe steam turbine which means the efficiency of the turbine is around 33 %. As has been seen with the COGES plant, the steam turbine's efficiency is very similar over its load factor. The limiting factor in this powerplant is however the reactor which power output remains constant and is difficult to adjust.

The properties of the powerplant are shown in Table 40.

Table 40: SMR Properties

40 MW SMR								
MicroURANUS			Containment Building			Steam Turbine		
								
Diameter	3	m	Length	15	m	Length	16	m
Height	9	m	Width	25	m	Width	3,4	m
			Height	15	m	Height	5	m
Weight	200	t	Weight⁶	≈3 500	t	Weight	105	t
P_thermal	60	MW				P_B	20	MW
Lifetime	40	years				P_{max}	140	Bar
						T_{max}	540	°C
						N_{max}	12 000	Rpm
						Efficiency	33	%

⁶ 0,8 m thick reinforced concrete (IAEA, 2020)

As explained before, this concept has no fuel cost and its capex can be estimated at \$ 126,04 million (Alex Dopico, 2020; Mihelčič et al., 2020).

While the containment unit makes the power plant very heavy, without a fuel tank the overall weight is still lower than previous concepts. The general arrangement of the powerplant is shown in Figure 53. With the steam turbines [1], generator & compressor [2], and containment unit [3] which houses the reactors.

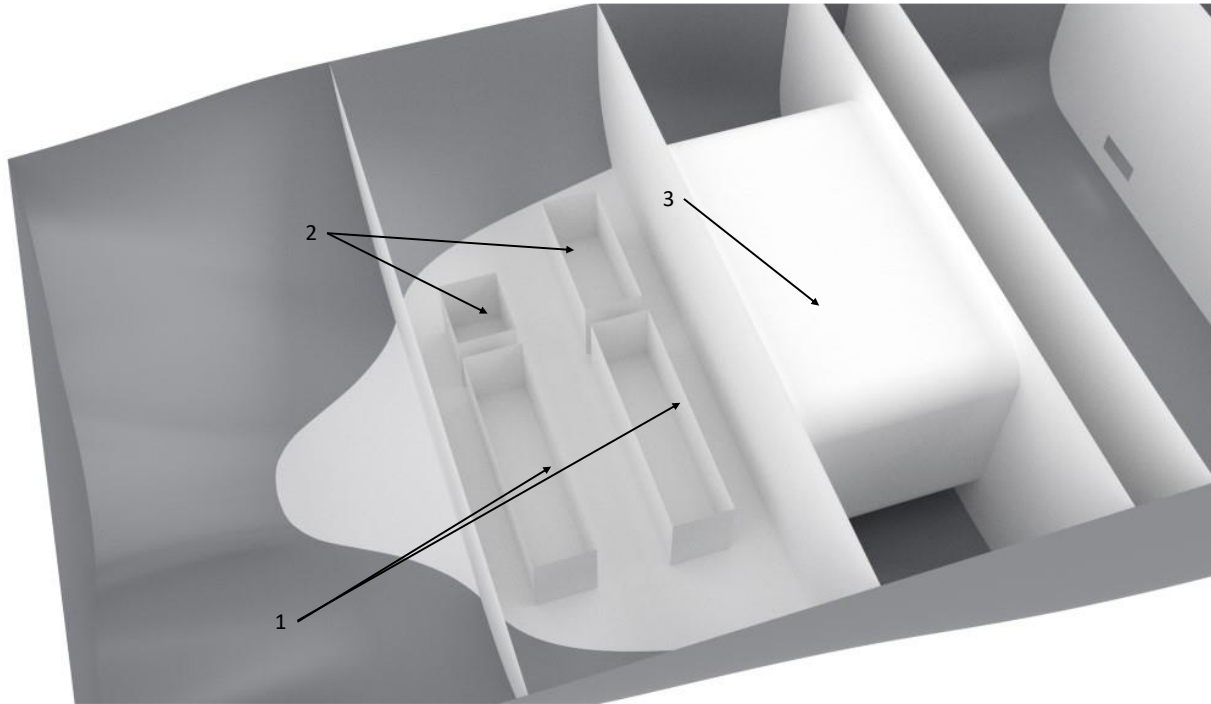


Figure 53: SMR General Arrangement

As it is difficult to adjust the power output of this powerplant, an energy storage solution is needed to balance the power load on the reactors. With the two reactors, one reactor could be switched off for lower power loads. This can however only be done a couple times a year without damaging the reactor. In the harbor, the ship's load is too low, and the reactors will have to be shut down.

8 Discussion

From the literature up to the powerplant concepts, a lot of knowledge gaps have been filled in the field of deep-sea mining and the future of powerplant in a low emission future. But it also showed that DSM is still a new industry with a lot of unknowns which offer opportunity for new solutions. This chapter will attempt to highlight these opportunities and points of discussion that have been encountered along the way.

8.1 Vessel systems

The DSM production support vessel has a multitude of function and a large amount of system aboard. As seen in the literature research, for each function different approaches with different system are available. The systems aboard are also dependent on the scale of the operation. As different systems work better at different production rates.

With the scale of the mining operation up for debate, it's worth to have a sensitivity analysis of scaling the different systems. For this thesis the 400 t/h production rate was chosen as previous research and economical research focused on this metric and offers a good basis to build upon. Going below this level, is considered economically unfeasible at this stage, and scaling up would invoke economies of scale but also increase the upfront investment. So, taking a look at the different systems in place, how sensitive are they to scaling and what alternative systems are worth a second look?

- Seabed Collector:

Starting from the ground up, the Coanda-effect collector is currently the best solution for the chosen production rate. It does however still have a significant effect on the marine environment and could as such prove an unsustainable method. With less disturbing methods like mechanical collection being advocated. Mechanical collection is best suited for small production rates and can be combined with a simpler vertical transport system, as nodule can be transported as bulk in this case.

The Coanda based collector can be easily scaled up by increasing its width with additional collector heads. A wider collector will be heavier and increasingly difficult to launch overboard. The 16-meter-wide collector pushes the maximum of current A-frames and AHC knuckle-boom cranes. But with larger offshore cranes, bigger collectors could be deployed. It will however be more interesting to first scale up with more collectors on the ground, before scaling the collectors themselves.

- Vertical transport System:

The vertical transport system (VTS) has been extensively examined in this thesis, with both the hydraulic- and airlift-concept. Both systems have however only been tested in model scale and further test will have to show if the theoretical conclusions carry over in practice. The VTS production rate can be controlled to a certain level by adjusting the flowrate. With the hydraulic pumps, this becomes a power balance as at a certain flow rate it is more advantageous to increase the diameter rather than the pump pressure. With the airlift system, this is more

difficult to control. As large airflow rates create annular flow inside the pipe whereby air dominates the pipe and leaves little room to transport the nodule slurry. So, this is an optimization process with having an airflow at a certain diameter to create a bubbly- or slug-airflow to allow a high nodule density in the pipe. Current oil & gas riser pipes are however not wider than 50 cm ID, increasing the pipe diameter above this would require a custom-made system. So, this could become a bottleneck when scaling up the operation, as riser dynamics will also have to be analysed when changing the riser pipe.

- Dewatering plant:

The dewatering process is quite straightforward, but the whole vessel design has struggled with where to place this process. As keeping the nodules slurry wet until the transport vessel would make ship-to-ship transfer easier and eliminate the need for a dewatering plant aboard the production vessel. The dewatering system itself is custom-made for this production rate. Increasing it would require a lot of power and deck space or comes with a lower efficiency. As hydrocyclones and logwasher are more difficult to scale-up compared to dewatering- and vibration-screens. This means that an increase in production needs to outweigh the drop in dewatering efficiency.

8.2 Vessel design

In general, four processes need to happen offshore: Collection, Vertical transport, dewatering, and transport to shore. Dewatering is deemed necessary as transporting the nodules as a fluid is both very inefficient and brings stability concerns. In this thesis most of these functions are fulfilled by the production support vessel, this has been done for the sake of simplicity. It has however become clear that other configurations may also be advantageous. Cause having all these systems on one vessel makes the vessel quite large and heavy (> 100 000 DWT). It also makes the vessel expensive and if one system fails, the whole operation has to be shut down.

A separate support vessel could for example carry the collectors or assemble the VTS, and as such spread the systems out over multiple smaller vessels. An interesting alternative to the current configuration is sketched in Figure 54.

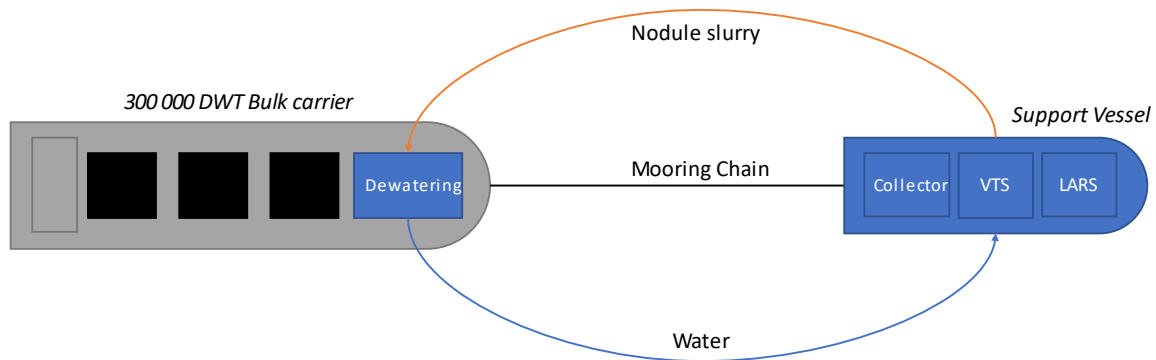


Figure 54: Alternative mining configuration

In this scenario, the support vessel only carries the mining equipment and could be substantially smaller, functioning something like a combine harvester. With a bulk carrier being connected with a dewatering module, making the offloading process continuous. This way a large bulk carrier could be modified with a dewatering module and slowly fill up. Such a configuration could easily scale up by increasing the flow rate and make wet offloading a robust solution. With a 300 000 DWT bulk carrier, as seen in the sketch, the loading would take roughly a month. Which would only require two bulk carrier to be operational, and maintenance on the mining system could be carried out in-between.

On the other hand, it remains a question if this would cause a significant size reduction of production vessel, as a lot of mining equipment requires deck space. Could some of the equipment be placed in the hull, to reduce the size of the support vessel?

8.3 Powerplant

With the powerplant concept, a strong emphasis was put on emissions. As it can be expected that the DSM industry and the marine industry as a whole will be subject to ever stricter emission legislation. IMO has adopted the vision to reduce carbon dioxide emissions with 50 % by 2050 compared to 2008 levels. Achieving this has proven difficult, generally engines have become more efficient, but CO₂ will remain the same per unit of fuel burned. By using LNG, CO₂ is reduced by roughly a third. CO₂ storage has also been examined but does require having basically two fuel tanks aboard and the CO₂ still needs to go somewhere. Getting rid of this CO₂ could become a big problem, definitely if this becomes a household practice. So, while LNG is a helping hand, meeting this goal set by IMO proves difficult with current powerplants.

With this in mind, nuclear energy was examined as alternative. Nuclear energy proved quite advantageous in several ways. It pretty much eliminates operational emissions, but its also significantly cheaper over its lifetime, gets rid of offshore bunkering, and is even a bit lighter (incl. fuel). This is however highly dependent on fuel prices, if LNG prices drop back to \$ 400 – 500 as in 2020 – 2021, nuclear is economically unfeasible. But looking at the current situation, LNG is likely to stay around \$ 1 500 and may even rise further as LNG demand keeps rising. If this stays the case, a strong environmental- and economical argument can be made for nuclear power.

With the DSM vessel operating in international waters and not needing to be in specific ports, this also makes nuclear more feasible as doesn't have to fear to be denied port entry due to its nuclear powerplant.

8.4 Energy storage – LAES

In pursuit of minimizing fuel costs and running the powerplants more efficiently, energy storage has played a large part in the powerplant concepts. With storage requirements between 10's and 100 MWh, batteries are not always the preferred solution due to their weight, space, and price. Fuel cells can prove a good alternative to store energy in chemical compounds which can be stored in large tanks.

With the airlift system however, an alternative was found with liquid air energy storage (LAES). Which compresses and cools air to store it in liquid form. Which is an interesting concept that proved compelling due to the cold form the LNG and compressor from the airlift which could work together to make this system work. This is however a very unknown system that has a lot of room for improvement. The system boosts efficiencies over 100 % as the cold energy from the LNG adds more energy than is put into the system through the compressor.

By releasing the air from its liquid and compressed storage, energy can be generated as its expands and heat's up. The process of this is shown in Figure 55.

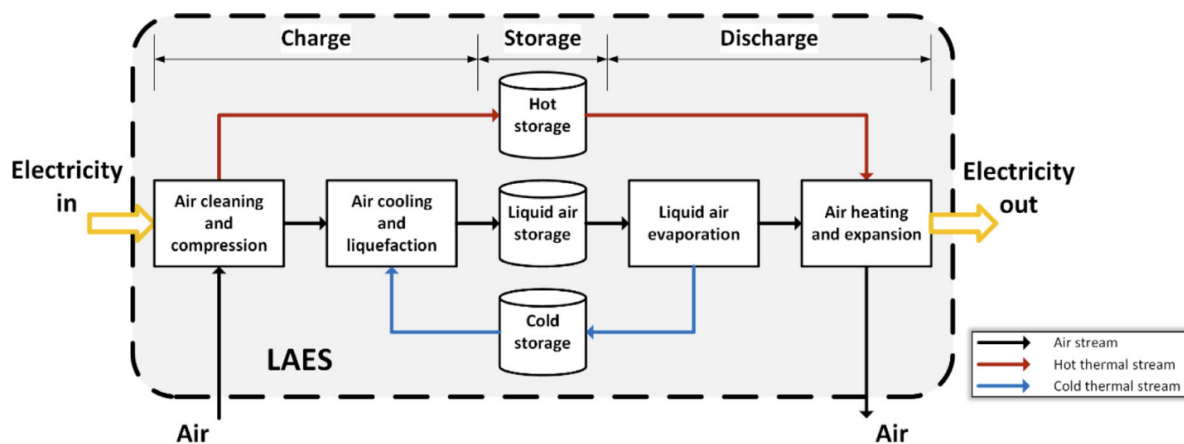


Figure 55: LAES (Vecchi et al., 2021)

For this air to become liquid it must be compressed and cooled to the critical point or below. This is shown in Figure 56.

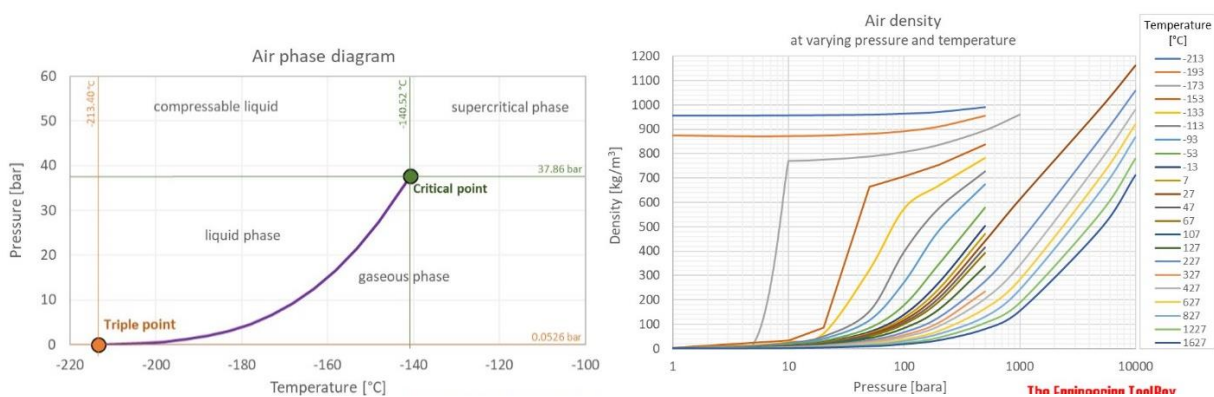


Figure 56: Air Phase Diagram (a) & Air Density (b) (Engineering ToolBox, 2018)

The air can then be further compressed as a compressible liquid, or the air will be in supercritical state once heated up above its critical temperature of 133 Kelvin. The density of liquid air is significantly higher than compressed gaseous air, as can be seen in Figure 56b. With a density around 800 kg/m³.

A concept of a Liquid air energy storage system with LNG powered cooling is shown in Figure 57.

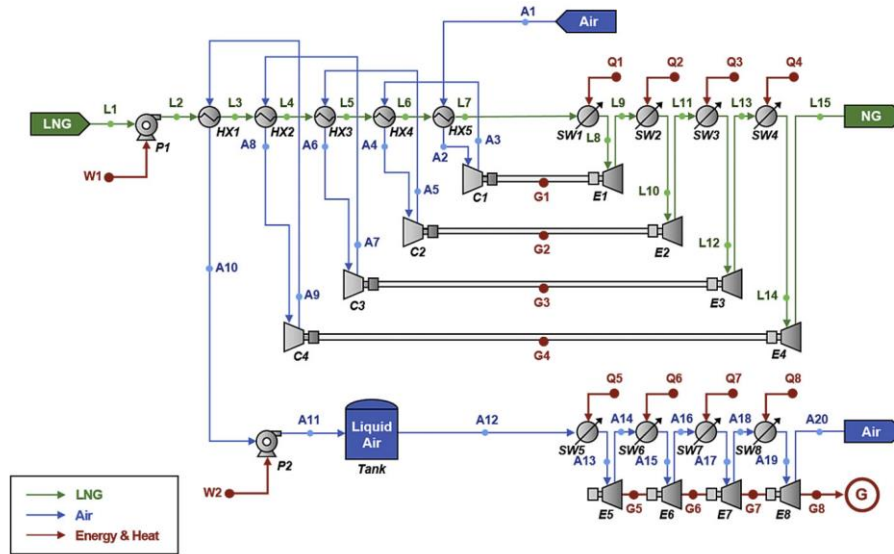


Figure 57: LAES (Lee et al., 2017)

In this case the air is cooled down and compressed in stages to get the gaseous air into its liquid state. The T-s diagram of this process is shown in Figure 58. The heat exchange between air and LNG is done by a direct contact cooler (DCC). This is however only the case for high temperature differences (ΔT). this means that when the LNG is above $-60\text{ }^{\circ}\text{C}$, a DDC cannot be longer efficiently used to cool the air. The remaining cold from the LNG can be extracted by using a cooling fluid in a Rakine-, or Brayton-cycle (Lee et al., 2017).

This concept uses the expansion of the LNG to drive a turbo to compress the air. This could also be done in this case, but as the compressor is already installed onboard doing the work, this will be left out for now. But may prove an option for increasing efficiency in the future.

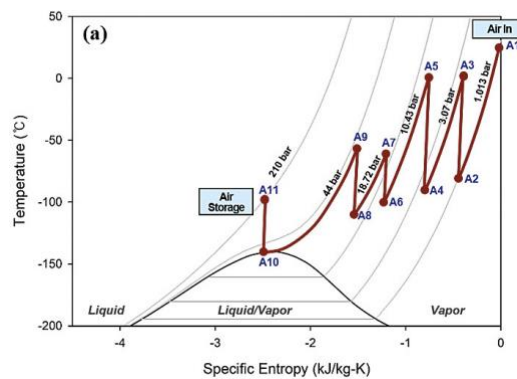


Figure 58: T-s Diagram dry air (Lee et al., 2017)

So, by further customizing the solution to the compressor size with the accompanying LNG flowrate, a more efficient and larger energy storage solution can be achieved.

It may also be beneficial to use the compressor to increase the flowrate rather than the compression ratio, as the density of liquid air is more dependent on temperature rather than pressure. Compressed air is also a form of energy storage but would require significantly higher pressures than needed for the airlift system and require much stronger storage tanks.

The energy captured and released by the LAES system is at a constant rate. This means a battery-electric storage buffer is needed to be able to deal with power variations.

Ideally this solution would allow for running in higher engines modes during transit and LARS 1, to harvest energy. This energy can then be used for peak load during offloading and with the necessary modifications can be used to run solely on the energy storage in low power modes, like during harbor visits or DP operations.

9 Recommendations

With the information gathered and analyzed in this thesis, points of interest are noted down in this section which require further research.

1. **Production rate of the mining operation**

In this thesis a production rate of 400 t/h was chosen, as most information is available at this scale. Looking at the systems analyzed in this thesis, chosen a smaller size looks achievable and offers a small-scale start-up solution. Scaling up the systems with a higher production rate could also increase the revenue of the operation significantly. Hereby the onboard storage will need to be reassessed based on the offloading interval. The research in this thesis did not support 400 t/h as a local or global optimum for the scale of the operation.

2. **Compact & low-power large scale dewatering**

Wet-offloading was discharged in this thesis as a second dewatering plant on the transport vessel would be too large and require too much power. If a compact footprint dewatering system with acceptable power draw can be achieved, wet-offloading can become a better alternative to the dry-offloading. The efficiency of the dewatering plant will have to be re-evaluated together with the chosen grain size of the nodules.

3. **Increasing operability of offloading methods**

The dry-offloading method chosen in this thesis has a limited operational window. While dry-offloading seems the better choice, the offloading boom will have large vertical movements if the vessel is subject to roll. An active heave compensation system may be able to decrease the relative movement of the boom and increase the operability of the offloading system.

4. **Continuous offloading & eliminate onboard storage**

Storing the nodules aboard and then offloading them at a very high rate requires both a lot of volume and power. By having a continuous offloading process, the onboard storage can be eliminated, and the offloading process can be a smaller scale. This would yield a smaller vessel with a lower power requirement. But if the chosen production rate of 400 t/h is best suited needs analyzing, as a higher production rate would likely suit such a solution better.

5. **Liquid Air Energy Storage**

The COGES powerplant concept for the airlift system opens up the possibility for LAES. The cold from the LNG can be used to cool compressed air from the compressor into its liquid state. This is however a complex solution which is best suited for large scale energy storage between 10's – and 100's MWh's. It however reuses the cold from the LNG and as such increases the overall energy efficiency onboard. Can this complex system be integrated at this scale in a way to increase to powerplant efficiency?

6. **Small Nuclear Reactor dynamic performance**

Using an SMR as powerplant proves a good solution in terms of power, weight, and costs. The reactor can't however be throttled up or down like an engine. The control rods offer a way to reduce power, but at which rate and to which level remains uncertain. How can this be controlled, and which systems can be put in place to ensure smooth dynamic power delivery?

7. **Liquid CO₂ storage**

Storing the CO₂ from the exhaust gasses in a liquid form onboard, is a good solution to significantly reduced the vessels emissions. But with CO₂ tank needing to be even bigger than the fuel tank, this solution requires a lot of volume. Sizing down the fuel tank or CO₂ tank would help a lot but decrease the operationality of the vessel. Could a compromise be found here, which would result in a compact vessel design and is it required to match the CO₂ tank to the fuel tank?

10 Conclusion

Combining the different subsystems identified in the introduction, a DSM production support ship has been put together by using modularity to have the comparison between different solutions for some of the subsystems.

10.1 Modular design – subsystems

The five main subsystems for the vessel with their solutions are summed up below.

- Mining: Coanda-effect collector which sucks up a slurry of nodules, sand, and water. The collector is launched and recovered with its umbilical using an A-frame.
- VTS: An oil & gas riser system consisting of riser joints fitted with buoyancy elements is used to transport the slurry to the surface. A derrick tower can assemble the system in around half a day. Both an airlift- and hydraulic system is considered.
- Dewatering: For the dewatering process, the Boskalis Chatham rock phosphate mining concept is chosen. As it has a high dewatering efficiency, can filter down to 1 mm particles, and is well suited for the scale required in this concept.
- Storage: Storage for 9 mining days is selected based on the blue nodules mining project, which considers offloading every 7th mining day and having a 2-day buffer for contingency.
- Unloading: The dry nodules are offloaded by a conveyor belt system fitted underneath the cargo holds. The nodules are moved above deck by being trapped between two conveyor belts. A 76-meter-long offloading boom is situated on portside and dumps the nodules into a bulk carrier.

With the vertical transport system, both the options were considered. The hydraulic transport system with a series of booster stations is the more convenient solution with known systems from dredging but is time consuming in maintenance and prone to clogging with the moving parts so far underwater. The airlift concept is quite unknown and only tested on small scale. With the compressor onboard, maintenance and downtime can easily be dealt with, but this comes at a 10 MW power penalty.

Both dry offloading with conveyor belts, and wet offloading with pumping a water-nodules slurry through a floating pipeline were considered. Dry offloading can only be undertaken up to 2-meter wave height, ensuring a 43 % operability, but this method is selected as there is a lot of room for improvement and imposes minimal constraints on the transport vessel. As the transport vessel can be a DP2 equipped bulk carrier. In contrast, wet offloading requires an additional dewatering plant which would require additional power and deck space.

The choice of offloading system will however have no significant impact on the ship design and only lead to a small change in power requirement.

10.2 Ship design

Putting all the subsystems together with the added peripherals to make it all work, a preliminary ship design is generated, shown in Figure 59.

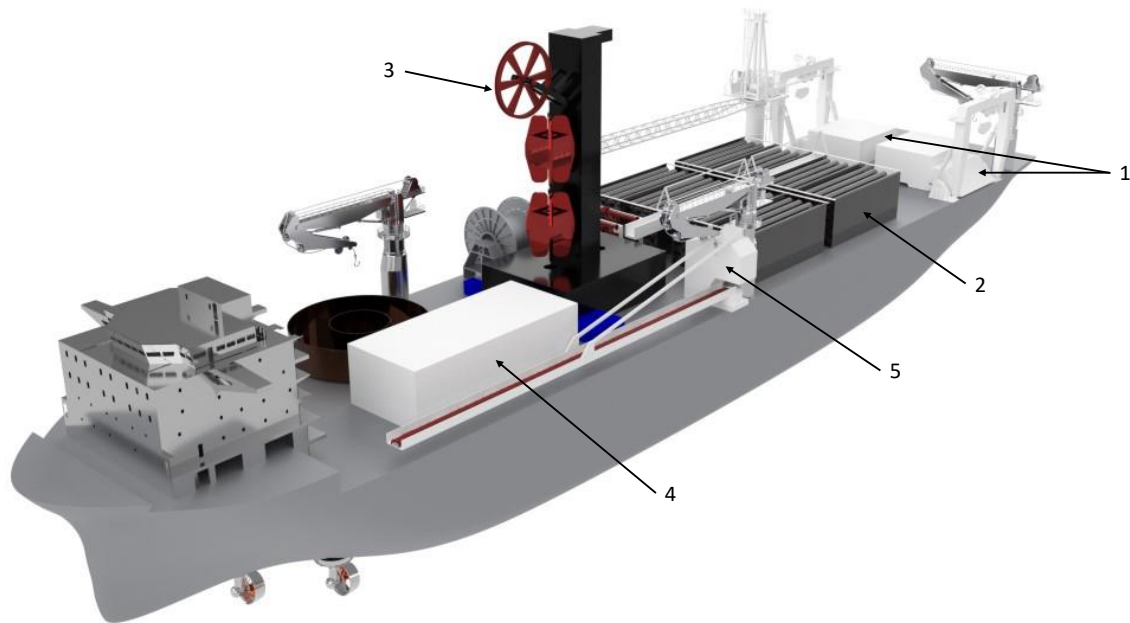


Figure 59: Complete vessel design

The collectors [1] are stored at the stern, with the riser joint storage [2] in front of it. The assembly tower [3] for the riser is situated over the moonpool which measures 25,6 meters by 12,5 meters. The nodules slurry goes through the dewatering plant [4], before being stored in the cargo holds situated in the hull. The offloading boom [5] on portside swings out to dump the nodules into a bulk carrier.

The vessel is propelled by three azimuth thrusters at the stern, capable of achieving 17,5 knots. With three additional retractable azimuths in the bow for DP operations.

Hull properties			
Length o.a.	247 m	Block coef.	0,79
Beam	47,5 m	Depth	20 m
Transit		Mining	
Draft	7,4 m	Draft	12,8 m
Displacement	62 818 t	Displacement	117 863 t
GM	16,18 m	GM	10,93 m

The effect of the VTS on the ship design is minimal, with the addition of a large compressor in the engine room in case of airlift. While the hydraulic system requiring an additional 150 m² of deck space to fit the hydraulic pumps. The placement of the collector and riser joint storage at the stern does make the vessel stern-heavy, but this is chosen as it's the best compromise for assembling the mining systems and when all the equipment is deployed, the vessel's balance shifts to its center.

10.3 Powerplant concepts

With the preliminary ship design complete, powerplant concepts for both VTS concepts were worked out. The powerplants are designed within the emission targets set and with an eye on their capital- and operational- expenditure. Two concepts for both VTS configuration are worked out and listed in Table 41.

Table 41: Powerplant concepts

	Hydraulic VTS – 32 MW		Airlift VTS – 42 MW		
Revenue	\$ 1 452 mil		\$ 1 545 mil		
	DF-engine	SMR	COGES	SMR	
CAPEX	\$ 8 mil	\$ 102 mil	\$ 33 mil	\$ 126 mil	
OPEX ⁷	\$ 53 mil	/	\$ 79 mil	/	
lightweight	650 t	3 055 t	600 t	4 210 t	
Fuel (LNG)	2 622 t	/	4 051 t	/	
Deadweight⁸	3 272 t	3 055 t	5 851 t	4 210 t	
Energy Storage	1 MWh Battery	10 MWh Battery	1 MWh Battery	10 MWh Battery	

Hydraulic VTS:

- The first concept consists of four diesel generators. LNG is chosen as fuel to reduce the emissions to mostly carbon dioxide. To reduce this as well, the carbon dioxide is collected from the exhaust gasses. This is achieved by a stripper and an adsorber which separate the CO₂ based on its higher density. By using the cold from the LNG through a heat exchanger, the CO₂ can be cooled into liquid form, where it has a density of 1032 kg/m³ making it able to store it in a pressurized tank onboard.
- The second concept uses a Small Nuclear Reactor (SMR), to get rid of the CO₂ conundrum. The reactor is placed within a water filled reinforced concrete box to ensure it meets the safety requirements. This means a heavier powerplant, but without a fuel tank it remains lighter overall. The SMR is slower in ramping up or down, which means a larger energy storage is needed to deal with low power variations. This has resulted in a 10 MWh battery.

⁷ 2022 Bunker price LNG = \$ 1 800

⁸ Includes energy storage solution

Airlift VTS:

- With the larger power needed for airlift, a COGES powerplant offers better efficiency and emissions over diesel-generators. This does come at an increase in powerplant cost.
- While the COGES plant is very efficient and relatively low in emissions, an SMR solution as with the hydraulic VTS is a promising alternative, as it eliminates the remaining emissions and eliminates annual fuel costs running in the tens of millions. Two separate reactors are installed to deal with the larger energy need and add a level of redundancy. The two reactors also allow to run on lower power modes.

While nuclear energy can be interpreted as a holy grail in these settings, it is politically and socially challenging, its cost is also a very rough estimate and can easily rise significantly as this industry doesn't commercially exist. With rising fuel prices and tightening emissions regulations, it is a promising alternative with very low operational costs.

With SMR's being able to generate lots of power, increasing the power output to be able to run an airlift system only costs \$ 24 million, while increasing the yearly revenue by \$ 93 million. Making this a compelling cost-effective upgrade.

For the diesel generators and COGES powerplant it is another story, as high fuel prices eat into the advantage of airlift. Airlift fuel costs are 49 % higher than a hydraulic system. While over time the airlift system will compound its gains and become the more profitable solution, the hydraulic system with diesel generators offers a cheap and technologically ready design.

Appendix A – Riser Assembly Power Breakdown

Hydraulic Riser																					
Assembly	14142 kW	Hydraulic Power	max rated			usage factor		Power		Riser assembly Time/Joint # joints time Riser Joint 3 212 636 [min] Booster Joint 30 6 180 [min] Total 13.6 [hours]											
			min use	max use	min	max	min	max													
Riser Up	5200 kW	907	50	900 t	6%	99%	1634	8160													
Drawworks	860 kW	910	50	900 t	5%	99%	287	5160													
Top drive (no torque needed)		50 l/min					47	851													
Riser Spider	1000 kW	1000	50	900 t	5%	90%	50	900													
Riser Tensioner	100 kW	320 l/min																			
Carwalk	100 kW	100	100	100 kW	100%	100%	100	100													
Riser crane	1500 kW	400	0	348 t	0%	87%	0	1306													
Riser Return	1500 kW	400	0	348 t	0%	87%	0	1306													
Tensioner 1	1500 kW	400	0	348 t	0%	87%	0	1306													
Tensioner 2	2660 kW	650	0	0 t	0%	0%	0	0													
A&R Winch	172 kW	172	0	172 kW	0%	100%	0	172													
Carousel	250 kW	250	250	250 kW	100%	100%	250	250													
ROV	500 kW	500	500	500 kW	100%	100%	500	500													
Jumper hose	400 kW	400	400	400 kW	100%	100%	400	400													
Hydraulics	670 l/min						1634	10944													
<table border="1"> <thead> <tr> <th colspan="2">Return riser length</th> </tr> </thead> <tbody> <tr> <td>length</td> <td>6000 m</td> </tr> <tr> <td>Weight/m</td> <td>190 kg/m</td> </tr> <tr> <td>Hydrostatic force</td> <td>10781 kN</td> </tr> <tr> <td>Gravitational force</td> <td>17614 kN</td> </tr> <tr> <td>Sub. Weight</td> <td>696 t</td> </tr> </tbody> </table>										Return riser length		length	6000 m	Weight/m	190 kg/m	Hydrostatic force	10781 kN	Gravitational force	17614 kN	Sub. Weight	696 t
Return riser length																					
length	6000 m																				
Weight/m	190 kg/m																				
Hydrostatic force	10781 kN																				
Gravitational force	17614 kN																				
Sub. Weight	696 t																				

Airlift Riser										
Assembly	12842 kW	Hydraulic Power	max rated			usage factor		Power		Riser assembly Time/Joint # joints time Riser Joint 3 217 651 [min] Injection Joint 15 1 15 [min] Total 11.1 [hours]
			min use	max use	min	max	min	max		
Riser Up	4300 kW	680	50	600 t	7%	88%	316	3794		
Drawworks	860 kW	910	50	600 t	5%	66%	47	567		
Top drive (no torque needed)		50 l/min								
Riser Spider	1000 kW	750	50	600 t	7%	80%	67	800		
Riser Tensioner	100 kW	320 l/min								
Carwalk	100 kW	100	100	100 kW	100%	100%	100	100		
Riser crane	1500 kW	400	0	348 t	0%	87%	0	1306		
Riser Return	1500 kW	400	0	348 t	0%	87%	0	1306		
Tensioner 1	1500 kW	400	0	348 t	0%	87%	0	1306		
Tensioner 2	2660 kW	650	0	0 t	0%	0%	0	0		
A&R Winch	172 kW	172	0	172 kW	0%	100%	0	172		
Carousel	250 kW	250	250	250 kW	100%	100%	250	250		
ROV	500 kW	500	500	500 kW	100%	100%	500	500		
Jumper hose	400 kW	400	400	400 kW	100%	100%	400	400		
Hydraulics	670 l/min						1180	8695		

Collector										
Collector	300 kW	Hydraulic Power	max rated			usage factor		Power		Collector Lowering speed distance time A-frame 0.5 5000 15 [min] Lowering 166,667 15 [min] Touchdown 15 [min] Total 3.027778 [hours]
			min use	max use	min	max	min	max		
A-frame	1000 kW	425 l/min	150	120 t	0%	80%	0	800		
AH&C Winch	230 kW	425 l/min	230	230 kW	0%	100%	0	425		
Hydraulics							0	1225		

Appendix B – Operational Profile Hydraulic Transport

	Transit [12 knfs]		DP 1		DP 2		LARS 1 [15h]		LARS 2 [15h]		Assembled Steady		Mining 1		Mining 2		Offloading 1 [17h]		Offloading 2 [17h]		Survival		Harbor		
	Sea State	Mild	Mild	Mild	High	High	Mild	Mild	Heavy	Heavy	Mild	Mild	Mild	Heavy	Heavy	Mild	Mild	Heavy	Heavy	Mild	Heavy	Extreme	Extreme	/	/
	5%	5%	4%	4%	1%	1%	2%	2%	2%	2%	4%	4%	45%	45%	19%	19%	4%	4%	2%	2%	7%	7%	4%	4%	
Max Power [kW]																									
Riser/LARS	10944	10944					10944	10944	10944	10944															
Collector LARS	1225	1225					1225	1225	1225	1225															
Accommodation	3000	3000	3000	3000	3000	3000	3000	3000	3000	3000	3000	3000	3000	3000	3000	3000	3000	3000	3000	3000	3000	3000	3000	3000	3000
Propulsion / DP	27000	18613	8209	8209	13790	13790	8209	8209	13790	13790	8209	8209	8209	8209	13790	13790	8209	8209	8209	8209	13790	13790	13790	13790	18613
Collector	1000										100	100	1000	1000	1000	1000	1000	1000	1000	1000	1000	1000	1000	1000	
Vertical Transport	8100										900	900	7200	8100	8100	8100	7200	7200	7200	7200	8100	8100	8100	8100	
Dewatering	1542												1542	1542	1542	1542	1542	1542	1542	1542	1542	1542	1542	1542	
Offloading																		4047	4047	4047	4047	4047	4047	4047	
Total		21613	11209	16790	23378	28959	12209	20951	27432	24998	31479	21613	3000												

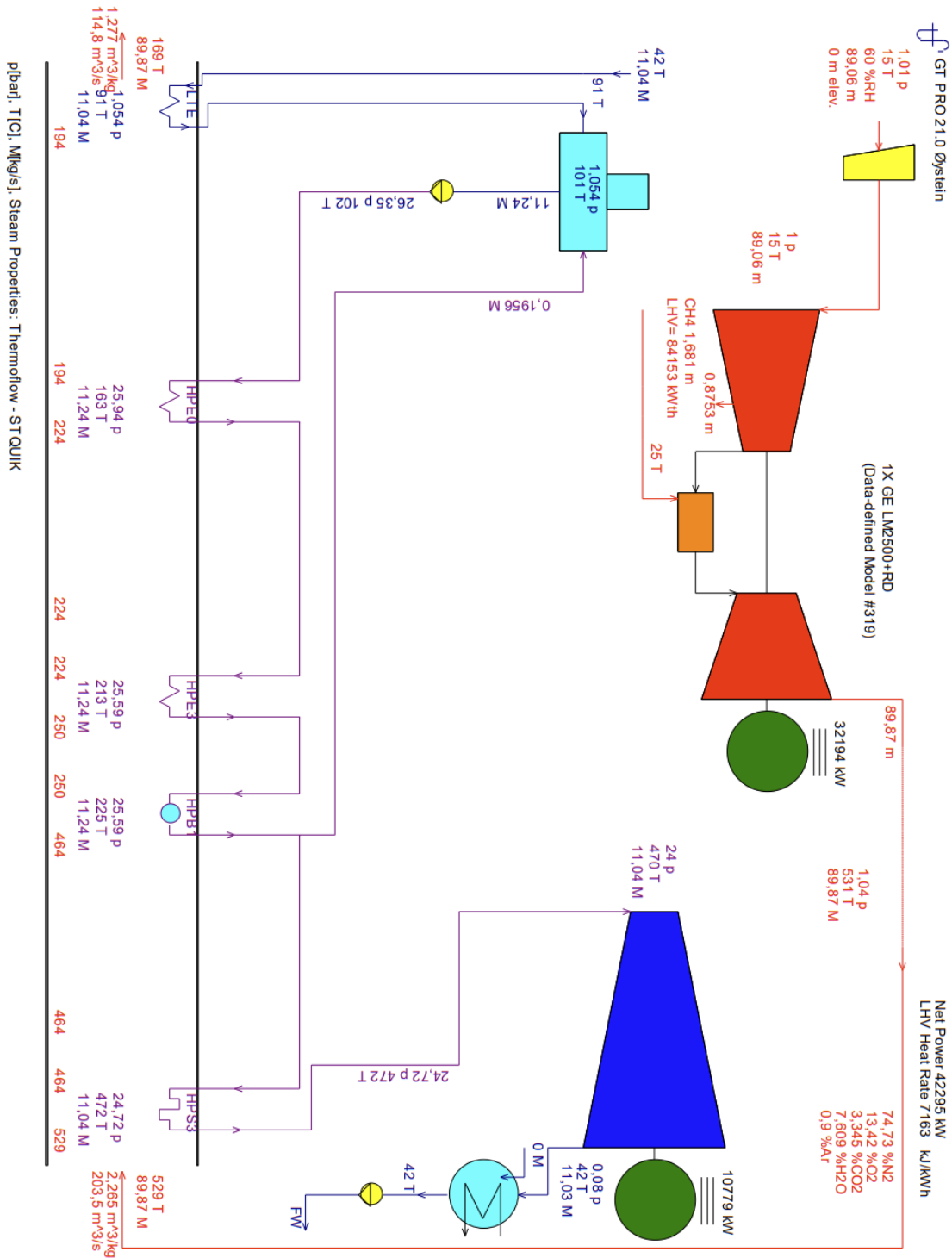
	Transit [12 knfs]		DP 1		DP 2		LARS 1 [15h]		LARS 2 [15h]		Assembled Steady		Mining 1		Mining 2		Offloading 1 [17h]		Offloading 2 [17h]		Survival		Harbor		
	Sea State	Mild	Mild	Mild	High	High	Mild	Mild	Heavy	Heavy	Mild	Mild	Mild	Heavy	Heavy	Mild	Mild	Heavy	Heavy	Mild	Heavy	Extreme	Extreme	/	/
	5%	5%	4%	4%	1%	1%	2%	2%	2%	2%	4%	4%	45%	45%	19%	19%	4%	4%	2%	2%	7%	7%	4%	4%	
Max Power [kW]																									
Riser/LARS	10944	10944					10944	10944	10944	10944															
Collector LARS	1225	1225					1225	1225	1225	1225															
Accommodation	3000	3000	3000	3000	3000	3000	3000	3000	3000	3000	3000	3000	3000	3000	3000	3000	3000	3000	3000	3000	3000	3000	3000	3000	3000
Propulsion / DP	27000	18613	8209	8209	13790	13790	8209	8209	13790	13790	8209	8209	8209	8209	13790	13790	8209	8209	8209	8209	13790	13790	13790	13790	18613
Collector	1000										100	100	1000	1000	1000	1000	1000	1000	1000	1000	1000	1000	1000	1000	
Vertical Transport	8100										900	900	7200	8100	8100	8100	7200	7200	7200	7200	8100	8100	8100	8100	
Dewatering	1542												1542	1542	1542	1542	1542	1542	1542	1542	1542	1542	1542	1542	
Offloading																		2050	2050	2050	2050	2050	2050	2050	
Total		21613	11209	16790	23378	28959	12209	20951	27432	24998	31479	21613	3000												

Appendix C – Operational Profile Airlift Transport

	Sea State [%]	Transit [12 knts]		DP 1		DP 2		LARS 1 [15h]		LARS 2 [15h]		Assembled Standby		Mining 1		Mining 2		Offloading 1 [17h]		Offloading 2 [17h]		Survival Extreme		Harbor /			
		Mild	5%	Mild	5%	High	2%	Mild	1%	Mild	2%	Heavy	2%	Mild	2%	Mild	47%	Heavy	21%	Mild	4%	Heavy	2%	Survival Extreme	7%	Harbor /	
Riser LARS	8695																										
Collector LARS	1225																										
Accommodation Propulsion / DP	3000		3000		3000		3000		3000		3000		3000		3000		3000		3000		3000		3000		3000		3000
Collector	1000		18613		8209		13790		8209		13790		8209		1000		1000		1000		1000		1000		1000		18613
Vertical Transport	23300														800		22500		23300		22500		23300		23300		23300
Dewatering	1542																1542		1542		1542		1542		1542		1542
Offloading	4047																				4047		4047		4047		4047
Total			21613		11209		16790		21129		26710		12109		36251		42632		40298		46679		21613		3000		3000

	Sea State [%]	Transit [12 knts]		DP 1		DP 2		LARS 1 [15h]		LARS 2 [15h]		Assembled Standby		Mining 1		Mining 2		Offloading 1 [17h]		Offloading 2 [17h]		Survival Extreme		Harbor /			
		Mild	5%	Mild	5%	High	2%	Mild	1%	Mild	2%	Heavy	2%	Mild	2%	Mild	47%	Heavy	21%	Mild	4%	Heavy	2%	Survival Extreme	7%	Harbor /	
Riser LARS	8695																										
Collector LARS	1225																										
Accommodation Propulsion / DP	3000		3000		3000		3000		3000		3000		3000		3000		3000		3000		3000		3000		3000		3000
Collector	1000		18613		8209		13790		8209		13790		8209		100		1000		1000		1000		1000		1000		18613
Vertical Transport	23300														800		22500		23300		22500		23300		23300		23300
Dewatering	1542																1542		1542		1542		1542		1542		1542
Offloading	2050																				2050		2050		2050		2050
Total			21613		11209		16790		21129		26710		12109		36251		42632		38301		44682		21613		3000		3000

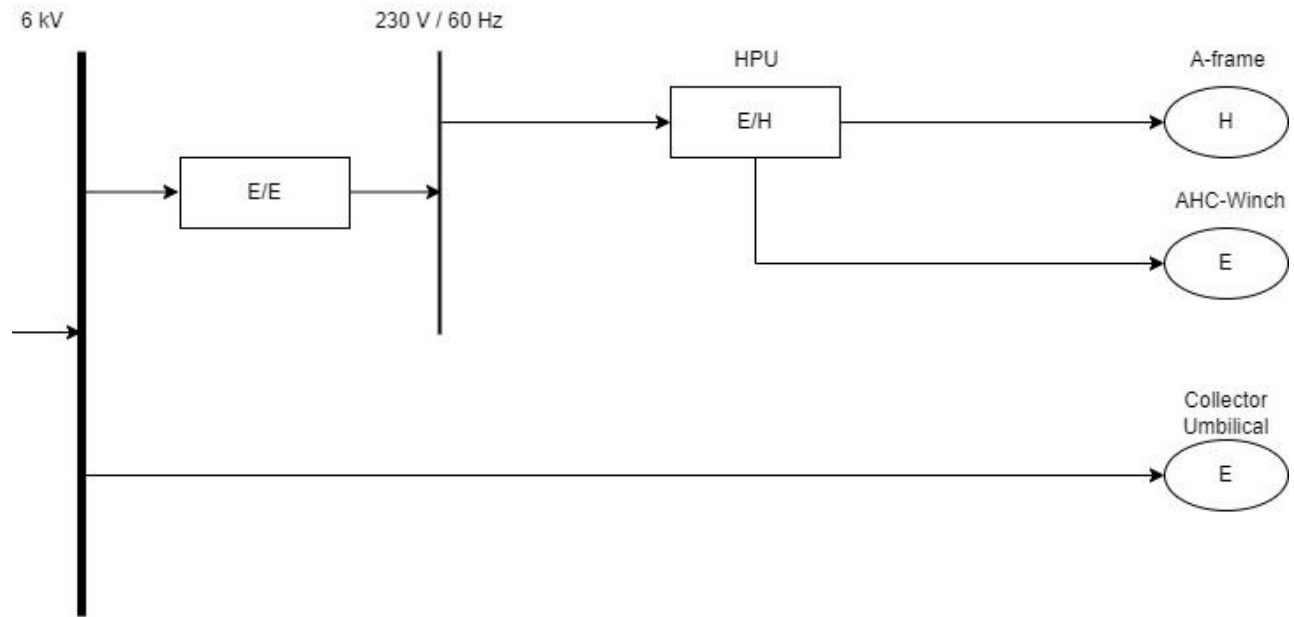
Appendix D – COGES Plant Schematic



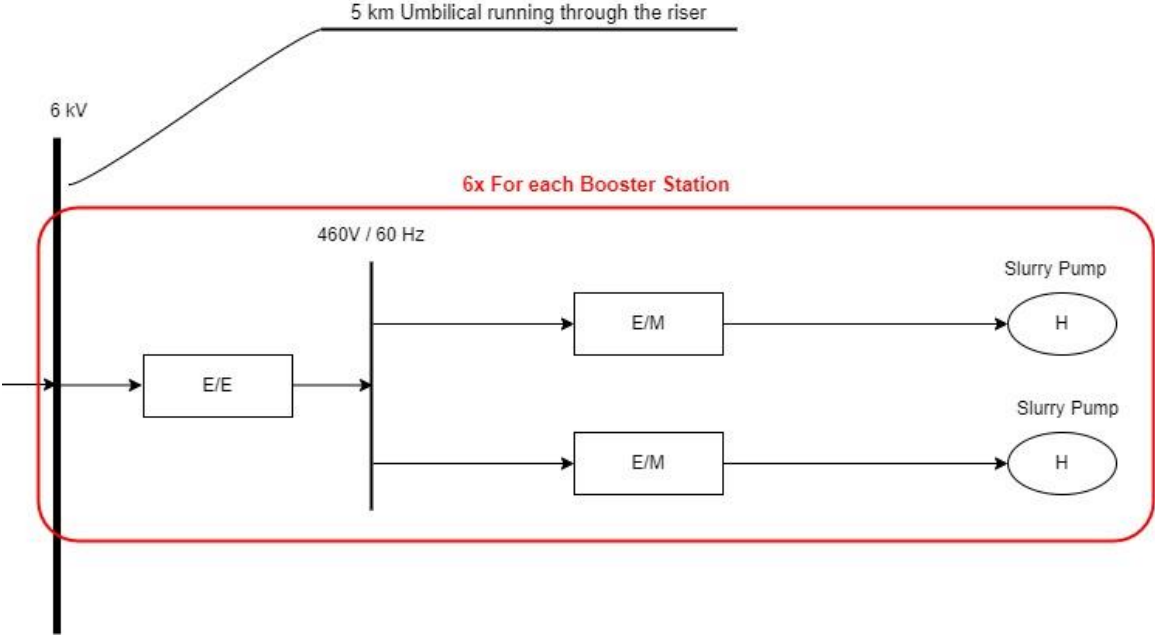
(Flatebø, 2012)

Appendix E – Energy Flow Diagram

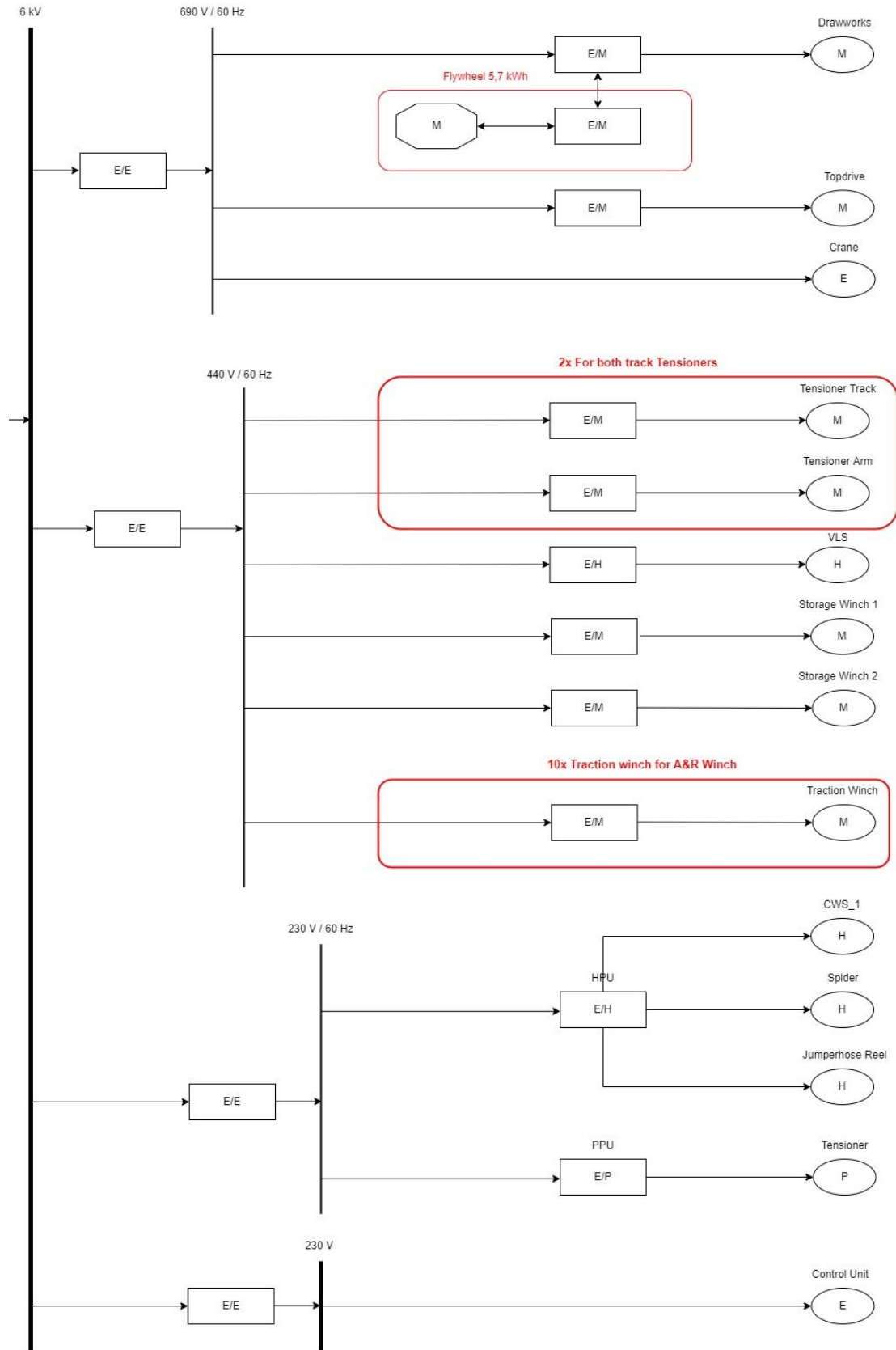
Collector – EFD



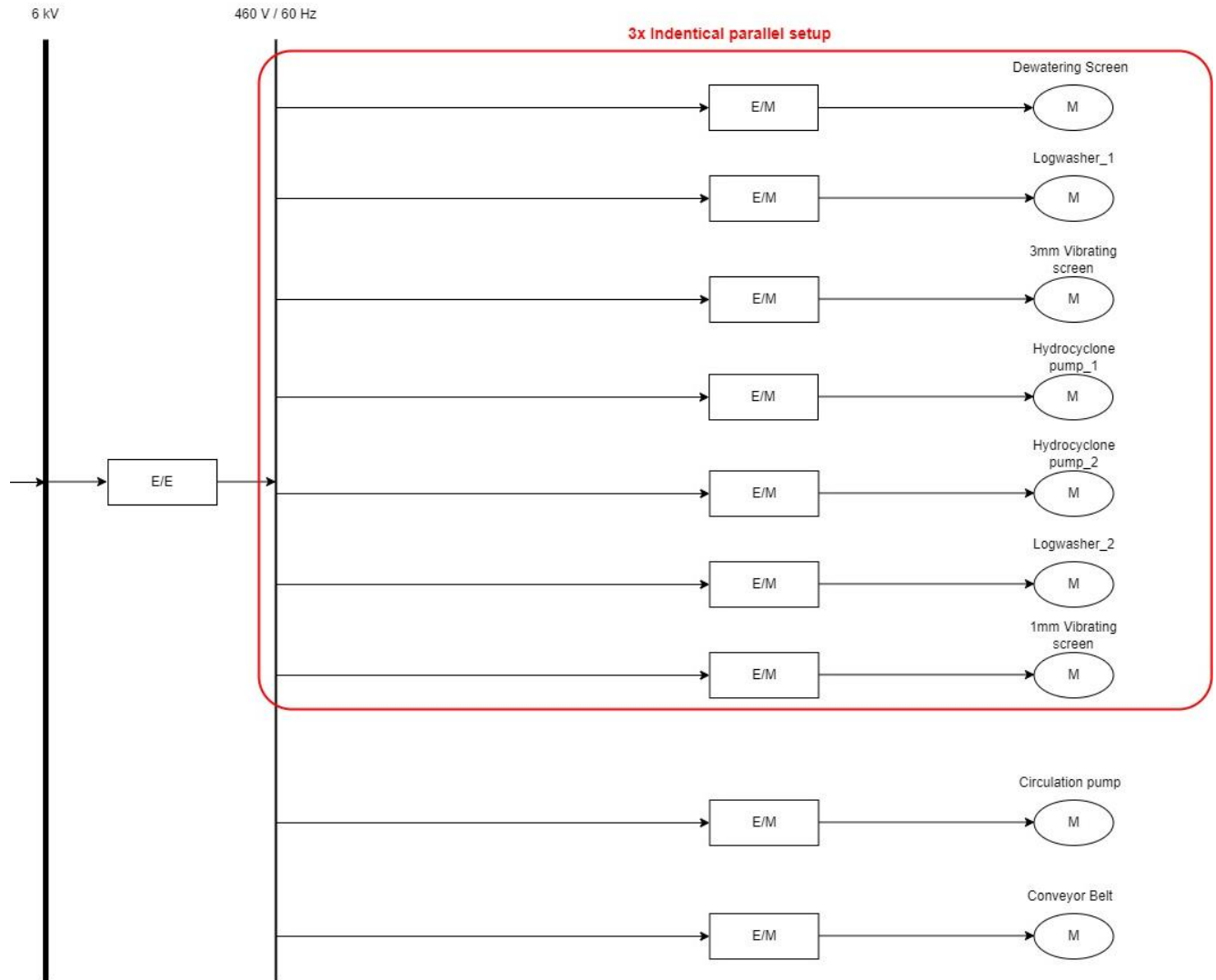
Hydraulic VTS – EFD



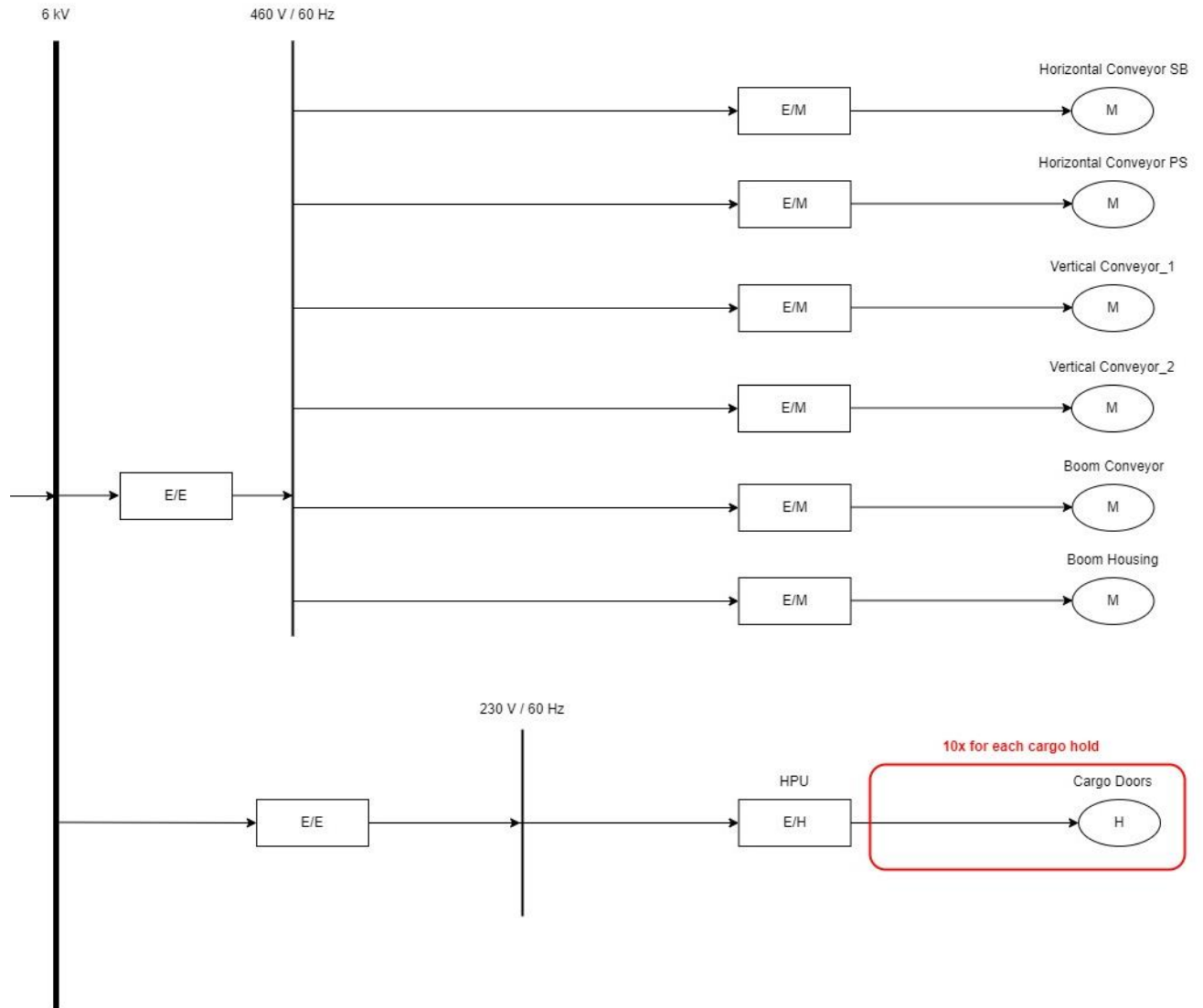
Riser Assembly – EFD



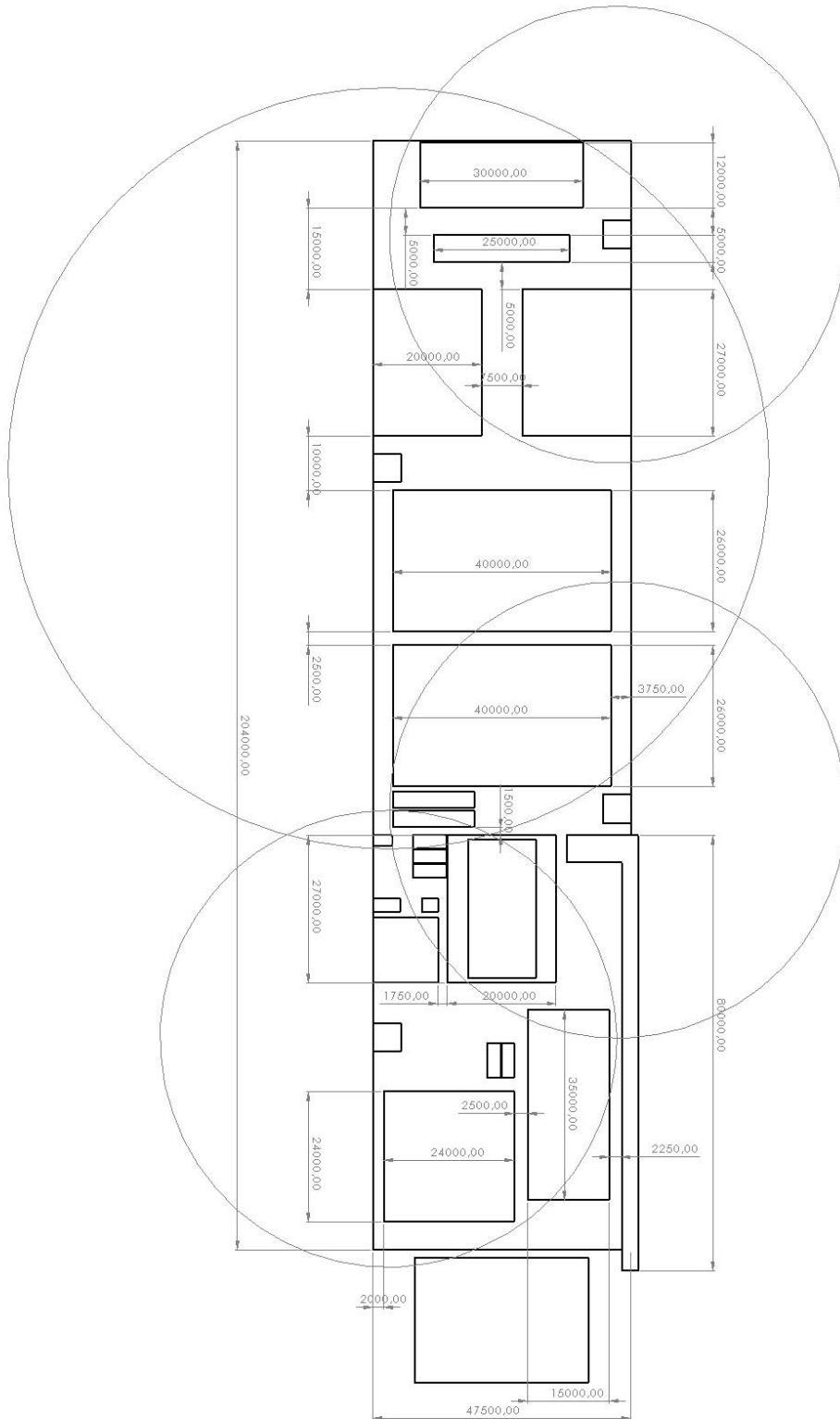
Dewatering – EFD

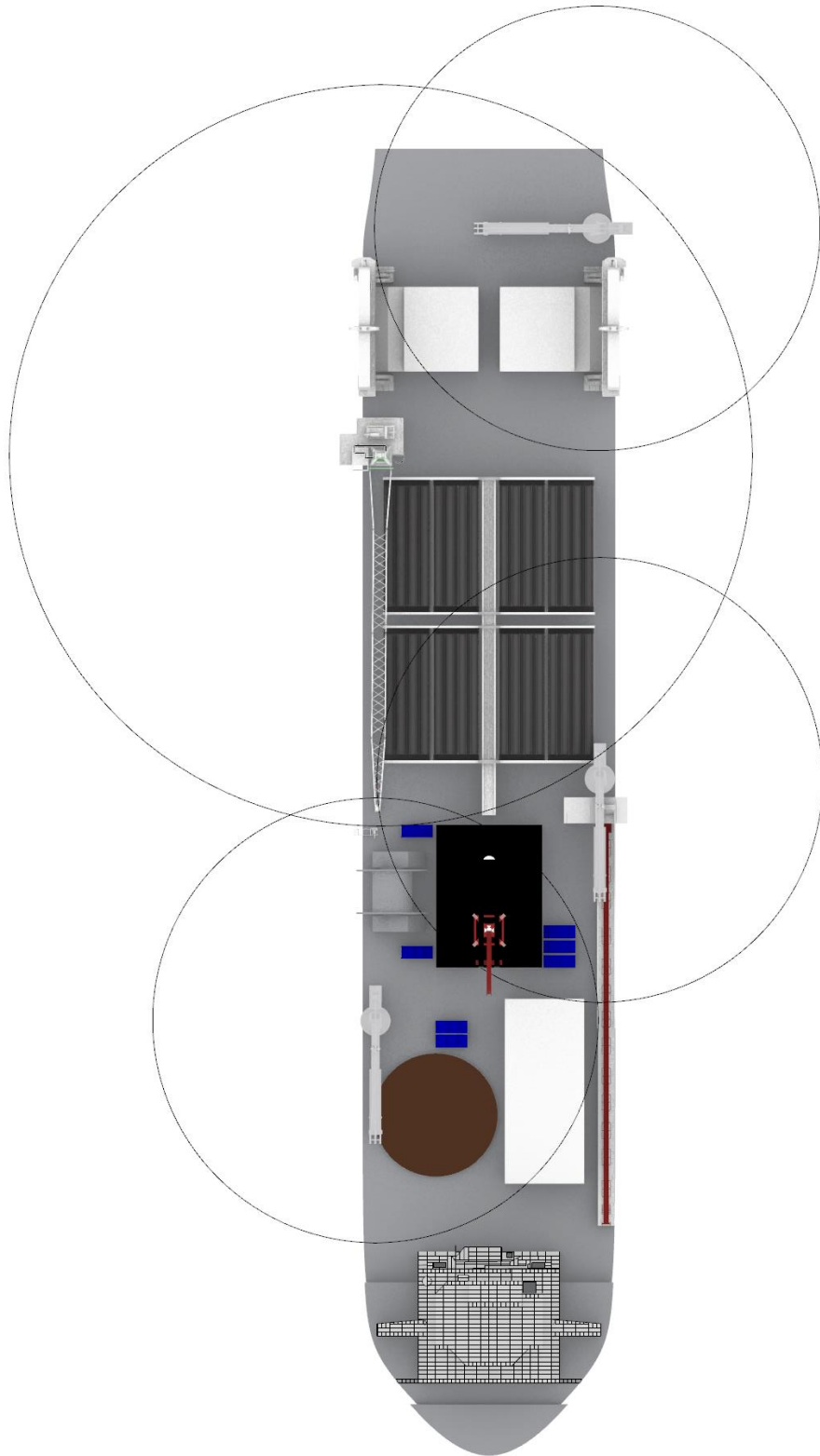


Dry – Offloading – EFD

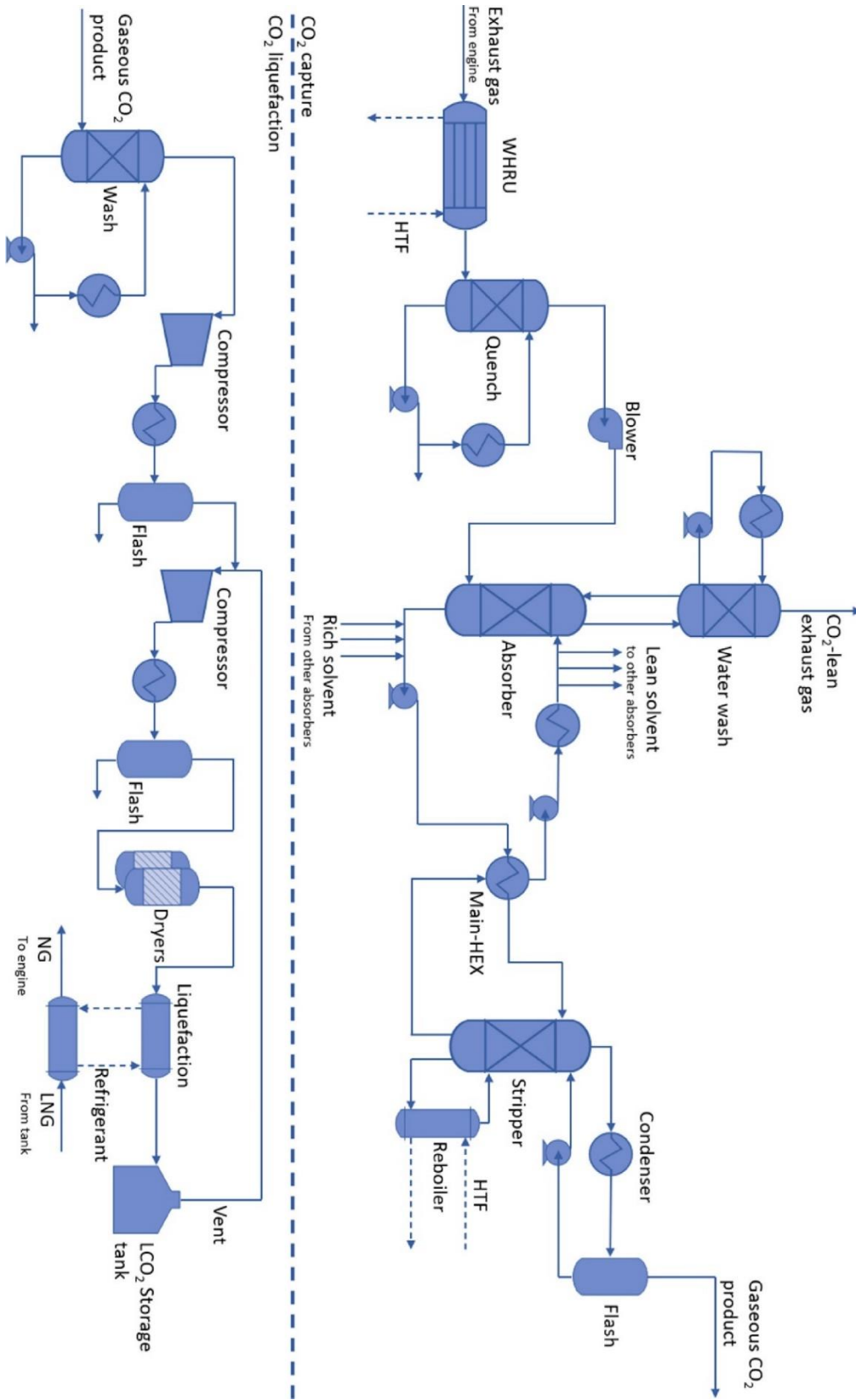


Appendix F – Deck Layout





Appendix H – Sleipnir LNG-fueled Ship Based Carbon Capture



(Ros et al., 2022)

Appendix J – DP Vessel force Calculation (MATLAB)

```

clear all
close all
clc

%% Max Conditions

Wave = 5.4;      % Max significant wave condition [m]           [0 2.4 3.4 5.4]
Wind = 20;      % Max wind speed condition [m/s]              [0 9 11 20]
Current = 1.5; % Max current speed condition [m/s]            [0 0.431 0.5 1.5]

%% Wave Force
% Wave Parameters

Hs = [0:0.1:Wave]; % Significant wave height [m]
Tp = 7;           % Wave Period [s]
g = 9.81;         % Gravitational constant [N/kg]
rho = 1025;       % Water Density [kg/m3]

zeta = Hs/2;      % Significant wave amplitude [m]
f = 1/Tp;         % Wave Frequency [Hz]
omega = 2*pi*f;   % Angular velocity [rad/s]
k = (omega^2)/g;  % Dispersion relation;
lambda = 2*pi/k;  % Wavelength [m]

L = 239.47;
B = 47.5;
T = 13;

% Plane Coordinates
x = [-L/2 L/2];
y = [-B/2 B/2];
z = [-T:1:0];

% Moonpool Coordinates
x_m = [128.5-(L/2) 154.1-(L/2)];
y_m = [-6.25 6.25];

t = [0:0.01:25];

% Vertical wall in infinite water depth

for i=1:length(t)
    for j=1:length(zeta)
        FK_x_1(i,j) = ((y(2)-y(1))*rho*zeta(j)*g*(1/k)*(exp(k*z(2))-
exp(k*z(1)))*cos(k*x(2) + omega*t(i)));
        FK_x_2(i,j) = -((y(2)-y(1))*rho*zeta(j)*g*(1/k)*(exp(k*z(2))-
exp(k*z(1)))*cos(k*x(1) + omega*t(i)));
        FK_x_3(i,j) = -((y_m(2)-y_m(1))*rho*zeta(j)*g*(1/k)*(exp(k*z(2))-
exp(k*z(1)))*cos(k*x_m(2) + omega*t(i)));
        FK_x_4(i,j) = ((y_m(2)-y_m(1))*rho*zeta(j)*g*(1/k)*(exp(k*z(2))-
exp(k*z(1)))*cos(k*x_m(1) + omega*t(i)));

        FK_y_1(i,j) = ((x(2)-x(1))*rho*zeta(j)*g*(1/k)*(exp(k*z(2))-
exp(k*z(1)))*cos(k*y(2) + omega*t(i)));
        FK_y_2(i,j) = -((x(2)-x(1))*rho*zeta(j)*g*(1/k)*(exp(k*z(2))-
exp(k*z(1)))*cos(k*y(1) + omega*t(i)));
    end
end

```

```

        FK_y_3(i,j) = -((x_m(2)-x_m(1))*rho*zeta(j)*g*(1/k)*(exp(k*z(2))-
exp(k*z(1)))*cos(k*y_m(2) + omega*t(i)));
        FK_y_4(i,j) = ((x_m(2)-x_m(1))*rho*zeta(j)*g*(1/k)*(exp(k*z(2))-
exp(k*z(1)))*cos(k*y_m(1) + omega*t(i)));

        FK_x(i,j) = FK_x_1(i,j) + FK_x_2(i,j) + FK_x_3(i,j) + FK_x_4(i,j);
        FK_y(i,j) = FK_y_1(i,j) + FK_y_2(i,j) + FK_y_3(i,j) + FK_y_4(i,j);
    end

end

figure(1)
subplot(1,2,1)
mesh(Hs,t,FK_x)
subplot(1,2,2)
mesh(Hs,t,FK_y)

F_x_1_c = (10^-3)*mean(abs(FK_x(:,j)));
F_x_1_m = (10^-3)* max(max(FK_x));
F_y_1_c = (10^-3)*mean(abs(FK_y(:,j)));
F_y_1_m = (10^-3)* max(max(FK_y));

%% Wind force
% Parameters
alpha_w = [0:10:180]; % Wind angle [deg]
Freeboard = 7; % Deck height above waterline [m]
M = 10; % Number of masts/kingposts in the lateral projection;
C = 75; % Distance from bow to centroid of lateral projected area [m];
S = 400; % Length of perimeter of lateral projection [m];
rho_air = 1.2; % Air density @ 20 degrees [kg/m3]
V_w = 0:0.5:Wind; % Wind speed [m/s]

% X Wind resistance coefficients
A_0 = [2.152 1.714 1.818 1.965 2.333 1.726 0.913 0.457 0.341 0.355 0.601 0.651 0.564 -
0.142 -0.677 -0.723 -2.148 -2.707 -2.529];
A_1 = (10)*[-0.5 -0.33 -0.397 -0.481 -0.599 -0.654 -0.468 -0.288 -0.091 0 0 0.129
0.254 0.358 0.364 0.314 0.256 0.397 0.376];
A_2 = [0.243 0.145 0.211 0.243 0.247 0.189 0 0 0 0 0 0 0 0 -0.175 -0.174];
A_3 = [-0.164 -0.121 -0.143 -0.154 -0.190 -0.173 -0.104 -0.068 -0.031 0 0 0 0 0.047
0.069 0.064 0.081 0.126 0.128];
A_4 = [0 0 0 0 0 0.348 0.482 0.346 0 -0.247 -0.347 -0.582 -0.748 -0.7 -0.529 -0.475 0
0 0];
A_5 = (10)*[0 0 0 0 0 0 0 0 0 0 0 0 0 0 0.127 0.181 0.155];
A_6 = [0 0 0.033 0.041 0.042 0.048 0.052 0.043 0.052 0.018 -0.02 -0.031 -0.024 -0.028
-0.032 -0.032 -0.027 0 0];

% Y Wind resistance coefficients
B_0 = [0 0.096 0.176 0.225 0.329 1.164 1.163 0.916 0.844 0.889 0.799 0.797 0.996 1.014
0.784 0.536 0.251 0.125 0];
B_1 = [0 0.22 0.71 1.38 1.82 1.26 0.96 0.53 0.55 0 0 0 0 0 0 0 0];
B_2 = [0 0 0 0 0 0.121 0.101 0.069 0.082 0.138 0.155 0.151 0.184 0.191 0.166 0.176
0.106 0.046 0];
B_3 = [0 0 0 0.023 0.043 0 0 0 0 0 0 0 0 -0.029 -0.022 -0.012 0];
B_4 = [0 0 0 0 -0.242 -0.177 0 0 0 0 -0.212 -0.280 -0.209 -0.163 0 0 0];
B_5 = [0 0 0 -0.29 -0.59 -0.95 -0.88 -0.65 -0.54 -0.66 -0.55 -0.55 -0.66 -0.69 -0.53 0
0 0];
% B_6 = [0 0 0 0 0 0 0 0 0 0.34 0.44 0.38 0.27 0 0 0 0];

% M Wind resistance coefficients
M_0 = [0 0.0596 0.1106 0.2258 0.2017 0.1759 0.1925 0.2133 0.1827 0.2627 0.2102 0.1567
0.0801 -0.0189 0.0256 0.0552 0.0881 0.0851 0];
M_1 = [0 0.061 0.204 0.245 0.457 0.573 0.480 0.315 0.254 0 0 0 0 0 0 0 0];

```

```

M_2 = [0 0 0 0 0 0 0 0 0 0 0 0 -0.0195 -0.0258 -0.0311 -0.0488 -0.0422 -0.0381 -0.0306 -
0.0122];
M_3 = [0 0 0 0 0.0067 0.0188 0.0115 0.0081 0.0053 0 0 0 0 0.0101 0.01 0.0109 0.0091
0.0025 0];
M_4 = [0 0 0 0 0 0 0 0 0 0 0.0335 0.0497 0.074 0.1128 0.0889 0.0689 0.0366 0 0];
M_5 = [0 -0.074 -0.170 -0.380 -0.472 -0.523 -0.546 -0.526 -0.443 -0.508 -0.492 -0.457
-0.396 -0.42 -0.463 -0.476 -0.415 -0.22 0];

% Lateral projected wind area
A_L = L*Freeboard + 23*14 + 35*10 + 27*10 + 60*7.5 + 25*10 + 25*10 + 22*8;

% Transverse projected wind area
A_T = B*Freeboard + 32*14 + (60+10-14)*7.5;

for i=1:length(alpha_w)
    % Longitudinal wind resistance coefficient
    C_w_x(i) = A_0(i) + A_1(i)*(2*A_L)/(L^2) + A_2(i)*(2*A_T)/(B^2) + A_3(i)*(L/B) +
A_4(i)*(S/L) + A_5(i)*(C/L) + A_6(i)*M;
    C_w_y(i) = B_0(i) + B_1(i)*(2*A_L)/(L^2) + B_2(i)*(2*A_T)/(B^2) + B_3(i)*(L/B) +
B_4(i)*(S/L) + B_5(i)*(C/L);
    C_w_m(i) = M_0(i) + M_1(i)*(2*A_L)/(L^2) + M_2(i)*(2*A_T)/(B^2) + M_3(i)*(L/B) +
M_4(i)*(S/L) + M_5(i)*(C/L);
    for j=1:length(V_w)
        % Wind force
        F_w_x(i,j) = (1/2)*rho_air*C_w_x(i)*A_T*V_w(j)^2;
        F_w_y(i,j) = (1/2)*rho_air*C_w_y(i)*A_L*V_w(j)^2;
        M_w_z(i,j) = (1/2)*rho_air*C_w_m(i)*A_L*L*V_w(j)^2;
    end
end

figure(2)
subplot(1,3,1)
mesh(V_w,alpha_w,F_w_x)
subplot(1,3,2)
mesh(V_w,alpha_w,F_w_y)
subplot(1,3,3)
mesh(V_w,alpha_w,M_w_z)

F_x_2 = (10^-3)*max(F_w_x(:,j));
F_y_2 = (10^-3)*max(F_w_y(:,j));
M_z_2 = (10^-3)*max(M_w_z(:,j));

%% Current Force

alpha_3 = [0:10:180]; % Current direction [deg]
alpha_c = (pi/180)*alpha_3;
S_w = L*(B+2*T); % wetted surface [m2]
V_c = [0:0.01:Current]; % Current Speeds [m/s]
nu = 1.002; % Dynamic viscosity [Pa s]

% Current coefficients
b = [0.908 0 -0.116 0 -0.033];
c = (1/10)*[-0.252 -0.904 0.032 0.109 0.011];

for l=1:length(V_c)
    for n=1:length(alpha_c)
        Rn(l,n) = (V_c(l)*abs(cos(alpha_c(n)))*L)/nu;
        F_c_x(l,n) = (0.075/((log(Rn(l,n))-
2)^2))* (1/2)*rho*abs(cos(alpha_c(n)))*cos(alpha_c(n))*V_c(l)^2;
    end
end

```

```

C_c_y(n) = b(1)*sin(alpha_c(n))+ b(2)*sin(2*alpha_c(n)) +
b(3)*sin(3*alpha_c(n)) + b(4)*sin(4*alpha_c(n)) + b(5)*sin(5*alpha_c(n));
C_c_m(n) = c(1)*sin(alpha_c(n))+ c(2)*sin(2*alpha_c(n)) +
c(3)*sin(3*alpha_c(n)) + c(4)*sin(4*alpha_c(n)) + c(5)*sin(5*alpha_c(n));

F_c_y(1,n) = (1/2)*rho*C_c_y(n)*(L*T)*V_c(1)^2;
M_c_z(1,n) = (1/2)*rho*C_c_m(n)*(L*T)*L*V_c(1)^2;
end
end

figure(3)
subplot(1,3,1)
mesh(alpha_3,V_c,F_c_x)
subplot(1,3,2)
mesh(alpha_3,V_c,F_c_y)
subplot(1,3,3)
mesh(alpha_3,V_c,M_c_z)

F_x_3 = (10^-3)*max(F_c_x(1,:));
F_y_3 = (10^-3)*max(F_c_y(1,:));
M_z_3 = (10^-3)*max(M_c_z(1,:));

%% Peak and nominal maximums

F_x_c = F_x_1_c + F_x_2 + F_x_3
F_y_c = F_y_1_c + F_y_2 + F_y_3

F_x_m = F_x_1_m + F_x_2 + F_x_3
F_y_m = F_y_1_m + F_y_2 + F_y_3

```

Table 42: Vessel forces results from MATLAB

	Mild		High		Extreme	
	Fx [kN]	Fy [kN]	Fx [kN]	Fy [kN]	Fx [kN]	Fy [kN]
Wave Amplitude $F_{FK} \sim f(H_s, t)$	171	1 815	243	2 571	386	4083
Wave Average $F_{FK} \sim f(H_s)$	109	1 140	155	1 615	246	2564
Wind $F_w \sim f(v_w, \alpha_w)$	74	156	111	232	368	769
Current $F_c \sim f(v_c, \alpha_c)$	0	292	0	395	0	3558
Total Continuous	183	1 588	262	2 242	614	6 891
Total Peak	245	2 263	354	3 198	754	8 410

Appendix K – Hydraulic VTS spc

Fuel Properties			
	Density	Energy Density	Bunker Rate
LNG	0.425 t/m ³	53600 kJ/kg	1800 USD/t
MGO	0.84 t/m ³	44000 kJ/kg	1140 USD/t
HFO	0.97 t/m ³	41000 kJ/kg	840 USD/t

Required SFE	
CO2	/ g/kWh
NOx	2.5 g/kWh
SOx	2 g/kWh
PM	2 g/kWh
CO	/ g/kWh
UHC	/ g/kWh

Hydraulic VTS													
Operating mode	Transit	DP 1	DP 2	Lars 1	LARS 2	sembled Stan	Mining 1	Mining 2	Offloading 1	Offloading 2	Survival	Harbor	Total
days	20	15	5	8	8	15	163	70	15	6	25	15	363
Production	5%	4%	1%	2%	2%	4%	45%	19%	4%	2%	7%	4%	100%
Power	21613	11209	16790	23378	28959	12209	20561	27432	24998	31479	21613	3000	2,3368 \$ 1,451.68 Mil. \$/year
							20561 kW						186 GWh
							4047 kW						
4x Wärtsilä 7L46DF Dual Fuel Engine (4x 8 015 kW) - HFO													
sfc	194	203	198	184	182	203	198	181	198	181	181	203	total 365 days 186 GWh
t/d	111	60	88	114	139	65	110	131	131	150	103	16	yearly 108 111 \$ 32,986,027.45
t/year	2214	901	439	908	1113	981	17851	9176	1960	903	2582	241	17 GWh
30 days mining Endurance													
days	15.3	8.3	1.8	0.7	0.7	1.1	131	131	150	103	1.1	1.1	17 GWh
t/d	110	110	131	131	150	103	131	131	150	103	1.1	1.1	17 GWh
t	2108	1084	232	107	107	107	107	107	107	107	107	107	17 GWh
CO2	604	632	617	573	567	632	617	564	617	564	632	632	122300 t 655.78 g/kWh CO2 3114.4 g/kg
SOx	4	4	4	4	4	4	4	4	4	4	4	4	4.04 g/kWh SOx 19.2 g/kg
PM	1.1	1.1	1.1	1.0	1.0	1.1	1.1	1.0	1.1	1.0	1.1	1.1	214 t 1.15 g/kWh PM 5.46 g/kg
CO	0.6	0.7	0.7	0.6	0.6	0.7	0.7	0.6	0.7	0.6	0.7	0.7	130 t 0.70 g/kWh CO 3.32 g/kg
UHC	0.3	0.3	0.3	0.3	0.3	0.3	0.3	0.3	0.3	0.3	0.3	0.3	57 t 0.31 g/kWh UHC 1.45 g/kg
4x Wärtsilä 7L46DF Dual Fuel Engine (4x 8 015 kW) - MGO													
sfc	180	187	183	173	170	187	177	171	177	171	172	187	total 365 days 186 GWh
t/d	103	55	81	107	130	60	98	124	117	142	98	15	yearly 99 117 \$ 41,033,877.07
t/year	2054	830	406	854	1040	904	15958	8669	1752	853	2454	222	17 GWh
30 days mining Endurance													
days	16	8	1.8	0.7	0.7	1.1	131	131	150	103	1.1	1.1	17 GWh
t/d	107	107	128	128	142	107	107	107	107	107	107	107	17 GWh
t	3216	3829	3666	565,41	565,41	565,41	565,41	565,41	565,41	565,41	565,41	565,41	17 GWh
CO2	577	600	587	555	545	600	567	548	567	548	551	600	115399 t 618.78 g/kWh CO2 3206 g/kg
SOx	0	0	0	0	0	0	0	0	0	0	0	0	66 t 0.35 g/kWh SOx 1.82 g/kg
PM	0.2	0.2	0.2	0.2	0.2	0.2	0.2	0.2	0.2	0.2	0.2	0.2	37 t 0.20 g/kWh PM 1.016 g/kg
CO	0.6	0.6	0.6	0.6	0.6	0.6	0.6	0.6	0.6	0.6	0.6	0.6	125 t 0.67 g/kWh CO 3.47 g/kg
UHC	0.3	0.3	0.3	0.3	0.3	0.3	0.3	0.3	0.3	0.3	0.3	0.3	55 t 0.29 g/kWh UHC 1.52 g/kg
4x Wärtsilä 7L46DF Dual Fuel Engine (4x 8 015 kW) - LNG													
sfc	148	153	150	143	139	153	144	140	144	140	141	153	total 365 days 186 GWh
t/d	84	45	66	88	106	49	80	101	95	116	80	12	yearly 81 189 \$ 52,906,984.43
t/year	1689	679	332	706	850	740	12983	7097	1425	698	2011	182	17 GWh
30 days mining Endurance													
days	15.3	8.3	1.8	0.7	0.7	1.1	131	131	150	103	1.1	1.1	17 GWh
t/d	107	107	128	128	142	107	107	107	107	107	107	107	17 GWh
t	2622	6170	4,720,383.36	4,720,383.36	4,720,383.36	4,720,383.36	4,720,383.36	4,720,383.36	4,720,383.36	4,720,383.36	4,720,383.36	4,720,383.36	17 GWh
CO2	407	421	413	393	382	421	396	385	396	385	421	421	80830 t 433.42 g/kWh CO2 2750 g/kg
NOx	0.7	0.7	0.7	0.7	0.7	0.7	0.7	0.7	0.7	0.7	0.7	0.7	139 t 0.75 g/kWh NOx 4.74 g/kg
SOx	0	0	0	0	0	0	0	0	0	0	0	0	0 t 0.00 g/kWh SOx 0 g/kg
PM	0.0	0.0	0.0	0.0	0.0	0.0	0.0	0.0	0.0	0.0	0.0	0.0	0 t 0.00 g/kWh PM 0.00117 g/kg
CO	1.4	1.4	1.4	1.3	1.3	1.4	1.3	1.3	1.3	1.3	1.4	1.4	274 t 1.47 g/kWh CO 9.33 g/kg
UHC	0.1	0.1	0.1	0.1	0.1	0.1	0.1	0.1	0.1	0.1	0.1	0.1	24 t 0.13 g/kWh UHC 0.8200233 g/kg
Gas Turbine - MGO													
sfc	230.0	250.0	235.0	220.0	213.0	248.0	223.0	214.0	218.0	210.0	218.0	250.0	total 365 days 186 GWh
t/d	131	74	104	136	163	80	123	155	144	175	124	36	yearly 125 149 \$ 52,906,063.06
t/year	2625	1110	521	1086	1303	1199	20105	10849	2158	1047	3110	546	17 GWh
30 days mining Endurance													
days	15.3	8.3	1.8	0.7	0.7	1.1	131	131	150	103	1.1	1.1	17 GWh
t/d	134	160	160	160	160	160	160	160	160	160	160	160	17 GWh
t	4034	4803	4,599,307.19	4,599,307.19	4,599,307.19	4,599,307.19	4,599,307.19	4,599,307.19	4,599,307.19	4,599,307.19	4,599,307.19	4,599,307.19	17 GWh
CO2	737	802	753	705	683	795	715	686	699	673	699	1475	146379 t 784.90 g/kWh CO2 3206 g/kg
NOx	14.0	15.2	14.3	13.4	13.0	15.1	13.6	13.0	13.3	12.8	13.3	28.0	1 t 0.01 g/kWh NOx 0.025 g/kg
SOx	0	0	0	0	0	0	0	0	0	0	0	0	0 t 0.00 g/kWh SOx 0 g/kg
PM	0.2	0.3	0.2	0.2	0.2	0.2	0.2	0.2	0.2	0.2	0.2	0.5	14 t 0.07 g/kWh PM 0.3 g/kg
CO	0.8	0.9	0.8	0.8	0.7	0.9	0.8	0.7	0.8	0.7	0.8	1.6	1 t 0.01 g/kWh CO 0.025 g/kg
UHC	0.3	0.4	0.4	0.3	0.3	0.4	0.3	0.3	0.3	0.3	0.3	0.7	14 t 0.07 g/kWh UHC 0.3 g/kg
Gas Turbine - LNG													
sfc	188.0	206.0	193.0	181.0	175.0	203.0	183.0	176.0	178.0	172.0	178.0	206.0	total 365 days 186 GWh
t/d	107	61	86	112	134	65	101	127	117	143	102	30	yearly 103 242 \$ 67,435,244.52
t/year	2145	914	428	894	1070	981	16499	8922	1762	858	2539	451	17 GWh
30 days mining Endurance													
days	15.3	8.3	1.8	0.7	0.7	1.1	131	131	150	103	1.1	1.1	17 GWh
t/d	110	110	131	131	150	103	131	131	150	103	1.1	1.1	17 GWh
t	3312	7793	5,961,368.70	5,961,368.70	5,961,368.70	5,961,368.70	5,961,368.70	5,961,368.70	5,961,368.70	5,961,368.70	5,961,368.70	5,961,368.70	17 GWh
CO2	603	660	619	580	561	651	587	564	571	551	571	1218	103026 t 552.44 g/kWh CO2 2750 g/kg
NOx	11.4	12.5	11.7	11.0	10.6	12.3	11.1	10.7	10.8	10.5	10.8	23.1	1 t 0.01 g/kWh NOx 0.025 g/kg
SOx	0	0	0	0	0	0	0	0	0	0	0	0	0 t 0.00 g/kWh SOx 0 g/kg
PM	0.2	0.2	0.2	0.2	0.2	0.2	0.2	0.2	0.2	0.2	0.2	0.4	0 t 0.00 g/kWh PM 0.0117 g/kg
CO	0.7	0.7	0.7	0.6	0.6	0.7	0.6	0.6	0.6	0.6	0.6	1.3	1 t 0.01 g/kWh CO 0.025 g/kg
UHC	0.3	0.3	0.3	0.3	0.3	0.3	0.3	0.3	0.3	0.3	0.3	0.6	31 t 0.16 g/kWh UHC 0.8200233 g/kg

Appendix L – Airlift VTS spc

Fuel Properties			
	Density	Energy Density	Bunker Rate
LNG	0.425 t/m ³	53600 kJ/kg	1800 USD/t
MGO	0.84 t/m ³	44000 kJ/kg	1140 USD/t
HFO	0.97 t/m ³	41000 kJ/kg	840 USD/t

Required SPE	
CO2	/ g/kWh
NOx	2.5 g/kWh
SOx	2 g/kWh
PM	2 g/kWh
CO	/ g/kWh
UHC	/ g/kWh

Airlift VTS														
Operating mode	Transit	DP 1	DP 2	Lars 1	LARS 2	embled Sta	Mining 1	Mining 2	Offloading	Offloading 2	Survival	Harbor	Total	
days	20	9	3	8	8	173	75	15	6	25	15		365	
Production	5%	2%	1%	2%	2%	2%	47%	21%	4%	2%	7%	4%	100%	
Power	21613	11209	16790	21129	26710	12109	36251	42632	36251	42632	21613	3000	286,0032 GWh	
Wet Offloading										2050 kW	38301	44682		
Dry Offloading										4047 kW	40298	46679		
6x Wartsila 7L46DF Dual Fuel Engine (4x 8 015 kW) - HFO														
sfoc	203	203	203	202	199	203	180	184	180	185	199	203	365 days	
t/d	116	60	90	113	140	65	172	207	172	208	114	16	159	
t/year	2317	541	270	901	1123	519	29802	15532	2584	1249	2839	241	57917	
30 days mining Endurance										days	19.3	8.4	1.7	0.7
										t/d	172	207	172	208
										t	3324	1732	288	139
CO2	g/kWh	632	632	632	629	620	632	561	573	561	576	620	632	
NOx	g/kWh	11.4	11.4	11.4	11.4	11.4	10.5	10.7	10.5	10.8	11.4	11.4	11.4	
SOx	g/kWh	4	4	4	4	4	4	3	4	3	4	4	4	
PM	g/kWh	1.1	1.1	1.1	1.1	1.1	1.0	1.0	1.0	1.0	1.1	1.1	1.1	
CO	g/kWh	0.7	0.7	0.7	0.7	0.7	0.6	0.6	0.6	0.6	0.7	0.7	0.7	
UHC	g/kWh	0.3	0.3	0.3	0.3	0.3	0.3	0.3	0.3	0.3	0.3	0.3	0.3	
6x Wartsila 7L46DF Dual Fuel Engine (4x 8 015 kW) - MGO														
sfoc	187	187	187	185	179	187	171	168	170	168	181	187	365 days	
t/d	107	55	83	103	126	60	164	189	163	189	103	15	148	
t/year	2134	498	249	826	1010	478	28312	14181	2440	1134	2582	222	54066	
30 days mining Endurance										days	19.3	8.4	1.7	0.7
										t/d	164	189	163	189
										t	3157	1582	272	127
CO2	g/kWh	600	600	600	593	574	600	548	539	545	539	580	600	
NOx	g/kWh	11.4	11.4	11.4	11.4	11.4	10.5	10.7	10.5	10.8	11.4	11.4	11.4	
SOx	g/kWh	0	0	0	0	0	0	0	0	0	0	0	0	
PM	g/kWh	0.2	0.2	0.2	0.2	0.2	0.2	0.2	0.2	0.2	0.2	0.2	0.2	
CO	g/kWh	0.6	0.6	0.6	0.6	0.6	0.6	0.6	0.6	0.6	0.6	0.6	0.6	
UHC	g/kWh	0.3	0.3	0.3	0.3	0.3	0.3	0.3	0.3	0.3	0.3	0.3	0.3	
6x Wartsila 7L46DF Dual Fuel Engine (4x 8 015 kW) - LNG														
sfoc	153	153	153	152	147	153	140.5	138	140	138	148	153	365 days	
t/d	87	45	68	85	104	49	134	155	134	155	84	12	122	
t/year	1746	407	203	678	829	391	23262	11649	2010	932	2111	182	44401	
30 days mining Endurance										days	19.3	8.4	1.7	0.7
										t/d	134	155	134	155
										t	2594	1299	224	104
CO2	g/kWh	421	421	421	418	404	421	386	380	385	380	407	421	
NOx	g/kWh	0.7	0.7	0.7	0.7	0.7	0.7	0.7	0.7	0.7	0.7	0.7	0.7	
SOx	g/kWh	0	0	0	0	0	0	0	0	0	0	0	0	
PM	g/kWh	0.0	0.0	0.0	0.0	0.0	0.0	0.0	0.0	0.0	0.0	0.0	0.0	
CO	g/kWh	1.4	1.4	1.4	1.4	1.4	1.3	1.3	1.3	1.3	1.4	1.4	1.4	
UHC	g/kWh	0.1	0.1	0.1	0.1	0.1	0.1	0.1	0.1	0.1	0.1	0.1	0.1	
COGES - MGO														
sfoc	190.0	310.0	265.0	190.0	180.0	310.0	163.0	163.0	163.0	190.0	190.0	460.0	365 days	
t/d	108	92	117	106	127	99	156	183	156	183	108	96	146	
t/year	2168	826	352	848	1015	793	26987	13759	2340	1101	2710	546	53446	
30 days mining Endurance										days	19.3	8.4	1.7	0.7
										t/d	156	183	156	183
										t	3010	1534	261	123
CO2	g/kWh	609	994	850	609	577	994	523	523	523	609	1475	171348 t	
NOx	g/kWh	11.6	18.8	16.1	11.6	10.9	18.8	9.9	9.9	9.9	11.6	28.0	1 t	
SOx	g/kWh	0	0	0	0	0	0	0	0	0	0	0	0 t	
PM	g/kWh	0.2	0.3	0.3	0.2	0.2	0.3	0.2	0.2	0.2	0.2	0.5	16 t	
CO	g/kWh	0.7	1.1	0.9	0.7	0.6	1.1	0.6	0.6	0.6	0.7	1.6	1 t	
UHC	g/kWh	0.3	0.5	0.4	0.3	0.3	0.5	0.2	0.2	0.2	0.3	0.7	16 t	
COGES - LNG														
sfoc	156.0	260.0	215.0	156.0	145.0	156.0	134.0	134.0	134.0	156.0	156.0	380.0	365 days	
t/d	89	77	95	87	102	50	128	151	128	151	89	30	120	
t/year	1780	692	286	696	818	396	22186	11311	1924	905	2225	451	43671	
30 days mining Endurance										days	19.3	8.4	1.7	0.7
										t/d	128	151	128	151
										t	2474	1261	215	101
CO2	g/kWh	500	834	689	500	465	497	430	430	430	500	1218	120096 t	
NOx	g/kWh	9.5	15.8	13.1	9.5	8.8	9.4	8.1	8.1	8.1	9.5	23.1	1 t	
SOx	g/kWh	0	0	0	0	0	0	0	0	0	0	0	0 t	
PM	g/kWh	0.2	0.3	0.2	0.2	0.1	0.2	0.1	0.1	0.1	0.2	0.4	1 t	
CO	g/kWh	0.5	0.9	0.7	0.5	0.5	0.5	0.5	0.5	0.5	0.5	1.3	1 t	
UHC	g/kWh	0.2	0.4	0.3	0.2	0.2	0.2	0.2	0.2	0.2	0.2	0.6	36 t	

Bibliography

- A. Vrij, S. B. (2020). *Blue Nodules Deliverable report D4.5 Mining Platform Deliverable Report: Final (revised), issue date on 2020-10-13 Blue Nodules-Breakthrough Solutions for the Sustainable Harvesting and Processing of Deep Sea Polymetallic Nodules.*
- Alex Dopico. (2020). *How much does a GE steam turbine cost?* <https://panicjanet.com/how-much-does-a-ge-steam-turbine-cost/>
- Baker Hughes. (2022). *Centrifugal & axial compressors.* <https://www.bakerhughes.com/centrifugal-axial-compressors>
- Blue Nodules. (2017). *Blue Nodules Deliverable Report D2.4 Initial Design of Vehicle Propulsion and Propulsion Test Performance Deliverable Report: Final, issue date 18 September 2017 Blue Nodules-Breakthrough Solutions for the Sustainable Harvesting and Processing of Deep Sea Polymetallic Nodules.*
- Blue Nodules. (2020). *Blue Nodules Summary - Deep sea mining.* <https://www.youtube.com/watch?v=pCus0hTsibc&t=1s>
- Brekke, J., Chakrabarti, S., & Halkyard, J. (2005). *Drilling and Production Risers.*
- by Elaine Baker, E., & Beaudoin, Y. (2013). *Manganese Nodules A physical, biological, environmental, and technical review.*
- Chatham Rock Phosphate Limited. (2014). *Marine Consent Application and Environmental Impact Assessment Volume One.*
- CSL Group. (2021). *GRAVITY-FED SELF-UNLOADERS.* <https://www.cslships.com/en/our-operations/self-unloaders/how-it-works/gravity-fed-self-unloaders>
- Drammen Offshore Leasing. (2022). *Offshore Cable Carousels available for rent.*
- Engineering ToolBox. (2018). *Air - Properties at Gas-Liquid Equilibrium Conditions.* https://www.engineeringtoolbox.com/air-gas-liquid-equilibrium-condition-properties-temperature-pressure-boiling-curve-d_2008.html
- Flatebø, Ø. (2012). *Off-design Simulations of Offshore Combined Cycles.*
- Fontelle, J.-P., Fridell, E., Grigoriadis, A., Hill, N., Kilde, N., Lavender, K., Mamarikas, S., Reynolds, G., Rypdal, K., Thomas, R., Webster, A., & Winther, M. (2019). *International maritime and inland navigation, national navigation, national fishing, recreational boats International maritime navigation, international inland navigation, national navigation (shipping), national fishin.*
- Frederico, C., Matt, T., Matt, C. F., Vieira, L. S. R., Soares, G. F. W., & de Faria, L. P. T. (2005). *Optimization of the Operation of Isolated Industrial Diesel Stations BENEFICE-Building Resources Management towards flexible Contracted Power View project Sustainable Systems and Ecosystems Engineering View project 6 th World Congress on Structural and Multidisciplinary Optimization*

- Optimization of the Operation of Isolated Industrial Diesel Stations.*
<https://www.researchgate.net/publication/240851584>
- Glover, A. G., Dahlgren, T. G., Wiklund, H., Mohrbeck, I., & Smith, C. R. (2016). An end-to-end DNA taxonomy methodology for benthic biodiversity survey in the Clarion-Clipperton Zone, central Pacific abyss. *Journal of Marine Science and Engineering*, 4(1).
<https://doi.org/10.3390/jmse4010002>
- GSR. (2018). *Environmental Impact Statement.*
- Hydralift. (1997). *200-250 Ton A-frame K4226 spec.*
- IAEA. (2020). *ADVANCES IN SMALL MODULAR REACTOR TECHNOLOGY DEVELOPMENTS 2020 Edition A Supplement to: IAEA Advanced Reactors Information System (ARIS)* <http://aris.iaea.org>
<http://aris.iaea.org>
- IHC Merwede. (2022). *D1 PS Rubber ring gate valve.*
- IMECA. (2016). *4 TRACKS TENSIONERS.* www.imeca.reel.fr
- IMO. (2014). *GUIDELINES FOR THE REDUCTION OF UNDERWATER NOISE FROM COMMERCIAL SHIPPING TO ADDRESS ADVERSE IMPACTS ON MARINE LIFE.*
- IMO. (2018). *2018 GUIDELINES ON THE METHOD OF CALCULATION OF THE ATTAINED ENERGY EFFICIENCY DESIGN INDEX (EEDI) FOR NEW SHIPS.*
- imo. (2018). *INITIAL IMO STRATEGY ON REDUCTION OF GHG EMISSIONS FROM SHIPS.*
<http://www.imo.org>
- ISA. (2006). *Polymetallic Nodules.*
- ISA. (2011). *International Seabed Authority ISBA/17/LTC/7 Legal and Technical Commission Environmental Management Plan for the Clarion-Clipperton Zone.*
- ISA. (2019). *Draft regulations for exploitation of mineral resources in the Area Draft regulations on exploitation of mineral resources in the Area.*
- IsherWood, R. M. (1972). *Wind Resistance of Merchant Ships.*
- Kai Levander. (2012). *System Based Ship Design.*
- Keppel. (2015). *Winches - Equipment & Systems.*
- Kortlever, R. (2021). *Electrochemical Devices and Summary Electrochemical Energy Storage (ME45201).*
- Kristian, E., Frimanslund, T., & Løve, S. (2016). *Feasibility of Deep-Sea Mining Operation Within Norwegian Jurisdiction.*
- Lee, I., Park, J., & Moon, I. (2017). Conceptual design and exergy analysis of combined cryogenic energy storage and LNG regasification processes: Cold and power integration. *Energy*, 140, 106–115.
<https://doi.org/10.1016/j.energy.2017.08.054>

Ma, W., van Rhee, C., & Schott, D. (2017). Technological and profitable analysis of airlifting in deep sea mining systems. *Minerals*, 7(8). <https://doi.org/10.3390/min7080143>

MacGregor. (2021). *Offshore AHC cranes*.

Maersk Drilling. (2021). *Maersk Valiant*.

MAN Diesel & Turbo. (2022). *RB Barrel type centrifugal compressors*.

Marine Solutions, W. (2017). *Wärtsilä Steerable Thruster Retractable Underwater Mountable (WST-RU)*. www.wartsila.com

Maxime Lesage. (2020). *A framework for evaluating deep sea mining systems for seafloor massive sulfide deposits*.

McLanahan. (2022). *DEWATERING SCREENS*.

McLanahan. (2022a). *Log-Washer_Brochure_NA_Digital*.

McLanahan. (2022b). *SeparatorS™ How It Works*.

McLanahan. (2022c). *TRIPLE-SHAFT HORIZONTAL SCREEN*.

MDL. (2022). *350Te Reel Drive System*. <https://maritimedevelopments.com/products/reel-drive-systems//350te-reel-drive-system>

Mihelčič, A., Jožef, ", Pungerčič, A., & Snoj, L. (2020). *Modelling of OPEN100 Reactor with Serpent-2*.

Mike Gawinski. (2020). *BELT CONVEYOR POWER CALCULATION PROGRAM FOR BULK HANDLING APPLICATIONS*. <https://rulmecacorp.com/bulk-handling-power-calculation-program/>

NORI. (2021). *Collector Test Study - EIS*.

NOV. (2018). *Product Reference Guide*. www.nov.com

NOV. (2022). *OC3550L Lattice Boom Offshore Cranes*.

NOV LH. (2018). *Lifting & Handling product portfolio*.

OCIMF. (2018). *"Guidelines for Offshore Tanker Operations" (GOTO)*.

Offshore Crane. (2022). *65 TON KNUCKLE BOOM CRANE FOR SALE*.

ONSITE SYCOM Energy Corporation. (2000). *The Market and Technical Potential for Combined Heat and Power in the Industrial Sector*.

Orientflex. (2021). *Floating Dredging Hose*. <https://www.orient-hose.com/project/floating-dredging-hose/>

Palfinger Marin. (2021). *DECK EQUIPMENT AND LIFESAVING APPLIANCES PRODUCT CATALOGUE*
APPLIANCES PRODUCT CATALOGUE.

- Preston, J. F. (2013). *L5.-Low Power and Shutdown PSA ANSN Regional Workshop on Integrated Deterministic Safety Analysis (DSA) and Probabilistic Safety Assessment (PSA) for Risk Management of Nuclear Power Plant Manila, PNRI, Philippines.*
- QUASAR. (2022). *DRILL SUPPORT/GENERAL WORK CLASS ROV.*
- Remery, G. F. M., & van Oortmerssen, G. (1973). *The Mean Wave, Wind and Current Forces on Offshore Structures and Their Role in the Design of Mooring Systems.*
- Romas Marine. (2022). *200te 4-Track Tensioner Equipment Data Sheet.*
- Ros, J. A., Skylogianni, E., Doedée, V., van den Akker, J. T., Vredeveldt, A. W., Linders, M. J. G., Goetheer, E. L. V., & G M-S Monteiro, J. (2022). Advancements in ship-based carbon capture technology on board of LNG-fuelled ships. *International Journal of Greenhouse Gas Control*, 114. <https://doi.org/10.1016/j.ijggc.2021.103575>
- Schulte, S. A. (2013a). *Vertical transport methods for Deep Sea Mining Section of Dredging Engineering.*
- Schulte, S. A. (2013b). *Vertical transport methods for Deep Sea Mining Section of Dredging Engineering.*
- Seatools. (2002). *Deep water excavation grab - GES.*
- Sun, L., Zhu, X., Li, B., & Ai, S. (2018). Coupled dynamic analysis of deep-sea mining support vessel with dynamic positioning. *Marine Georesources and Geotechnology*, 36(7), 841–852. <https://doi.org/10.1080/1064119X.2017.1391901>
- Tim Matzke. (2021). *Four Design Decisions To Prepare For When Purchasing A Bucket Elevator.*
- van den Akker, J. T. (2017). *CARBON CAPTURE ONBOARD LNG-FUELED VESSELS A FEASIBILITY STUDY.* <http://repository.tudelft.nl>
- van der Stoep, C., & Peters, O. A. J. (1997). *A dynamically positioning system for the drillship "Gusto 10000" written by.*
- van Nijen, K., van Passel, S., Brown, C. G., Lodge, M. W., Segerson, K., & Squires, D. (2019). The Development of a Payment Regime for Deep Sea Mining Activities in the Area through Stakeholder Participation. In *International Journal of Marine and Coastal Law* (Vol. 34, Issue 4, pp. 571–601). Brill Nijhoff. <https://doi.org/10.1163/15718085-13441100>
- Vecchi, A., Li, Y., Ding, Y., Mancarella, P., & Sciacovelli, A. (2021). Liquid air energy storage (LAES): A review on technology state-of-the-art, integration pathways and future perspectives. In *Advances in Applied Energy* (Vol. 3). Elsevier Ltd. <https://doi.org/10.1016/j.adapen.2021.100047>
- Volkman, S. E., Kuhn, T., & Lehnen, F. (2018). A comprehensive approach for a techno-economic assessment of nodule mining in the deep sea. *Mineral Economics*, 31(3), 319–336. <https://doi.org/10.1007/s13563-018-0143-1>
- Volkman, S. E., & Lehnen, F. (2018). Production key figures for planning the mining of manganese nodules. *Marine Georesources and Geotechnology*, 36(3), 360–375. <https://doi.org/10.1080/1064119X.2017.1319448>

Warman. (2009). *MC Pump range for Mill Circuit applications WARMAN® Centrifugal Slurry Pumps*.

WARMAN. (2009). *Warman - MC Pump Range*.

Wärtsilä. (2017). *Wärtsilä Underwater Mountable (UWM) Thrusters*.

Yue, Z., Zhao, G., Xiao, L., & Liu, M. (2021). Comparative Study on Collection Performance of Three Nodule Collection Methods in Seawater and Sediment-seawater Mixture. *Applied Ocean Research*, 110. <https://doi.org/10.1016/j.apor.2021.102606>